

MODE CONVERSION OF PLASMA WAVES

Anna Maria Woods

A Thesis Submitted for the Degree of PhD
at the
University of St Andrews



1987

Full metadata for this item is available in
St Andrews Research Repository
at:

<http://research-repository.st-andrews.ac.uk/>

Please use this identifier to cite or link to this item:

<http://hdl.handle.net/10023/13965>

This item is protected by original copyright

MODE CONVERSION OF PLASMA WAVES

ANNA MARIA WOODS

THESIS SUBMITTED FOR THE DEGREE OF DOCTOR OF PHILOSOPHY
OF THE UNIVERSITY OF ST ANDREWS



ProQuest Number: 10171005

All rights reserved

INFORMATION TO ALL USERS

The quality of this reproduction is dependent upon the quality of the copy submitted.

In the unlikely event that the author did not send a complete manuscript and there are missing pages, these will be noted. Also, if material had to be removed, a note will indicate the deletion.



ProQuest 10171005

Published by ProQuest LLC (2017). Copyright of the Dissertation is held by the Author.

All rights reserved.

This work is protected against unauthorized copying under Title 17, United States Code
Microform Edition © ProQuest LLC.

ProQuest LLC.
789 East Eisenhower Parkway
P.O. Box 1346
Ann Arbor, MI 48106 – 1346

Th 17486

MODE CONVERSION OF PLASMA WAVES

Abstract

Linear mode conversion processes are much studied in plasma physics because they determine the efficiency of any radio frequency heating scheme. Mode coupling model equations, extracted with varying degrees of rigour from the Maxwell-linearised kinetic equations, are usually fourth or higher order O.D.E's. These are solved by complicated methods to obtain transmission, conversion, reflection and absorption coefficients. Recently, Fuchs et al and Cairns and Lashmore-Davies (C.L-D.) have postulated second order O.D.E's to describe pairwise coupling events. The second order theories have reproduced results previously obtained by much more sophisticated treatments.

In this thesis, we firstly examine the hybrid resonances in a cold plasma and show that they have a mode conversion interpretation in the framework of the C.L-D. model. The Budden tunnelling coefficients are recovered for this case.

Next, mode conversion between the fast and slow electromagnetic waves in the lower hybrid frequency range is considered. This phenomenon determines the accessibility of the lower hybrid resonance to the slow wave, and is also of theoretical interest because the mode coupling differs in certain aspects from cases previously investigated by C.L-D. A second order approximation to the dispersion relation is used in the mode conversion region leading to Weber's equation from which transmission coefficients are then

obtained in various cases.

Finally, we provide justification for the use of Weber's equation. The exact fourth order system of O.D.E's for the problem is set down, and a linear transformation, which is an extension of that given by Heading, reveals the second order nature of the coupling process.

Numerical solutions of the fourth order system yield transmission coefficients in excellent agreement with the second order theory, and also demonstrate that the electric field variation across the mode conversion region is well approximated, via the above transformation, by our second order theory.

ACKNOWLEDGEMENTS

I would like to thank my supervisor, Dr Alan Cairns of the Applied Mathematics Department, for his help and encouragement throughout this work.

I would also like to thank Dr C N Lashmore-Davies of Culham Laboratory for monitoring this project.

I wish to thank Miss Shiela Wilson for typing this thesis so expertly.

I am grateful to the Science and Engineering Research Council and Culham Laboratory for financial support.

CERTIFICATE

I certify that Anna M Woods has satisfied the conditions of the Ordinance and Regulations and is thus qualified to submit the accompanying application for the degree of Doctor of Philosophy.

POSTGRADUATE CAREER

I was admitted into the University of St Andrews as a research student under Ordinance General No. 12 in October 1982 to work on the theory of radio frequency heating under the supervision of Dr R A Cairns. I was admitted under the above resolution as a candidate for the degree of Ph.D. in October 1983.

DECLARATION

I declare that the following thesis is a record of research work carried out by me, that the thesis is my own composition, and that it has not been previously submitted in application for a higher degree.

This thesis is dedicated to my parents.

CONTENTS

	<u>Page</u>
Ch. 1 INTRODUCTION	1
1.1 Radio Frequency Heating in Tokamak Plasmas	1
1.2 Linear Mode Conversion	8
1.3 Full Wave Calculations	12
1.4 Second Order Theories	15
1.5 Outline of the Thesis	20
 Ch. 2 THE HYBRID RESONANCES IN A COLD PLASMA	 22
2.1 The C.L-D. mode conversion model	22
Applications:	26
2.2 The upper hybrid resonance	26
2.3 The two-ion hybrid resonance	29
 Ch. 3 MODE CONVERSION BETWEEN FAST AND SLOW LOWER HYBRID WAVES	 35
3.1 Accessibility of slow waves to the lower hybrid resonance	35
3.2 Dispersion curves in the ω - k_{\perp} plane	39
3.3 Construction of model Weber equation	40
3.4 The result for a plasma with a linear density profile	47
3.5 Inclusion of a magnetic field gradient in the calculation	49
3.6 Mode conversion at low plasma densities	52

Ch. 4	DERIVATION OF SECOND ORDER THEORY FROM EXACT FOURTH ORDER EQUATIONS	56
4.1	The cold-plasma wave equation	56
4.2	Heading's transformation	58
4.3	Application and extension of Heading's transformation	65
4.4	Conservation of energy	68
4.5	Properties of the transformed system	72
4.6	Approximate expressions for the electromagnetic fields	78
 Ch. 5	 SOME NUMERICAL COMPARISONS	 81
5.1	Transmission coefficients	81
5.2	Electric field variation in the mode coupling region	84
	 CONCLUSIONS	 90
	APPENDIX	93
	REFERENCES	111

CHAPTER 1

INTRODUCTION

1.1 Radio Frequency heating in tokamak plasmas

A tokamak is a toroidal device for the production, confinement and heating of plasma. The magnetic field required for stable confinement has two components: a toroidal field, which is provided by external coils, and a much weaker poloidal field, which is generated by a toroidal electrical current flowing in the plasma. This current is induced by the action of a transformer and heats the plasma by ohmic dissipation. On the JET tokamak, 3MA current pulses lasting several seconds have produced electron temperatures of 1-3 keV (Bickerton, 1984). However, ohmic heating is less efficient at high temperatures due to the $T^{-3/2}$ dependence of the plasma resistivity and the fact that the current in a given device is limited by gross stability considerations. Since the threshold temperature above which fusion reactions can self-heat a deuterium-tritium plasma is $\gtrsim 10$ keV, some form of auxiliary heating is necessary.

In radio frequency (R.F.) heating schemes, (Fielding, 1981), energy is carried into the plasma by electromagnetic waves. Once in the plasma, the waves propagate, without loss, to a localised region where they are absorbed by one of several mechanisms, thus transferring their energy to the particles. All R.F. schemes consist of the same general layout which offers several desirable features; namely, an efficient high power generator remote from the plasma, a

low loss transmission line and an efficient antenna which couples the electromagnetic energy to the plasma. A further advantage of such schemes is that the location of the absorption zone is externally controllable.

The flexibility of R.F. heating lies in the variety of wave modes which can exist in a hot, magnetised plasma. Waves with phase velocities well above particle thermal velocities are adequately described by the cold plasma approximation (Boyd and Sanderson, 1969; Cairns, 1985) in which the plasma pressure is zero and linearised fluid equations are coupled to Maxwell's equations via the Lorentz force. However, for certain values of plasma parameters the refractive index of one of the two fundamental electromagnetic modes becomes infinite. In the vicinity of these cold plasma resonances, the wave phase velocity drops to thermal levels and strong interaction between wave and particles can occur. A fuller kinetic description invoking the Vlasov-Maxwell equations (Stix, 1962; Clemmow and Dougherty, 1969) resolves the refractive index infinities into short wavelength propagating modes and also reveals a plethora of new waves which propagate close to the ion and electron cyclotron frequencies ($\Omega_{i,e}$) and their harmonics. Moreover, the kinetic theory predicts collisionless damping of waves as a direct result of their interaction with the particles. This damping is governed by the resonance condition

$$\omega - k_{\parallel} v_{\parallel s} - n\Omega_s = 0; \quad n = 0, 1, 2, \dots \quad (1.1)$$

where ω is the wave frequency, k_{\parallel} the wave vector component along the equilibrium magnetic field direction and $v_{\parallel s}$, Ω_s are the parallel

streaming velocity and cyclotron frequency respectively, of particle species s . In (1.1), $n=0$ corresponds to Landau damping (Chen, 1984) which is important for waves with nonzero E_{\parallel} propagating obliquely to the magnetic field. Energy is transferred to the parallel degrees of freedom by the E_{\parallel} of the wave. On the other hand, $n \neq 0$ corresponds to cyclotron damping (Stix 1962). In this case, the left or right circularly polarised electric field component of the wave resonantly drives the perpendicular motion of the particles thereby increasing their perpendicular energy. The phenomena of Landau and cyclotron damping underpin any R.F. heating scheme since they provide the mechanisms by which energy can be absorbed from an incident waves.

The four principle R.F. heating schemes are, in order of increasing frequency, Alfvén wave heating, the ion cyclotron frequency range, (ICRF), lower hybrid resonance heating (LHRH) and electron cyclotron resonance heating (ECRH). Alfvén wave heating, at frequencies of a few MHz, involves two main mechanisms. The first is excitation of a localised Alfvén wave at a point where the local Alfvén velocity v_A is related to the frequency and parallel (to the magnetic field) wavenumber of the incident wave by $\omega = k_{\parallel} v_A$. The group velocity of the Alfvén wave is along the field so energy cannot propagate away across the field lines. The result is that the wave is resonantly excited and energy is fed into the plasma by its damping. At somewhat lower frequencies it is possible to excite so-called "global modes" which are eigenmodes of the toroidal system. A review of the theory has recently been given by Appert et al (1986) and of experimental results by Behn et al (1984).

ICRF (Swanson, 1985b) utilises frequencies of 25-100 MHz. Corresponding vacuum wavelengths are of the order of several metres, requiring the launch antenna to be wrapped around the poloidal

circumference of the torus. The fast magnetosonic wave, which is used to transport energy to the absorption region, is evanescent at the plasma edge. Consequently the antenna needs to be a few centimetres from the cutoff density for efficient coupling. In a single species plasma, the fast wave is strongly absorbed at the hot plasma second harmonic ($\omega \approx 2\Omega_1$) resonance by ion cyclotron damping. However, if two ion species (1 and 2, with $\Omega_1 > \Omega_2$) are present, then a cold plasma resonance also occurs at the two-ion hybrid frequency given by $\omega_{ii}^2 = (\omega_{p1}^2 \Omega_1^2 + \omega_{p2}^2 \Omega_2^2) / (\omega_{p1}^2 + \omega_{p2}^2)$, where $\Omega_1 > \omega_{ii} > \Omega_2$. On the high field side of this resonance, the fast wave connects smoothly onto the quasi-electrostatic ion Bernstein wave (Swanson, 1976). A fraction of the incident fast wave energy is transformed to slow waves by mode conversion. This process is inherent to all R.F. schemes and will be discussed in detail later. If ω_{ii} is well separated from Ω_1, Ω_2 , then the Bernstein waves can heat the electrons by Landau damping; but if the lighter species 1 is present in small concentration, $\omega_{ii} \approx \Omega_1$ and the Bernstein waves couple directly to the minority ions via cyclotron damping. Second harmonic and minority species heating have achieved significant ion temperatures on PLT (Hosea et al, 1982) and TFR (Equipe TFR, 1982). Recently, the possibility of heating at the third ion-cyclotron harmonic ($\omega = 3\Omega_1$) of deuterium has received some theoretical attention (Swanson, 1985a). This resonance is still strongly absorbing and the plasma core is accessible. Also, the higher wave frequencies involved make wave-guide launching an attractive feature of this scheme.

LHRH uses waves in the frequency range 1-10 GHz. At 3 GHz, the vacuum wavelength is 0.1m, thus allowing the energy to be launched by

means of waveguides. Another advantage of the scheme is that efficient, megawatt power sources are already available for these frequencies, so, unlike ECRH, little extra source development is required. The slow wave, which in the cold plasma approximation has a resonance at the lower hybrid frequency $\omega_{LH} = \omega_{pi} / (1 + \omega_{pe}^2 / \Omega_e^2)^{1/2}$, is used for heating. Propagation towards the centre of the plasma is only possible for waves with $n_{||} (= k_{||}c/\omega) > 1$. These waves are then evanescent at the plasma edge, but in practice the width of the evanescent layer $\ll c/\omega$ so that coupling is efficient. In fact, there will be a second region of evanescence between the plasma edge and the resonance unless the waves are launched with $n_{||}^2 > 1 + (\omega_{pe}^2 / \Omega_e^2)_{res}$, where res indicates quantities to be evaluated at the resonance. Accessibility of slow waves to the LHR layer is discussed in detail in Chapter 3. A "grill" antenna, which consists of an array of waveguides with a definite phase relation between adjacent elements, excites the required $n_{||}$ spectrum. The cold plasma slow wave is mode converted in the vicinity of the LHR layer to an ion Bernstein wave (Stix, 1965), which is then strongly absorbed as it crosses high ion cyclotron harmonics. Alternatively, $n_{||}$ can be chosen so that the slow wave Landau damps on the electrons before the mode conversion layer is reached (Brambilla, 1978). LHRH has achieved significant temperatures on, for example, PLT (Stevens et al, 1982) and ALCATOR C (Porkolab et al, 1984).

ECRH (Manheimer, 1979; Bornatici, 1983) is the simplest of the R.F. heating methods and will use waves in the frequency range 30-150 GHz. The main drawback to ECRH has so far lain with the

development of suitable high-power microwave sources (gyrotrons). However, gyrotrons in the lower half of the frequency range are now becoming available (Jory, 1984). In contrast to ICRH and LHRH there is no evanescent region between the vacuum and the absorption zone. As a result, power can be fed in by a small aperture waveguide which is retracted from the plasma. At these high frequencies, only electrons are heated directly. The electrons will then heat the ions by collisions. Both of the cold plasma waves penetrate to reasonable plasma densities and so can be used for heating. For propagation perpendicular to the equilibrium magnetic field (B_0), the extraordinary (X) mode is elliptically polarised with $E_{\perp} B_0$ and the ordinary (O) mode is linearly polarised with $E_{\parallel} B_0$. Density limitations on propagation, and therefore heating, are imposed by the existence of cutoffs at $\omega_{pe}^2 = \omega^2$ for the O mode, and $\omega_{pe}^2 = \omega(\omega \pm \Omega_e)$ for the X mode. The X mode has a cold plasma resonance at the upper hybrid frequency $\omega_{UH} = (\omega_{pe}^2 + \Omega_e^2)^{\frac{1}{2}}$, whereas the O mode, being independent of B_0 , does not possess such a resonance. However, both waves are found to have hot plasma resonances at $\omega = n\Omega_e$, ($n = 1, 2, \dots$). As usual, these resonances have a mode conversion interpretation (Cairns and Lashmore-Davies, 1982, 1983). In the vicinity of the upper hybrid or second harmonic resonance the X mode is converted to a Bernstein wave which will be cyclotron damped for nonzero k_{\parallel} , while the fundamental ($\omega = \Omega_e$) O and X mode resonances can be understood in terms of conversion to cyclotron harmonic waves which appear (Akhiezer et al, 1975) when second (or higher) order Larmor radius terms are included in the dispersion relation. It is noted that the propagation and

absorption of electron cyclotron waves may be profoundly affected, even in low temperature plasmas, by the velocity-dependent relativistic correction to the electron mass (Shkarofsky, 1966 a,b; Fidone et al, 1978, 1982). This makes the resonance condition (1.1) velocity-dependent even for exactly perpendicular propagation, resulting in wave damping where none existed before. The main scenarios for heating use the X mode at $\omega \approx 2\Omega_e$ or the O mode at $\omega \approx \Omega_e$, both waves being launched from the outside of the torus. Like ICRH, ECRH has the considerable advantage that the absorption region is controlled by matching the wave frequency to the gyro-frequency. The experimental programme on T-10 (Parail and Alikae, 1984) uses a bank of 4-6 gyrotrons at 84 GHz with a total power output of up to 1 MW. X mode ($\omega \approx 2\Omega_e$) and O mode ($\omega \approx \Omega_e$) heating have raised electron temperatures by 0.5 - 2 keV.

R.F. waves have one further, very interesting application: they can generate continuous toroidal electric currents which will sustain the poloidal magnetic field required for tokamak stability. This offers the possibility of steady-state tokamak operation without need of an ohmic heating transformer. Fisch (1978) proposed a scheme in which lower hybrid waves are launched unidirectionally around the torus. The waves resonantly drive superthermal electrons travelling in that direction by Landau damping. In this way a net toroidal current is produced. Recent results from PLT (Jobes et al, 1985) show significant current ramping when R.F. lower hybrid waves are applied. A basically different method (Fisch and Boozer, 1980) relies upon altering the collisionality of the plasma. The idea is

to preferentially heat electrons travelling in one direction, to the right, say. The right-moving electrons, being hotter, collide less frequently with the ions than do their left-moving counterparts. This results in a net motion of electrons to the right, and ions to the left, i.e. a current. This mechanism applies to electron cyclotron waves, which give energy to the perpendicular, rather than the parallel, motion of the electron. Electron cyclotron waves have driven currents of about 20 mA per Watt on the TOSCA (Robinson et al, 1982) experiment at Culham Laboratory.

1.2 Linear Mode Conversion

In wave propagation studies, the simplest examinable case is that of the infinite homogeneous medium. We look for small amplitude plane wave solutions of the form $\underline{A}_0 \exp(i\mathbf{k} \cdot \underline{x} - i\omega t)$, where \underline{A}_0 is a constant vector, and Fourier analyse the linearised governing equations to obtain a dispersion relation, $D(\omega, \mathbf{k}) = 0$, which determines the allowed modes of the system. These waves propagate independently throughout space. Suppose now that the medium is spatially varying on a length scale much greater than the wavelength. Intuitively we expect the solutions in a slowly varying medium to behave locally like the plane waves of the homogeneous case. For waves of a given frequency ω_0 , the wavenumber will evolve in space so as to satisfy at each point the dispersion relation

$$D(\omega_0, \mathbf{k}; \underline{x}) = 0, \quad (1.2)$$

whose parameters are now slowly varying functions of \underline{x} . This idea

forms the basis of the geometrical optics, or WKBJ, approximation, which can be applied to the Maxwell-linearised kinetic equations in the study of electromagnetic wave propagation in nonuniform plasmas (Bernstein and Friedland, 1983). However, for simplicity and in order to appreciate the limitations of the approximation, we consider a one-dimensional wave equation

$$\frac{\partial^2 u}{\partial x^2} = \frac{1}{c^2(x)} \frac{\partial^2 u}{\partial t^2},$$

where the wave speed c is allowed to vary in space. We factor out the time dependence by writing $u(x,t) = \varphi(x)\exp(i\omega t)$ and obtain an O.D.E.,

$$\frac{d^2 \varphi}{dx^2} + k^2(x)\varphi = 0; \quad k = \frac{\omega}{c}. \quad (1.3)$$

The solutions of (1.3) for constant k suggest trial solutions of the form $A_0 \exp\left(\pm i \int_0^x k(x')dx'\right)$, which, when substituted into (1.3) leaves a remainder term $\pm i dk/dx A_0$. The guess is then a reasonable one provided $|dk/dx| \ll k^2$, i.e. if $1/k |d(\ln c)/dx| \ll 1$, which recovers our original assumption that the fractional change in the parameter c over a local wavelength is much less than unity.

A better approximation to the solutions of (1.3) allows an amplitude as well as a phase variation. Taking

$$\varphi = A(x) \exp\left(\pm i \int_0^x k(x')dx'\right)$$

in (1.3) we obtain the exact relation

$$2kA' + k'A \mp iA'' = 0. \quad (1.4)$$

If the A'' term is neglected, $A \propto |k|^{-\frac{1}{2}}$, leading to the so-called

WKBJ approximate solutions

$$\varphi_{\pm} \propto |k|^{-\frac{1}{2}} \exp \left(\pm i \int_0^x k(x') dx' \right). \quad (1.5)$$

The fractional error involved in this procedure is then of order $k'/k^2 \propto 1/k \, d(\ln A)/dx$, where we have dropped a k'' term. Clearly the solutions (1.5) fail completely at a 'turning point' where $k=0$. In the neighbourhood of a cutoff, the wavelength becomes large compared with the scale length of the nonuniformities so that the original assumption underlying the method is violated. The other circumstance in which the WKBJ approximation breaks down is when the local wavelength is exceeded by its own gradient scale length. If $|k'/k^2| \gtrsim 1$, then the amplitude A varies rapidly indicating that the neglect of A'' compared with the other terms in (1.4) is no longer valid. This happens near a wave resonance as $k \rightarrow \infty$. Such behaviour can also occur at finite k , in regions where k' becomes large. These are precisely the regions where the mapping $k(x)$, as determined by (1.2), has a branch point so that, typically, two of the roots of the dispersion relation are almost coincident. Outside of such regions the two modes propagate independently and are described by the WKBJ approximation. Inside, however, the two modes have almost identical characteristics resulting in a 'mode conversion' process in which energy incident in one mode emerges from the region partitioned between the two modes. This process, which has no analogy in homogeneous media, is being extensively investigated in many areas of physics, including plasma physics (Zheleznyakov et al, 1983).

Mode conversion is a physical consequence of the mathematical fact that the WKBJ solutions φ_{\pm} cannot be continued analytically

through a turning point. The reason for this is that they are leading terms in asymptotic, not convergent, expansions. While φ_+ and φ_- are the leading terms of some pair of solutions of (1.3) sufficiently far on either side of a turning point, φ_+ , say, alone does not constitute the leading term of a continuous solution of (1.3) on both sides of a turning point simultaneously. This is the so-called Stokes phenomenon (see, for example, Heading, 1962). A continuous solution $\varphi(x)$ of the O.D.E. (1.3) is always expressible as the product of a convergent series with a factor incorporating the behaviour at a branch point or singularity. Any different expansion cannot hope to represent this function everywhere except by periodic changes in form. Thus the constant coefficients of the linear combination of φ_{\pm} which represents $\varphi(x)$ change abruptly as certain lines, Stokes lines, emanating in the complex plane from a turning point, are crossed. The occurrence of discontinuities in the representation of a continuous function is no contradiction when we realise that asymptotic series contain inherent errors, and that the discontinuities are always smaller in magnitude than these errors. Heading (1962) set down rules for tracing the asymptotic representation of the general solution of (1.3) across Stokes lines. These connection formulae, when the appropriate boundary condition is applied, tell us what fraction of the incident power flux is distributed in each mode after passing through the mode conversion, i.e turning point, region.

1.3 Full Wave Calculations

As we have seen, linear mode conversion is of particular relevance to R.F. heating since the efficiency of any heating scheme is determined by the fraction of incident electromagnetic energy that can be converted to a plasma wave which in turn is susceptible to a collisionless damping process. To date, many attempts at extracting mode coupling equations from the Vlasov-Maxwell equations have taken as their starting point the solutions for the homogeneous plasma. The method consists firstly of approximating the local dispersion relation by a polynomial in k^2 , usually a quadratic, where k is the wavenumber in the direction of the inhomogeneity. This is then associated with a differential equation via the identification $k \rightarrow -id/dx$. If the spatial variation of plasma parameters is linear in x , then the resulting fourth or higher order differential equation has coefficients which are linear in x . Such equations are amenable to treatment by Laplace transform theory (Smith, 1966), leading to a first order equation for the transform of the dependent variable. This is easily integrated to obtain the general solution of the original O.D.E. in the form of a contour integral. Different choices of contour produce different solutions, each valid for all complex z , where $x = \text{Re}(z)$. A set of contours can be found which represent the linearly independent solutions of the O.D.E. Connection formulae, and hence transmission, conversion and reflection coefficients, are obtained by evaluating the contour integrals in the two limits of large $\pm|z|$. These integrals can be done using the method of steepest descents (Murray, 1974). Application of the integral transform

technique to typical fourth order mode conversion equations is described in detail by Stix and Swanson (1983). The method was successfully used first by Stix (1965) to study mode conversion between the cold plasma electromagnetic wave and a warm ion or electron plasma wave in the vicinity of the lower or upper hybrid resonant layer respectively. Since then, the approach has been adopted by several authors including Fidone and Paris (1974) who examined lower hybrid wave conversion for a parabolic density profile. Swanson (1976) investigated mode coupling between the fast magnetosonic wave propagating perpendicularly to the magnetic field ($k_{\parallel} = 0$) and the ion Bernstein wave near the two-ion hybrid resonance. Ngan and Swanson (1977) considered mode coupling between the fast wave and the ion Bernstein wave at the second ion cyclotron harmonic ($\omega = 2\Omega_i$), again for the case of perpendicular propagation. Gambier and Schmitt (1983) presented an algorithm for calculating the connection formulae between the sets of propagating fast and slow wave solutions of a general n th order homogeneous O.D.E. whose coefficients are linear in x .

A variant of the integral transform method was developed by Swanson (1978, 1980) in order to study the effects of localised absorption on the mode conversion process at the second ion cyclotron harmonic. For propagation at nonzero k_{\parallel} , the Bernstein modes are strongly damped in the resonance region, and so there is competition between absorption and the conversion of fast wave energy to the Bernstein mode. The method of attack on these problems has been reviewed by Stix and Swanson (1983) and Swanson (1985b), so we outline it only briefly here. To include absorption effects, the plasma dispersion function, Z , which appears in the dispersion

relation must be retained in its general form. However, attempts at solving the associated fourth order O.D.E., which has the Z function on its coefficients, by direct numerical integration fail due to the presence of exponentially growing solutions. The idea then is to separate out the asymptotic from locally important terms of the O.D.E. by keeping the asymptotic form of the Z function terms on the l.h.s., while putting the difference of the asymptotic and general form of the Z function terms on the r.h.s. The r.h.s., which is zero far from the mode conversion region, is then treated as a source term, making the equation inhomogeneous. The next step is to construct a Green's function for the homogeneous fourth order O.D.E. given by l.h.s. $\equiv 0$. This requires knowledge of the solutions of the adjoint homogeneous equation. The end result is that the original O.D.E. is expressed as an integralequation involving the Green's function and the source term. This formulation is not subject to the previously encountered numerical instabilities, and can be solved by iteration, starting with solutions of the homogeneous O.D.E. as guess functions. The Green's function method has recently been applied to a sixth order O.D.E. (Swanson, 1985a) in a study of wave absorption at the third ion cyclotron harmonic. Also, the algorithm of Gambier and Schmitt (1983) has been extended (Gambier and Swanson, 1985) to calculate a complete set of solutions for the n th order equation, thus allowing construction of the Green's function and, therefore, treatment of localised source problems.

1.4 Second Order Theories

The method of associating an O.D.E. with the uniform warm plasma dispersion relation by taking a Fourier transform in the direction of variation has its limitations. The first is a technical one in that solving fourth or higher order model equations is, as we have seen, a complicated task. Much more serious is the fact that such equations are always ambiguous since there is no a priori prescription to determine whether terms such as $f(x)k$ in the dispersion relation will correspond to $-id/dx (f\phi)$, $-if d\phi/dx$ or some linear combination of both. The most severe restriction to the technique is that the Vlasov-Maxwell equations constitute a set of integro-differential equations and the uniform dispersion relation contains the transcendental plasma dispersion function which has $k_{||}$ as one of its arguments. Consequently, in cases where the variation is along the magnetic field direction we are not even able to approximate the dispersion relation by a polynomial in $k_{||}$, let alone make the translation to a differential equation form.

Recently, there have been attempts to simplify and generalise the theory of linear mode conversion. These have arisen from the suggestion that since, despite the multitude and complexity of possible modes in plasmas, in most cases, coupling involves only two waves at a time, the process might be described by a second order O.D.E. for the wave amplitude. A method has been developed by Fuchs et al (1981, 1985) for extracting pairwise coupling events "embedded" in general dispersion relations. Very briefly, the method focusses on the properties of the dispersion relation in the vicinity of the

branch and saddle points of the complex mapping of the spatial variable $x = \text{Re}(z)$ onto the complex wavenumber plane k , as determined by the dispersion relation

$$D(k, z; \omega) = 0. \quad (1.6)$$

In addition to the branches $k = f(z)$ of (1.6), important contours in the k plane are those on which the function $\partial D / \partial k$ vanishes. The mapping

$$D_k \equiv \frac{\partial D}{\partial k} = 0 \Leftrightarrow k = k_c(z) \quad (1.7)$$

defines contours on which the wave group velocity must vanish since

$$\frac{\partial \omega}{\partial k} = - \frac{\partial D / \partial k}{\partial D / \partial \omega}.$$

The branch points, z_b , of the mapping $k = f(z)$ are those for which df/dz diverges, and they are by definition, the only ones which map onto a single point k_s in the k plane, where k_s is the saddle point of the inverse mapping $z = f^{-1}(k)$. The branch and saddle points, z_b and k_s , of (1.6) are also solutions of (1.7) since

$$\frac{dk}{dz} = - \frac{\partial D / \partial z}{\partial D / \partial k},$$

and they are therefore the points at which the branches will couple. Also, the points (z_b, k_s) are the only common points of the branches $k = f(z)$ with the contours $k_c(z)$, and so the $k_c(z)$ can be taken as branch cuts. The dispersion relation is then expanded around $k = k_c(z)$ to second order in k yielding the embedded dispersion relation

$$D(k_c) + \frac{1}{2}(k - k_c)^2 D_{kk}(k_c) = 0. \quad (1.8)$$

In order to obtain transmission and conversion coefficients, a second order O.D.E. is attributed to (1.8). This can be done unambiguously by requiring that the turning points of the equation coincide with the branch points of the dispersion relation (1.8).

The O.D.E. must then be of the form

$$\frac{d^2 Y}{dz^2} + Q(z)Y = 0 \quad (1.9)$$

where the coupling potential Q is

$$Q = - \frac{2D(k_c)}{D_{kk}(k_c)}$$

Q vanishes when $z = z_b$ since $k_c(z_b) = k_s$, and the branch and saddle points satisfy the dispersion relation. Moreover, the wave amplitude

$$\Phi = Y \exp \left(- i \int k_c dz \right)$$

satisfies the equation

$$D \left(-i \frac{d}{dz}, z \right) \Phi = 0.$$

Hence (1.9) is the required representation. The transmission coefficients for any given Q will also depend on the boundary condition for the transmitted wave (Fuchs et al, 1985). This method claims for its advantages that it is neither restricted to dispersion relations which are polynomials in the wavenumber k , nor to plasma gradients which are linear in the spatial variable x .

A different approach was adopted by Cairns and Lashmore-Davies (C.L-D.) (1983) who assumed that a certain class of coupling events is more naturally described by a pair of coupled first order equations. They considered a local dispersion relation of the form

$$(\omega - \omega_1)(\omega - \omega_2) = \eta \quad (1.10)$$

where $\omega_{1,2}(k, x)$ are smooth differentiable functions of k and x , and η is a small positive quantity. It is instructive here to refer forward to Fig. 2.1 in Section 2.1 which shows the typical shape of the model ω - k dispersion curves given by (1.10). At points A or B on the diagram, the two uncoupled modes ω_1 and ω_2 , which are represented by the dotted lines, cross. The presence of the small parameter η leads to the characteristic shape of the dispersion curves in the neighbourhood of a mode crossing point A as shown. If a wave at fixed frequency ω_0 propagates through the inhomogeneous plasma, then coupling takes place in the vicinity of a point x_0 at which the wavenumbers $k_1(\omega_0, x)$ and $k_2(\omega_0, x)$ of the uncoupled modes have a common value k_0 . The dispersion relation (1.10) is then expanded about the point (k_0, x_0) writing

$$k = k_0 + \delta, \quad x = x_0 + \xi.$$

We have, to first order in the Taylor expansion,

$$\omega_1 = \omega_0 + a\delta + b\xi, \quad \omega_2 = \omega_0 + f\delta + g\xi$$

where a , b , f and g are the appropriate partial derivatives of ω_1 and ω_2 evaluated at the point (k_0, x_0) . Then around x_0 , k is given as a function of position by

$$(ak - ak_0 + b\xi)(fk - fk_0 + g\xi) = \eta_0 \quad (1.11)$$

where $\eta_0 = \eta(k_0, x_0)$.

In order to calculate transmission/conversion coefficients, (1.11) must be associated with a differential equation. The fact

that we are dealing with two modes which de-couple as $\eta_0 \rightarrow 0$ in (1.11) suggests introducing two wave amplitudes φ_1 and φ_2 instead of just one. Coupling between the two waves φ_1 and φ_2 is then described in a symmetric way by the pair of first order O.D.E's

$$\left. \begin{aligned} \frac{d\varphi_1}{d\xi} - i \left(k_0 - \frac{b}{a} \xi \right) \varphi_1 &= i\lambda \varphi_2 \\ \frac{d\varphi_2}{d\xi} - i \left(k_0 - \frac{g}{f} \xi \right) \varphi_2 &= i\lambda \varphi_1 \end{aligned} \right\} \quad (1.12)$$

where $\lambda = (\eta_0/af)^{\frac{1}{2}}$.

For the case where both waves have positive group velocities, i.e. $a, f > 0$, it is seen from (1.12) that

$$\frac{d}{d\xi} (|\varphi_1|^2 + |\varphi_2|^2) = 0. \quad (1.13)$$

The case where one wave is backward propagating is also treated by C.L-D. (1983). Thus, if the wave amplitudes are regarded as being normalised in such a way that $|\varphi_i|^2$, $i = 1, 2$, are the energy fluxes, we have energy conservation. Equations (1.12) are then combined to form Weber's equation from whose asymptotic solutions we obtain the transmission coefficient T . This gives the fraction of incident energy which is transmitted on the same mode as

$$T = \exp \left(- \frac{2\pi\eta_0}{|ag - bf|} \right) \quad (1.14)$$

while the fraction converted into the other mode is $1-T$. The C.L-D. method is easy to apply since in practice it involves elementary algebraic manipulations of the local dispersion relation to put it in the form (1.11), from which the parameters a , b , g , f and η_0 are then identified. However, the method is limited to dispersion

relations which are polynomials in k , and linear variations in plasma parameters. Both the C.L-D. and Fuchs et al approaches have been shown to reproduce results obtained by sophisticated mathematical treatments of higher order differential equations. The relative merits of the two methods are assessed in a joint study (Lashmore-Davies, Cairns and Fuchs, 1985) of a mode conversion between the fast and slow ion-cyclotron waves in a plasma with a longitudinally inhomogeneous equilibrium magnetic field.

So far, second order theories are able to extract in a simple way the same asymptotic connection formulae which have previously been derived from higher order O.D.E's. However, since the starting point for these theories is a reduced dispersion relation, it is not clear whether and how the amplitudes appearing in the second order equations are related to the physical electric field amplitudes in the mode conversion region. In this thesis, we examine a mode conversion between the two cold plasma electromagnetic waves for which the exact governing equation is a fourth order O.D.E. It will be shown for this problem that the field amplitudes in the mode conversion can be obtained from the solutions of a second order equation, thus providing an extension to the previous theory.

1.5 Outline of the Thesis

Firstly, in Chapter 2, we examine the cold plasma hybrid resonances and show that these have a mode conversion interpretation in the framework of the C.L-D. model. The remainder of the work

is concerned with a mode conversion between the fast and slow cold plasma waves in the lower hybrid frequency range. In Chapter 3 we show that this phenomenon determines the accessibility of the slow wave to the lower hybrid resonance. A second order approximation to the dispersion relation in the coupling region is associated with a second order O.D.E., Weber's equation, from which transmission and conversion coefficients are then obtained in various cases. The effect of including a magnetic field gradient in the calculation is also considered.

Next, in Chapter 4, we write down the exact fourth order system of O.D.E's for the problem, and use a linear transformation, which is an extension of that given by Heading (1961), to extract a second order O.D.E. describing the coupling process. Approximate expressions for the electromagnetic fields are then given, via our transformation, in terms of amplitudes associated with the second order equation.

Finally, in Chapter 5, we compare transmission coefficients obtained from numerical integration of the exact fourth-order system with those obtained from our second order theory of Chapter 3. Also, the approximate expressions for the electromagnetic fields, given in Chapter 4, are compared across the mode conversion region with the exact field solutions of the fourth order equations.

CHAPTER 2

THE HYBRID RESONANCES IN A COLD PLASMA

2.1 The C.L-D. mode conversion model

In this chapter, the mode coupling theory of Cairns and Lashmore-Davies (1983) is used to examine the transmission properties of cutoff-resonance doublets. These exist in layers of plasma where the incident wave frequency ω becomes equal to one of the hybrid frequencies, ω_h , defined by setting ϵ_1 equal to zero. For certain values of plasma parameters, the cutoff and resonance points may be closely spaced in which case significant transfer of wave energy through the evanescent layer is expected.

Consider two independently propagating disturbances described by

$$v_{gj} \frac{d\phi_j}{dx} + ia_j(x)\phi_j = 0; \quad j = 1, 2 \quad (2.1)$$

where v_{gj} is the group velocity of mode ϕ_j and functions $a_j(x)$ are determined by plasma inhomogeneity. C.L-D. have used the model equations

$$\begin{aligned} v_{g1} \frac{d\phi_1}{dx} + ia_1(x)\phi_1 &= i(\eta)^{\frac{1}{2}}\phi_2 \\ v_{g2} \frac{d\phi_2}{dx} + ia_2(x)\phi_2 &= i(\eta)^{\frac{1}{2}}\phi_1 \end{aligned} \quad (2.2)$$

to describe propagation in regions where ϕ_1 and ϕ_2 are coupled. The local dispersion relation associated with (2.2) is

$$(v_{g_1} k + a_1(x))(v_{g_2} k + a_2(x)) = \eta \quad (2.3)$$

where the left hand brackets refer to the dispersion of the two independent propagators (2.1). Note that C.L-D.'s analysis of (2.2) pertains to functions $a_j(x)$ which are linear in x . In practice, the C.L-D. method consists firstly of identifying the asymptotic dispersion of the two propagating modes. One must then factor the dispersion relation (usually a biquadratic in k) in the form (2.3) to extract the appropriate coefficients. However, if mode 1, say, is asymptotically resonant, then the task of factorisation is particularly simple because in this case (2.3) becomes

$$a_1(x)(v_{g_2} k + a_2(x)) = \eta \quad (2.4)$$

where $a_1(x)$ is yielded directly from the resonant terms of the original dispersion relation.

We will consider a geometry in which the magnetic field strength and (or) density vary in a direction perpendicular to the field so that $n_{||}$, the parallel refractive index along the field direction, is conserved, while the evolution of the perpendicular wavenumbers is given by the roots of the cold plasma dispersion relation

$$\epsilon_1 n_{\perp}^4 - [(\epsilon_1 + \epsilon_3)(\epsilon_1 - n_{||}^2) - \epsilon_2^2] n_{\perp}^2 + \epsilon_3((\epsilon_1 - n_{||}^2)^2 - \epsilon_2^2) = 0. \quad (2.5)$$

At points where ϵ_1 becomes zero, one of the roots of (2.5) has an infinity while the other remains finite. The general procedure

which we apply to these resonant mode problems is firstly to extract from (2.5) the resonant solution and note that it is of the form

$$k_{\perp}^2 \frac{c^2}{\omega^2} = \frac{A}{\omega^2 - \omega_h^2} . \quad (2.6)$$

We then write this as

$$(\omega^2 - \omega_h^2) k_{\perp}^2 c^2 / \omega^2 = A$$

where the left hand bracket represents the resonant (i.e. non-propagating) mode, and expand about the resonance to first order in x with

$$\omega^2 - \omega_h^2 = \lambda x, \quad A = A_0 + A_1 x$$

so that

$$\lambda x \left(k_{\perp}^2 - \frac{\omega^2 A_1}{c^2 \lambda} \right) = \frac{\omega^2}{c^2} A_0 . \quad (2.7)$$

The "mode conversion" point at which the two uncoupled solutions identified with the left hand brackets cross is given by

$$(k_{\perp}^2, x) = (k_0^2, 0); \quad k_0^2 = \frac{\omega^2 A_1}{c^2 \lambda}$$

Concentrating on the wave with positive k_{\perp} , we may write (2.7) in the vicinity of the crossover point as

$$x(k_{\perp} - k_0) = \frac{\omega^2 A_0}{2k_0 c^2 \lambda} . \quad (2.8)$$

Clearly (2.8) is a special case of the general form described in Chapter 1, and so we can use C.L-D's result to obtain the fraction of incident energy transmitted through the evanescent region between the resonance and cutoff points. This is

$$T = \exp\left(-\pi \frac{\omega^2 A_0}{c^2 k_0 \lambda}\right). \quad (2.9)$$

If the wave is incident from the transmission side of the cut-off, there will also be reflection. C.L-D. have given a simple justification, based on causality, for treating mode conversion which occurs between branches at a nonzero k_{\perp} separately from the reflection which may subsequently occur at a neighbouring cutoff. The argument says that a mode-converted wave cannot be reflected until it has first been excited by the incident wave. This allows us to trace the incident wave energy through all the accessible branches in the following manner. Consider Fig. 2.1 which shows typical dispersion curves for a wave resonant at $\omega = \omega_h$. Energy incident from the region $\omega/\omega_h > 1$ will firstly encounter the coupling region A where a fraction T is transmitted on the propagating branch, while the remainder $1-T$ proceeds to the cutoff C and is reflected there. All of the reflected energy then proceeds to the next coupling region B where a further fraction T is transmitted onto the resonant branch, so that the mode-converted energy is $T(1-T)$, while the fraction of energy converted to the backward propagating counterpart of the incident wave is $(1-T)^2$. Thus the reflection coefficient in this case is given by

$$R = (1-T)^2 \quad (2.10)$$

and the fraction of energy fed to the particles in the form of electrostatic oscillations at frequency $\omega = \omega_h$ is

$$A = T(1-T). \quad (2.11)$$

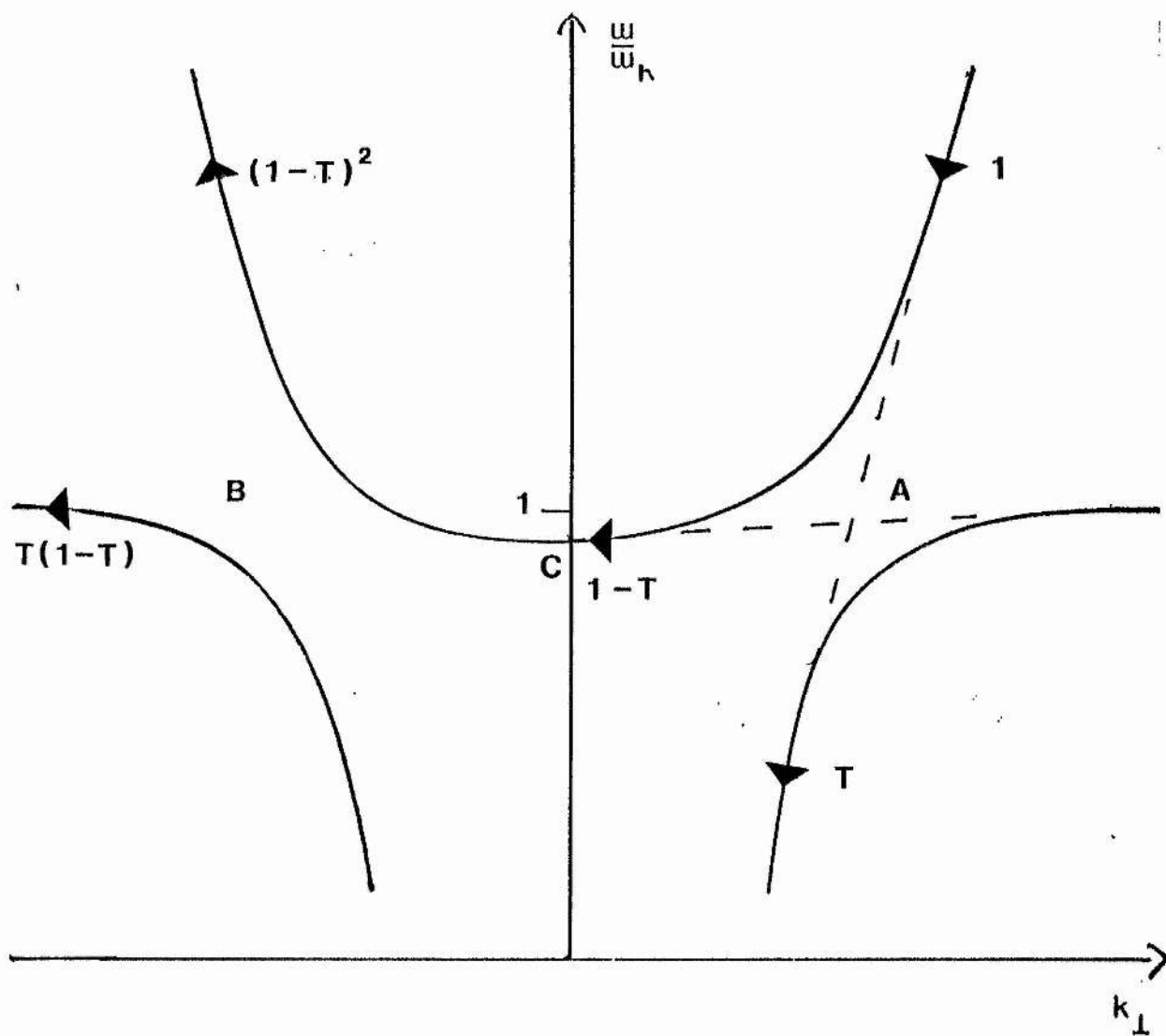


Figure 2.1 Typical dispersion curves for a wave which is resonant at a hybrid frequency ω_h .

Clearly A can never exceed 25%.

On the other hand, the cutoff C is not accessible to wave energy incident from the region $\omega/\omega_h < 1$, so for this case we have

$$R = 0 \quad \text{and} \quad A = 1 - T. \quad (2.12)$$

Note here that absorption can be total. Finally we remark that (2.9) and the arguments leading to (2.10), (2.11) and (2.12) predict the same transmission and reflection coefficients as would be obtained by treating the tunnelling problem in the usual way with Budden's equation (see Budden, 1961, p.476).

Applications:

2.2 The upper hybrid resonance

We consider an equilibrium in which the density is uniform and where the external magnetic field is given by

$$\underline{B} = B\hat{z}, \quad B = B_0 \left(1 + \frac{x}{R}\right).$$

In the simple case of perpendicular propagation, the dispersion relation for the X-mode is

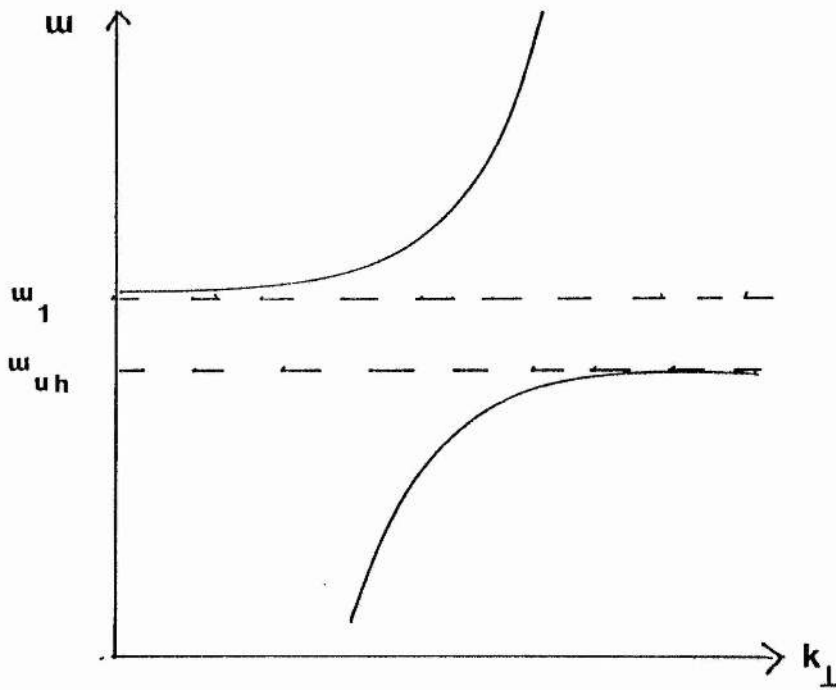
$$k_{\perp}^2 \frac{c^2}{\omega^2} = 1 - \frac{\omega_p^2}{\omega^2} \frac{(\omega^2 - \omega_p^2)}{(\omega^2 - \omega_p^2 - \Omega^2)} \quad (2.13)$$

where Ω , the electron cyclotron frequency, varies as

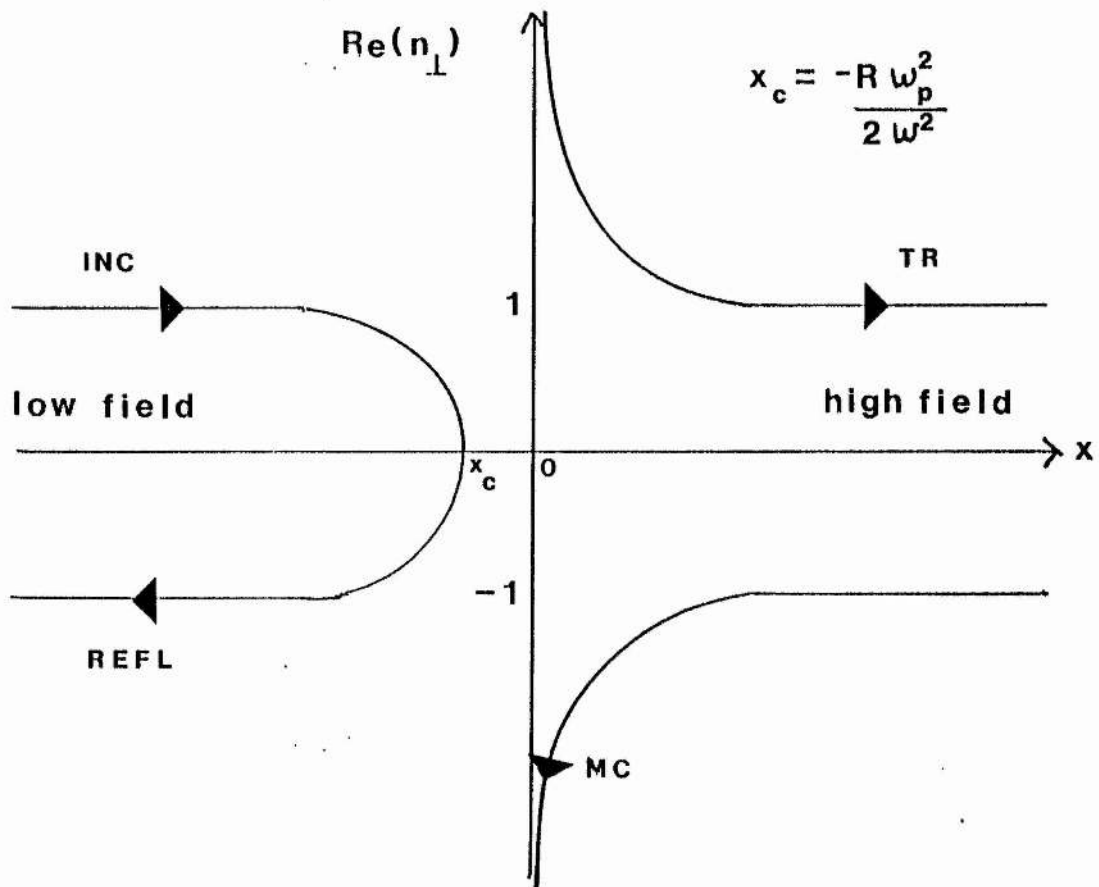
$$\Omega = \Omega_0 \left(1 + \frac{x}{R}\right) \quad \text{with} \quad \omega^2 = \omega_p^2 + \Omega_0^2.$$

The resulting dispersion curves are sketched in Fig. 2.2. If $\omega_p \ll \Omega$, then the upper hybrid frequency is close to the cutoff ω_1 and there

Figure 2.2



Dispersion curves for X-mode at perpendicular incidence where $\omega_{uh} = (\omega_p^2 + \Omega^2)^{\frac{1}{2}}$ and $\omega_1 = \frac{\Omega}{2} + \left(\frac{\Omega^2}{4} + \omega_p^2\right)^{\frac{1}{2}}$.



Real part of perpendicular refractive index as a function of distance from the resonance. Wave energy incident from the low field side is partially transmitted, reflected and mode-converted.

can be significant transmission through the evanescent layer.

Following the method of Section 2.1, we write (4.13) as

$$\begin{array}{ccc} (\omega^2 - \omega_p^2 - \Omega^2)(k_\perp^2 - \omega^2/c^2) = -\frac{\omega_p^2}{c^2}(\omega^2 - \omega_p^2) \\ \uparrow \qquad \qquad \qquad \uparrow \\ \text{resonant solution} \quad \text{vacuum solution} \end{array}$$

In the vicinity of the mode conversion point $(k_\perp, x) = (\omega/c, 0)$ this becomes

$$x(k_\perp - \omega/c) = R\omega_p^2/4c$$

and so, from (2.8) and (2.9), the transmission coefficient at perpendicular incidence is given by

$$T = \exp\left(-\frac{\pi R\omega_p^2}{2c(\omega_p^2 + \Omega_0^2)^{\frac{1}{2}}}\right). \quad (2.14)$$

Introducing a nonzero $n_{||}$ merely complicates the dispersion relation which is still of the general form (2.6). The resonant solution of (2.5) is given by

$$k_\perp^2 \frac{c^2}{\omega^2} = \frac{C + D}{\omega^2 - \omega_p^2 - \Omega^2}$$

where

$$\begin{aligned} C &= ((\epsilon_1 + \epsilon_3)(\epsilon_1 - n_{||}^2) - \epsilon_2^2) \frac{(\omega^2 - \Omega^2)}{2} \\ D &= [((\epsilon_1 - \epsilon_3)(\epsilon_1 - n_{||}^2) - \epsilon_2^2)^2 + 4\epsilon_3\epsilon_2^2n_{||}^2]^{\frac{1}{2}} \frac{(\omega^2 - \Omega^2)}{2} \end{aligned}$$

and

$$\epsilon_1 = 1 - \frac{\omega_p^2}{\omega^2 - \Omega^2}, \quad \epsilon_2 = -\frac{\omega_p^2\Omega}{\omega(\omega^2 - \Omega^2)}, \quad \epsilon_3 = 1 - \frac{\omega_p^2}{\omega^2}. \quad (2.15)$$

As usual, we write $\Omega^2 \approx \Omega_0^2 (1 + 2x/R)$ in (2.15), expanding C, D and $\omega^2 - \omega_p^2 - \Omega^2$ to $O(x)$. This gives

$$C \approx -\frac{\Omega_0^2}{2} \left(\frac{\omega_p^2}{\omega^2} (1 + n_n^2) + 2(1 - n_n^2) \left(1 + \frac{\Omega_0^2}{\omega^2} \right) \frac{x}{R} \right)$$

$$D \approx -\frac{\Omega_0^2}{2} \left(\frac{\omega_p^2}{\omega^2} (1 + n_n^2) + 2 \frac{\omega_p^2}{\omega^2} \frac{(1 + n_n^4)}{(1 + n_n^2)} \frac{x}{R} \right)$$

and
$$\omega^2 - \omega_p^2 - \Omega^2 \approx -2\Omega_0^2 \frac{x}{R} . \quad (2.16)$$

Substitution of (2.16) into (2.15) finally yields the standard dispersion relation in the vicinity of the conversion point $(k_0, 0)$,

$$x(k_{\perp} - k_0) = R \frac{\omega_p^2}{4k_0 c^2} (1 + n_n^2)$$

where

$$k_0 = \frac{\omega}{c} \left(\frac{1}{2} \left(1 + \frac{\Omega_0^2}{\omega^2} \right) (1 - n_n^2) + \frac{\omega_p^2}{2\omega^2} \frac{(1 + n_n^4)}{(1 + n_n^2)} \right)^{\frac{1}{2}} .$$

The corresponding transmission coefficient is then

$$T = \exp \left(- \frac{\pi R \omega_p^2 (1 + n_n^2)}{2k_0 c^2} \right) \quad (2.17)$$

with k_0 as above. The behaviour of (2.17) is illustrated in Fig. 2.3 where the numbers labelling the curves are values of $R\omega_p^2/(\omega c)$, the transmission coefficient depending only on this combination of parameters if $\omega_p^2/\omega^2 \ll 1$. Unless this condition is satisfied, T is essentially zero for reasonable values of the scale length R.

From the arguments discussed earlier, it can be shown that for a wave incident from the low field side there is a reflection

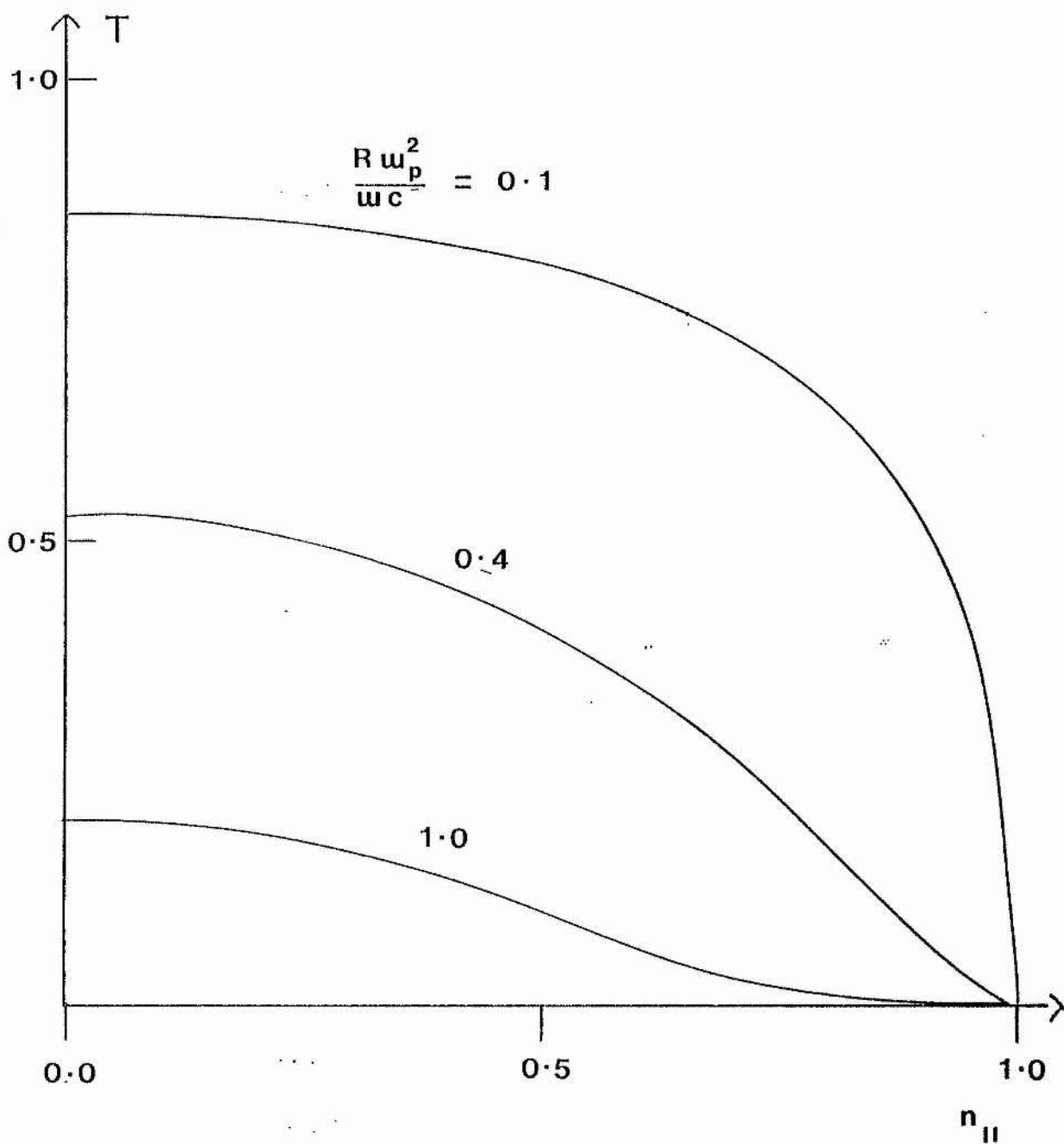


Figure 2.3 Transmission coefficients at the upper hybrid resonance.

coefficient given by $R = (1-T)^2$, while for incidence from the high field side there is no reflection. Previous authors to treat the upper hybrid resonance have taken a different equilibrium in which the density varies and the magnetic field is uniform. White and Chen (1974) have discussed the problem in the context of Budden's equation while Kuehl et al. (Kuehl, 1967; Kuehl et al., 1970; Shoucri and Kuehl, 1981) matched asymptotic solutions of a fourth order equation including thermal effects onto small argument approximations to the solutions of Budden's equation. Also, Tang (1970) treated the contour integral representation of the solutions of a fourth order O.D.E. by the method of steepest descents to obtain connection formulae.

2.3 The two-ion hybrid resonance

A resonant frequency in the ion cyclotron range is the ion-ion (Buchsbaum) resonance which only occurs when two or more ion species of differing charge to mass ratios are present. The frequency for two ion species is

$$\omega_{ii}^2 = \Omega_1 \Omega_2 \frac{(1 + n_2 m_2 / n_1 m_1)}{(m_2 q_1 / m_1 q_2 + n_2 q_2 / n_1 q_1)} \quad (2.18)$$

where n_i is the number density, and m_i , q_i are the mass and charge numbers of species i ; $i = 1, 2$.

We begin by deriving an approximate dispersion relation for waves in the frequency range $\Omega_1 < \omega < \Omega_2$. The wave equation in a cold, homogeneous magnetised plasma can be written in matrix form as

$$\begin{pmatrix} \epsilon_1 - n_{||}^2 & -i\epsilon_2 & n_{\perp} n_{||} \\ i\epsilon_2 & \epsilon_1 - n_{||}^2 - n_{\perp}^2 & 0 \\ n_{\perp} n_{||} & 0 & \epsilon_3 - n_{\perp}^2 \end{pmatrix} \begin{pmatrix} E_x \\ E_y \\ E_z \end{pmatrix} = 0. \quad (2.19)$$

In the frequency range of interest, $\omega \ll \omega_{pe}$ so that $|\epsilon_3| \gg |n_{\perp}^2|$, $|n_{\perp} n_{||}|$, and $|E_z| \ll |E_x|, |E_y|$. With these approximations (2.19) becomes

$$\begin{pmatrix} \epsilon_1 - n_{||}^2 & -i\epsilon_2 \\ i\epsilon_2 & \epsilon_1 - n_{||}^2 - n_{\perp}^2 \end{pmatrix} \begin{pmatrix} E_x \\ E_y \end{pmatrix} = 0$$

yielding the following dispersion relation for the fast magnetosonic (compressional Alfvén) wave.

$$n_{\perp}^2 = (\epsilon_1 - n_{||}^2) - \frac{\epsilon_2^2}{\epsilon_1 - n_{||}^2} \quad (2.20)$$

where

$$\epsilon_1 \approx -\frac{\omega_{p1}^2}{\omega^2 - \Omega_1^2} - \frac{\omega_{p2}^2}{\omega^2 - \Omega_2^2},$$

$$\begin{aligned} \epsilon_2 &\approx \frac{\omega_{pe}^2}{\omega \Omega_e} - \frac{\omega_{p1}^2 \Omega_1}{\omega(\omega^2 - \Omega_1^2)} - \frac{\omega_{p2}^2 \Omega_2}{\omega(\omega^2 - \Omega_2^2)} \\ &= -\frac{\omega_{p1}^2 \omega}{\Omega_1(\omega^2 - \Omega_1^2)} - \frac{\omega_{p2}^2 \omega}{\Omega_2(\omega^2 - \Omega_2^2)}. \end{aligned}$$

While approximation (2.20) preserves the correct behaviour for the fast wave cutoffs and is valid in regions away from resonance, its form means that the position of the resonance is now a function of $n_{||}$. This is incorrect as can be seen from the full dispersion relation (2.5) and expression (2.18). In our slab geometry, the

position of a resonance must be independent of $n_{||}$ since we are considering propagation at fixed $n_{||}$ in which case the direction of wave propagation is not constant. Thus as $n_{\perp}^2 \rightarrow \infty$, the wave vector tends to become perpendicular to the magnetic field direction and so the resonance at finite $n_{||}$ appears the same as for perpendicular incidence. We nevertheless use (2.20) for the purpose of analysis bearing in mind that it models a hybrid layer thicker than that described by the resonant solution of (2.5).

Introducing the notation

$$\alpha = \frac{q_2 n_2}{q_1 n_1}, \quad \mu = \frac{q_1 m_2}{q_2 m_1} \quad \text{and}$$

$$p = k_{||} \frac{v_A}{\Omega_2} \equiv k_{||} \frac{c\mu}{\omega_{p1}}$$

where v_A is the Alfvén speed of species 1, the resonant frequency is determined by the condition

$$\epsilon_1 - n_{||}^2 = 0$$

which gives

$$\left(\frac{\omega}{\Omega_1}\right)^4 \left(1 + \frac{\alpha}{\mu}\right) - \left(\frac{\omega}{\Omega_1}\right)^2 \left(1 + \alpha\mu + \frac{p^2}{\mu^2} (1 + \mu^2)\right) + \frac{p^2}{\mu^4} = 0. \quad (2.21)$$

Solving (2.21) we obtain the following expression for the two-ion hybrid frequency at finite $n_{||}$,

$$\omega_{ii}^2 = \frac{\Omega_1^2 \left(1 + \alpha\mu + p^2 \left(1 + \frac{1}{\mu^2}\right) + \left[\left(1 - \alpha\mu + \left(\frac{1}{\mu^2} - 1\right)p^2\right)^2 + 4\alpha\mu\right]^{\frac{1}{2}}\right)}{2(\mu(\mu + \alpha) + p^2)} \quad (2.22)$$

We investigate only the case where species 2, say, is present in small concentration and expand (2.22) for small α to obtain

$$\omega_{ii}^2 \approx \frac{\Omega_1^2}{\mu^2} \left(1 - \frac{\alpha\mu(1-\mu^2)}{\mu^2 + (1-\mu^2)p^2} \right) \equiv \Omega_1^2 f. \quad (2.23)$$

As before, we consider a uniform density profile and take a linear field variation, letting the cyclotron frequency vary as $\Omega_1 = \Omega_{10}(1 + x/R)$. The dispersion relation (2.20) is now expanded about the resonance ($x=0$) remembering that $\omega^2 = \Omega_{10}^2 f$.

Firstly,

$$\epsilon_1 - n_{ii}^2 \approx \frac{2\omega_{p1}^2}{\Omega_{10}^2} \frac{x}{R} \frac{\left((1+\alpha\mu)f + \frac{p^2}{\mu^2} ((\mu^2+1)f - 2) \right)}{f(f-1)(\mu^2 f - 1)} \left(1 + \frac{2x}{R} \left(\frac{1}{f-1} + \frac{1}{\mu^2 f - 1} \right) \right) \quad (2.24)$$

Also,

$$\epsilon_2 \approx - \frac{\omega_{p1}^2}{\Omega_{10}^2} \frac{f^{\frac{1}{2}} \mu^2 \left((1+\alpha)f - \left(\alpha + \frac{1}{\mu^2} \right) \right)}{(f-1)(\mu^2 f - 1)} \left(1 + \frac{2x}{R} \left[\frac{1}{f-1} + \frac{1}{\mu^2 f - 1} - \frac{\left(\alpha + \frac{1}{\mu^2} \right)}{(1+\alpha)f - \left(\alpha + \frac{1}{\mu^2} \right)} - \frac{1}{2} \right] \right) \quad (2.25)$$

Upon substitution of (2.24), (2.25) into (2.20) and keeping the $O(1/x)$ and $O(1)$ terms, we obtain

$$n_1^2 \approx \frac{A_0 + A_1 x}{x}$$

where

$$\left. \begin{aligned} A_0 &= - \frac{\omega_{p1}^2}{2\Omega_{10}^2} \frac{Rf^2 \mu^4 \left((1+\alpha)f - \left(\alpha + \frac{1}{\mu^2} \right) \right)^2}{(f-1)(\mu^2 f - 1) \left((1+\alpha\mu)f + \frac{p^2}{\mu^2} ((\mu^2+1)f - 2) \right)} \\ A_1 &= 2A_0 \left(\frac{1}{f-1} + \frac{1}{\mu^2 f - 1} + 1 - \frac{2 \left(\alpha + \frac{1}{\mu^2} \right)}{(1+\alpha)f - \left(\alpha + \frac{1}{\mu^2} \right)} \right) \end{aligned} \right\} \quad (2.26)$$

For small α , (2.26) becomes, upon substituting for f from (2.23),

$$A_0 \approx \frac{\omega_{p1}^2}{2\Omega_{10}^2} R\alpha\mu \left(\frac{\mu^2 - \mu + (1 - \mu^2)p^2}{\mu^2 + (1 - \mu^2)p^2} \right)^2, \quad \text{and}$$

$$A_1 \approx - \frac{\omega_{p1}^2}{\Omega_{10}^2} \left(\frac{\mu^2 - \mu + (1 - \mu^2)p^2}{\mu^2 + (1 - \mu^2)p^2} \right) \left(\frac{\mu^2 + \mu + (1 - \mu^2)p^2}{1 - \mu^2} \right).$$

Then the transmission coefficient for the fast wave at the minority two-ion hybrid resonance is given by

$$T = \exp(-\pi\eta) \quad \text{where}$$

$$\eta = \frac{\omega}{c} \frac{A_0}{A_1} \approx \alpha \frac{\omega_{p1} R}{2c} \left[\frac{\mu - \mu^2 - (1 - \mu^2)p^2}{\mu^2 + (1 - \mu^2)p^2} \right]^{3/2} \left[\frac{1 - \mu^2}{\mu + \mu^2 + (1 - \mu^2)p^2} \right]^{1/2} \quad (2.27)$$

to first order in α . As k_{\parallel} increases, η goes to zero and the mode conversion ceases.

In the case of a deuterium plasma with hydrogen impurities, $\mu = \frac{1}{2}$ and (2.27) becomes

$$\eta = \frac{\alpha\omega_p R}{2c} \left(\frac{1 - 3p^2}{1 + 3p^2} \right)^{3/2} \left(\frac{1}{1 + p^2} \right)^{1/2}.$$

This is the cold plasma limit of a result obtained by Swanson (1980) in a study of the effects of localised absorption on the mode conversion process. In a warm plasma, the fast wave solution connects smoothly onto the electrostatic Bernstein mode (Swanson, 1976) and all of the energy lost from the fast wave ends up on the slow branch which ultimately heats the electrons via electron Landau damping. However, Stix (1975) showed that with a minority species,

the two-ion hybrid resonance can occur sufficiently close to the minority ion cyclotron frequency so that the local left handed electric field component overlaps the absorption region leading to strong heating of the minority ions. Swanson (1980) set out to determine whether the total energy lost from the fast wave is increased by including these localised absorption effects. What he found, after a complicated analysis involving the numerical solution of a fourth order O.D.E. with a source term on the r.h.s. to represent the absorption, was that the transmission coefficient is nevertheless completely characterised by our quantity η and that the reflection coefficient for incidence from the high field side is still zero. However, the reflection coefficient for low field side incidence is less than its zero absorption limit if $(1-I)^2$.

We have shown that the hybrid resonances may be treated within the framework of C.L-D.'s method, the transmission and reflection coefficients being given by the same simple formulae as other mode coupling problems. In effect we interpret the problem as a mode conversion from an electromagnetic wave to a non-propagating electrostatic mode localised at the resonance. Results obtained in this way can be verified to be the same as those obtained if the dispersion relation is associated with Budden's equation.

CHAPTER 3

MODE CONVERSION BETWEEN FAST AND SLOW LOWER HYBRID WAVES

3.1 Accessibility of slow waves to the lower hybrid resonance

In the cold plasma approximation, two waves propagate, one of which, the slow mode, has a resonance at points where plasma parameters are such that

$$\omega^2 = \frac{\omega_{pe}^2 \Omega_e \Omega_i}{\omega_{pe}^2 + \Omega_e^2} \equiv \omega_{LH}^2$$

In a considerable number of experiments the slow mode is used for heating and for current drive.

As is well known, (Stix, 1962, p 64; Golant, 1972) there is a critical value, n_c , of the parallel refractive index for which, in slab geometry, the fast and slow waves have the same perpendicular refractive index at some point between the plasma edge and the resonance. For values of $n_{||}$ close to n_c we may expect partial mode conversion, with energy incident in one mode being split between the two modes after passing through the region where the two roots of n_{\perp}^2 are almost coincident. This phenomenon determines the sharpness of the transition between values of $n_{||}$ for which the lower hybrid resonance is accessible to the slow wave and those for which an incident slow wave is reflected on the fast mode.

Our aim in this chapter is to estimate the range of $n_{||}$ over which such an effect is significant. Firstly, the accessibility criterion pertaining to a plasma in a uniform magnetic field is

re-derived. Next, we discuss the general nature of the dispersion relation in the ω - k_{\perp} plane and find that this mode coupling problem is different in character from cases previously considered by Cairns and Lashmore-Davies (1983). An expansion about a saddle point of the dispersion relation is then used to construct a model second order O.D.E., Weber's equation, describing the coupling process. The equation has a first integral which is interpreted as a conservation law, allowing us to identify amplitudes appearing in the connection formula with incident, transmitted and converted wave amplitudes. In this way, transmission and conversion coefficients are obtained. Finally we apply the general theory to cases involving various spatial gradients. The result for a plasma with a linear density profile in a uniform field is given, while the inclusion of a magnetic field gradient in the calculation shifts the mode conversion region towards the plasma edge.

The question of our somewhat ad hoc arrival at a model second order O.D.E. for this problem is addressed in Chapter 4.

We consider a tokamak-like configuration in which the spatial gradients are taken to be perpendicular to the external magnetic field direction. Then locally, n_{\parallel} , the parallel refractive index along the field direction may be taken to be constant while n_{\perp} varies. Ray tracing studies in toroidal plasma (Bonoli and Ott, 1982) have shown that n_{\parallel} changes along the ray due to toroidal effects, but this can be neglected in the study of the localised process of mode conversion, remembering, however, that the n_{\parallel} of a wave when it undergoes conversion may not be that with which it was launched.

The cold plasma dispersion relation is

$$\epsilon_1 n_1^4 - [(\epsilon_1 - n_n^2)(\epsilon_1 + \epsilon_3) - \epsilon_2^2] n_1^2 + \epsilon_3 [(\epsilon_1 - n_n^2)^2 - \epsilon_2^2] = 0, \quad (3.1)$$

where the cold dielectric tensor elements $\epsilon_1, \epsilon_2, \epsilon_3$ are approximated in the lower hybrid frequency range $\Omega_i \ll \omega \ll \Omega_e$ by

$$\epsilon_1 \approx 1 + \frac{\omega_{pe}^2}{\Omega_e^2} - \frac{\omega_{pi}^2}{\omega^2}, \quad \epsilon_2 \approx \frac{\omega_{pe}}{\omega \Omega_e}, \quad \epsilon_3 \approx 1 - \frac{\omega_{pe}^2}{\omega^2}.$$

The condition for a confluence of the roots n_1^2 of (3.1) to occur is given by

$$[(n_n^2 - \epsilon_1)(\epsilon_1 - \epsilon_3) + \epsilon_2^2]^2 + 4\epsilon_2^2 \epsilon_3 n_n^2 = 0. \quad (3.2)$$

We use the following notations:

$$X \equiv \frac{\omega_{pe}^2}{\omega^2}, \quad y^2 \equiv \frac{\omega^2}{\Omega_i \Omega_e}, \quad \mu \equiv \frac{m_e}{m_i}$$

and assuming that X is the dominant parameter, (3.1) is approximated by

$$A n_1^4 - B n_1^2 + C = 0 \quad (3.3)$$

where

$$\left. \begin{aligned} A &= 1 - \mu X(1 - y^2) \\ B &= -X[1 - n_n^2 - \mu X(1 - 2y^2)] \\ C &= \mu y^2 X^3 \end{aligned} \right\} \quad (3.4)$$

Then condition (3.2) for a confluence of the fast and slow wave solutions becomes

$$X^2[\mu^2 X^2 - 2[n_{||}^2(2y^2 - 1) + 1]\mu X + (1 - n_{||}^2)^2] = 0. \quad (3.5)$$

If we suppose for now that the magnetic field is uniform and that the density varies linearly, then X is the spatial coordinate. In general (3.5) has two non-zero roots depending on $n_{||}^2$ and y^2 . If these are real and distinct, then there is a region between the plasma edge and the resonance where the solutions of (3.3) are complex conjugate corresponding to evanescent waves, while if (3.5) has no real roots the fast and slow waves can propagate independently from the plasma edge to the lower hybrid resonance. The transition between these two types of behaviour takes place at a critical value of $n_{||}^2$ given by

$$n_{||}^2 = \frac{1}{1 - y^2} = n_c^2 \quad (3.6)$$

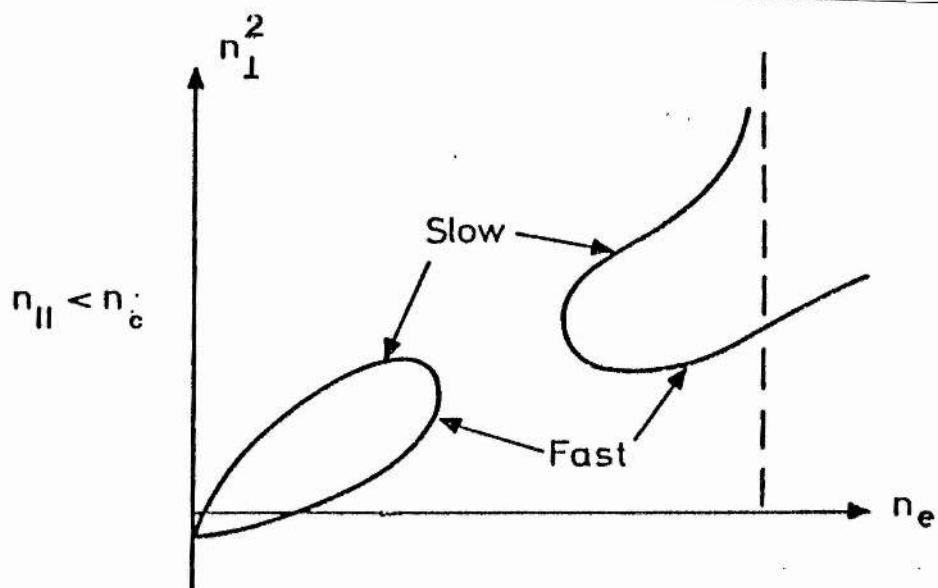
for which (3.5) has repeated roots at

$$X = \frac{1}{\mu} \frac{y^2}{1 - y^2} = X_0. \quad (3.7)$$

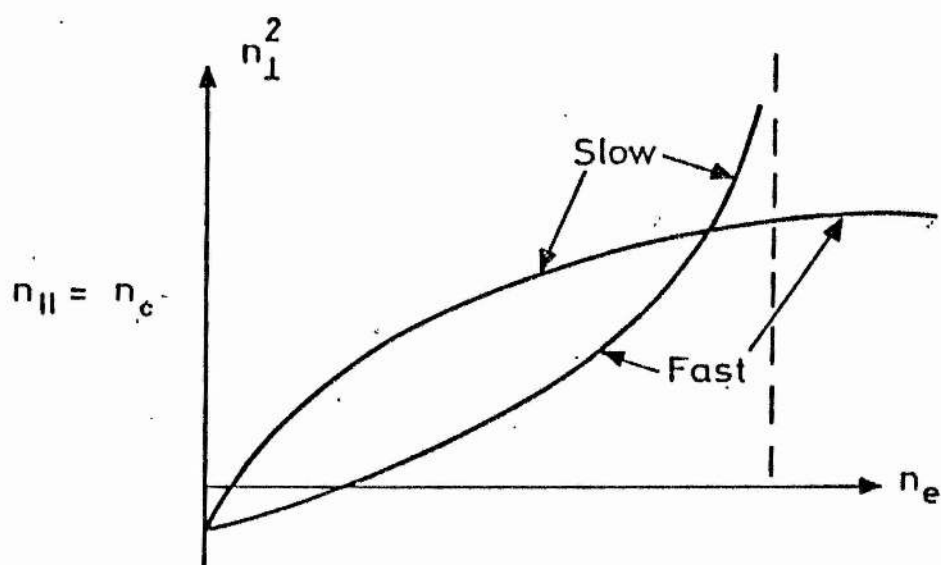
The spatial variation of $n_{||}^2$ for $n_{||} = n_c$ is shown in Fig 3.1b) (Bonoli and Ott, 1982). This behaviour has also been described in detail by Brambilla (1979).

Writing $n_{||} = n_c + \Delta n$ in (3.5) we find that for $\Delta n < 0$ (3.5) has two real roots given by

(a)



(b)



(c)

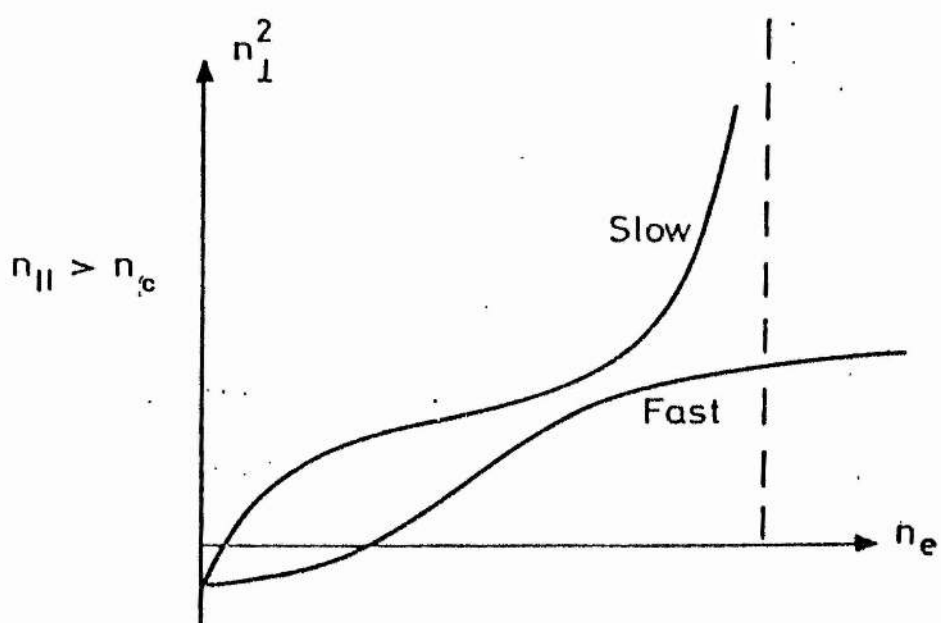


Fig.3.1 Variation of n_1^2 as a function of n_e (electron density),
 (a) $n_{||} < n_c$, (b) $n_{||} = n_c$ and
 (c) $n_{||} > n_c$ where $n_c^2 = \left(1 - \frac{\omega^2}{\Omega_e \Omega_1}\right)^{-1}$.

$$X \approx X_0 \pm \frac{2\sqrt{2}}{\mu} \frac{y}{(1-y^2)^{\frac{1}{4}}} |\Delta n|^{\frac{1}{2}}, \quad (3.8)$$

whereas for $\Delta n > 0$, (3.5) has no real roots. The two distinct topologies for $n_{||} < n_c$ and $n_{||} > n_c$ are shown in Figs 3.1a) and 3.1c) respectively.

3.2 Dispersion Curves in the ω - k_{\perp} plane

When two propagating modes approach each other closely or coincide as in Figs 3.1, we may expect a mode conversion process to lead to a partitioning of the energy between them. In mode conversions previously considered by Cairns and Lashmore-Davies, configurations in the k_{\perp} - x plane of the types shown in Figs 3.1 have been associated with ω - k_{\perp} diagrams which also exhibit a crossover of two distinct branches. However, for the present problem the dispersion relation plotted in the ω - k_{\perp} plane involves a single curve.

Figs 3.2 illustrate the relation between the k_{\perp} - x diagrams for lower hybrid waves and their dispersion curves in the ω - k_{\perp} plane.

We can write the dispersion relation as

$$\omega = f(k_{\perp}, x) \quad (3.9)$$

where plasma inhomogeneities are contained in the x variation. At points between the plasma edges and the resonance, the incident wave frequency, ω_{inc} , is above the lower hybrid frequency as shown. A

Figure 3.2a) Dispersion curves for lower hybrid waves with

$$1 < k_{\parallel} \frac{c}{\omega_{inc}} < n_c.$$

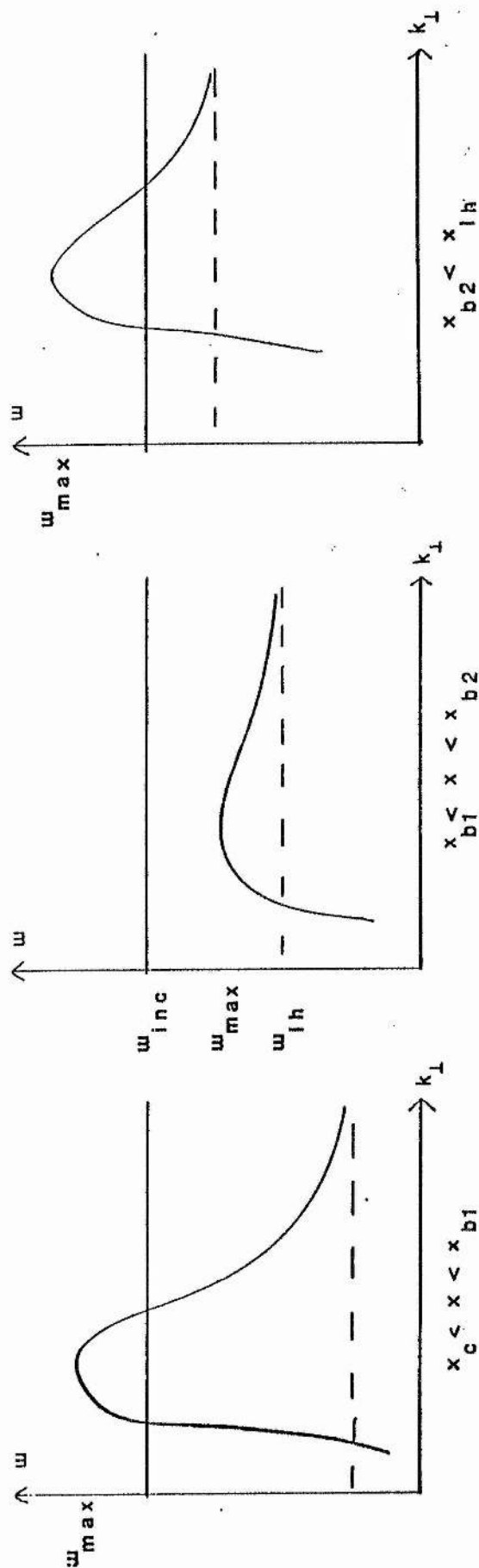
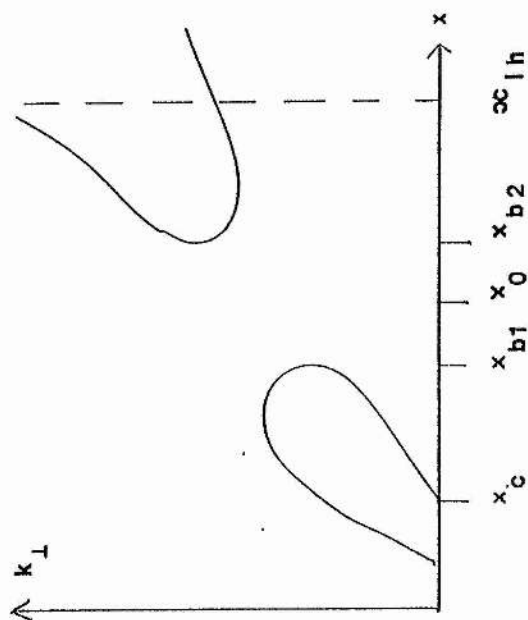


Figure 3.2b) Dispersion curves for lower hybrid waves with

$$1 < k_{\parallel} \frac{c}{\omega_{inc}} = n_c.$$

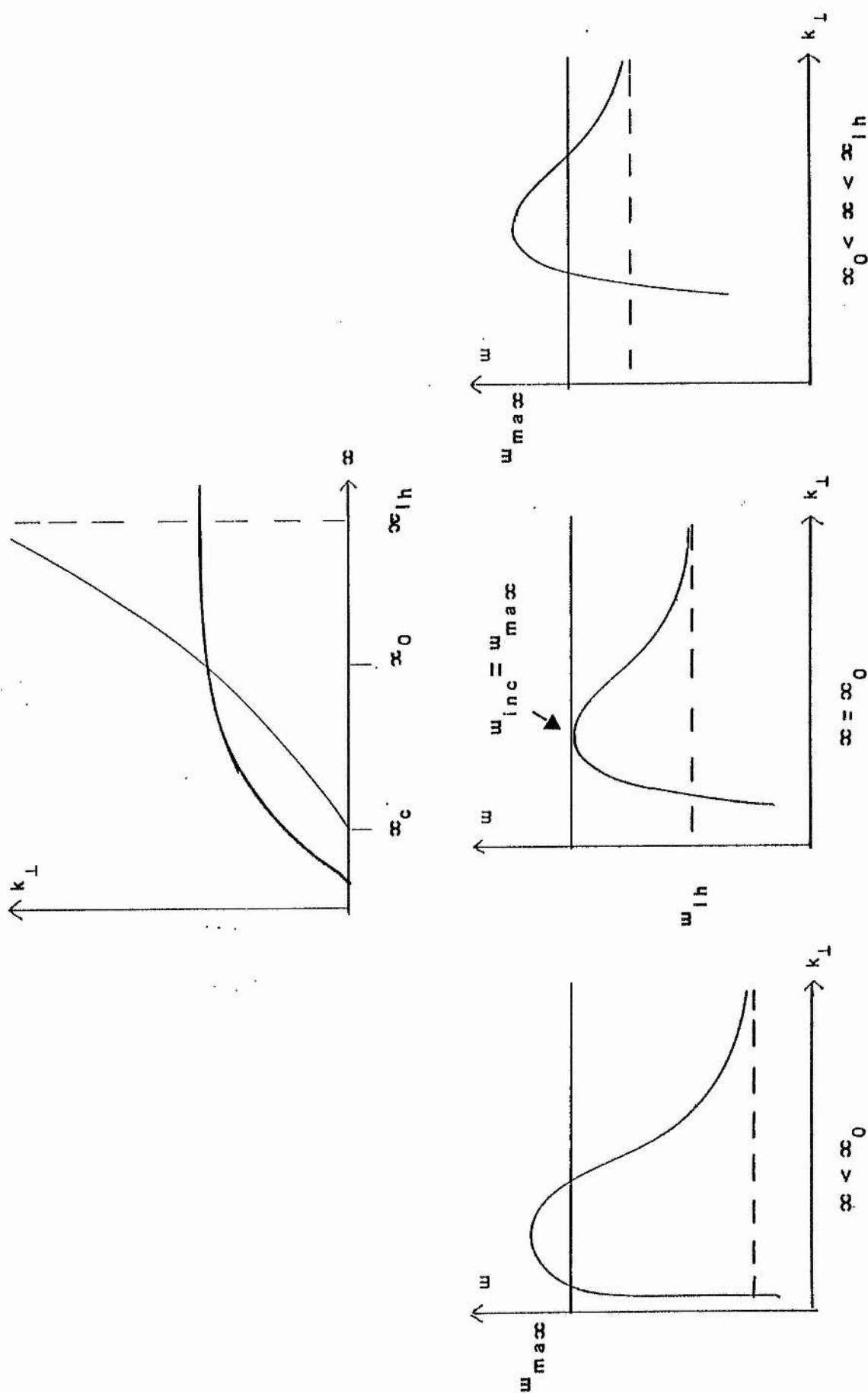
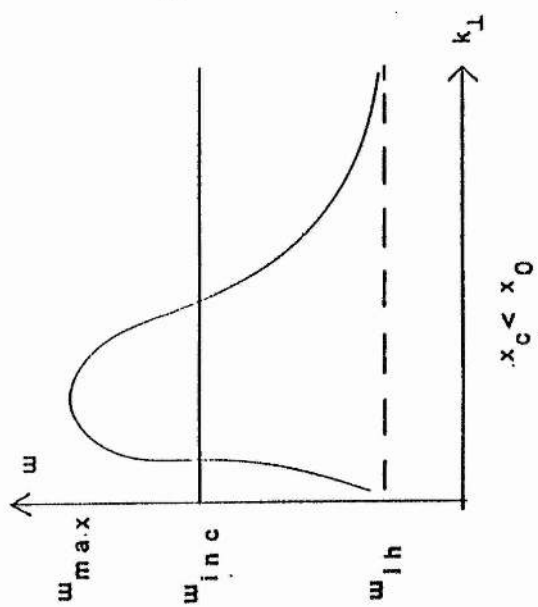
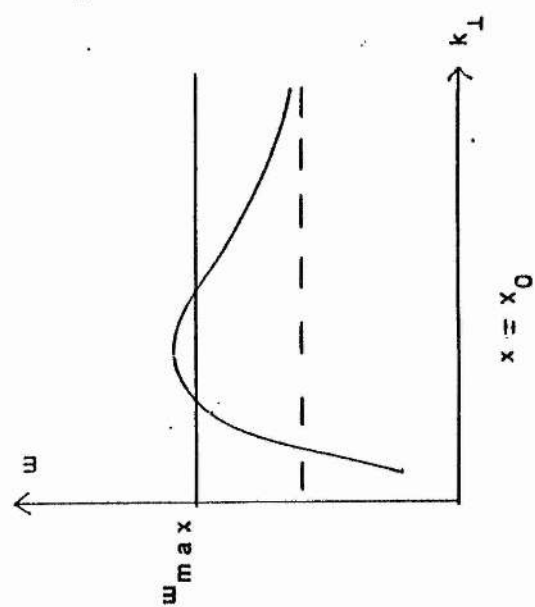
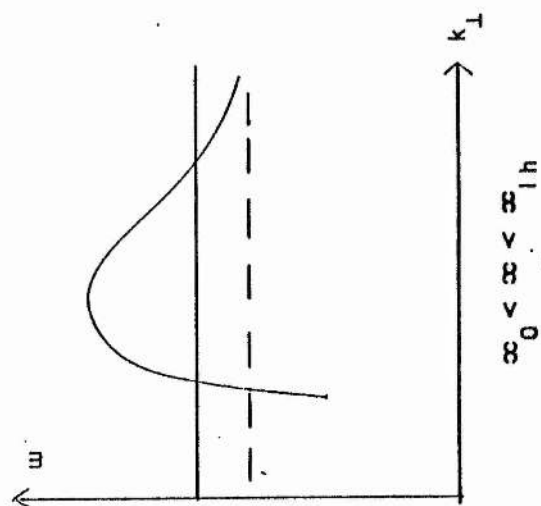
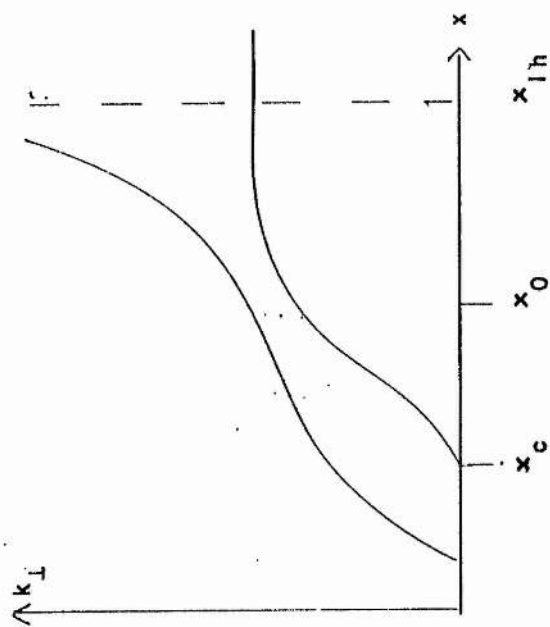


Figure 3.2c) Dispersion curves for lower hybrid waves with

$$1 < n_c < k_{\parallel} \frac{c}{\omega_{inc}}$$



family of $\omega-k_{\perp}$ curves such as in Figs 3.2 is generated at different x values, for each of which f has a maximum at some value of k_{\perp} . As the wave propagates into the plasma and x increases, the maximum, $\omega_{\max}(x)$, in the $\omega-k_{\perp}$ plane moves to lower values of ω , then moves up again. That is, ω_{\max} has a minimum as a function of x . In Fig 3.2a) for which $k_{\perp}c/\omega_{\text{inc}} < n_c$, ω_{\max} falls below ω_{inc} and we encounter an evanescent region, while in Fig 3.2c) for which $k_{\perp}c/\omega_{\text{inc}} > n_c$, ω_{\max} always lies above ω_{inc} ensuring two real k_{\perp} solutions. In Fig 3.2b) where $k_{\perp}c/\omega_{\text{inc}} = n_c$ and for which the two propagating modes have a single confluence at the point (k_0, x_0) , $\omega_{\max}(x)$ takes its minimum value at x_0 , and $\omega_{\max}(x_0) = \omega_{\text{inc}}$.

Thus (k_0, x_0) is a saddle point of (3.9) where

$$\frac{\partial f}{\partial k_{\perp}}(k_0, x_0) = \frac{\partial f}{\partial x}(k_0, x_0) = 0.$$

For points (k_{\perp}, x) near to (k_0, x_0) , (3.9) is approximately given by

$$\begin{aligned} \omega_{\text{inc}} - \omega_0 - \frac{1}{2} \frac{\partial^2 f}{\partial k_{\perp}^2}(k_0, x_0)(k_{\perp} - k_0)^2 - \frac{\partial^2 f}{\partial k_{\perp} \partial x}(k_0, x_0)(k_{\perp} - k_0)(x - x_0) \\ - \frac{1}{2} \frac{\partial^2 f}{\partial x^2}(k_0, x_0)(x - x_0)^2 = 0. \end{aligned} \quad (3.10)$$

where

$$\omega_0 = \omega_{\max}(x_0) = f(k_0, x_0).$$

3.3 Construction of Model Weber Equation

Factorising the last three terms of (3.10), the equation can be written as

$$(k_{\perp} - k_0 - a_1 \xi)(k_{\perp} - k_0 - a_2 \xi) = \eta \quad (3.11)$$

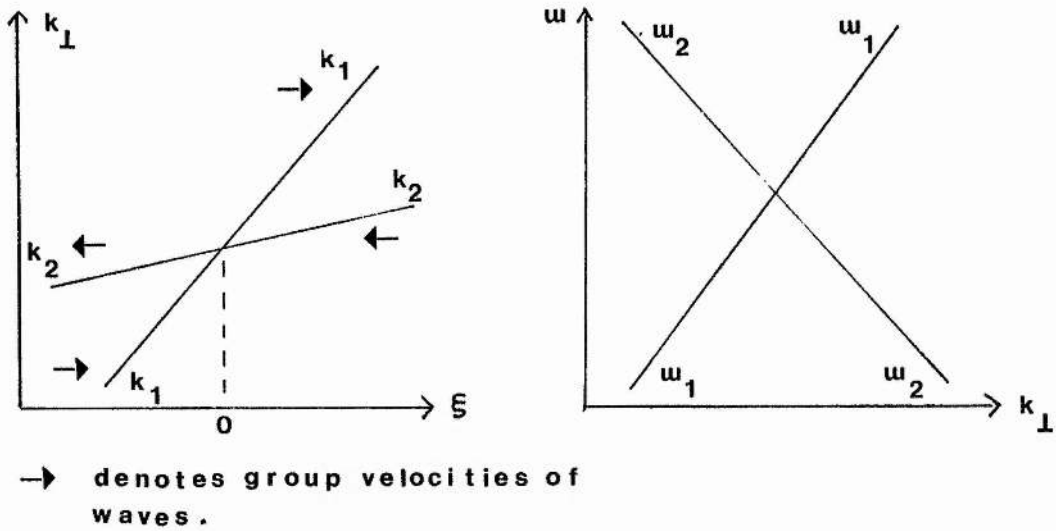
where $\xi = x - x_0$ and $a_1 \xi$, $a_2 \xi$ are the (real) roots of

$$\left. \begin{aligned} &A(k_{\perp} - k_0)^2 + B(k_{\perp} - k_0) + C = 0 \\ \text{with} \quad &A = \frac{1}{2} \frac{\partial^2 f}{\partial k_{\perp}^2}(k_0, 0) \\ &B = \frac{\partial^2 f}{\partial k_{\perp} \partial \xi}(k_0, 0) \xi \\ &C = \frac{1}{2} \frac{\partial^2 f}{\partial \xi^2}(k_0, 0) \xi^2 \\ \text{and} \quad &\eta = 2 \frac{(\omega_0 - \omega_{inc})}{\left| \frac{\partial^2 f}{\partial k_{\perp}^2}(k_0, 0) \right|} \end{aligned} \right\} \quad (3.12)$$

We now wish to associate the local dispersion relation (3.11) with a differential equation, making the correspondence $k_{\perp} \rightarrow -i d/d\xi$. This cannot be done uniquely since $k_{\perp} \xi$ terms go to some undetermined linear combination of $-i d/d\xi (\xi \varphi)$ and $-i \xi d\varphi/d\xi$. We remove this ambiguity by choosing the combination producing an equation with a conserved quantity which is then interpreted as the total energy.

Cairns and Lashmore-Davies (1983) achieved this using two coupled first order equations in which the amplitudes φ_1 and φ_2 were identified directly with the transmitted and converted waves. It is worthwhile to point out how such a representation arises naturally for the class of problems considered by these authors but not for the present case. The local dispersion relation (3.11) when $\eta = 0$ has two smoothly varying solutions $k_1(\xi)$, $k_2(\xi)$ given by

the factors on the l.h.s. In the C.L-D. coupling model for waves with anti-parallel group velocities these are associated with two independently propagating "modes" $\omega_1(k_\perp, \xi)$ and $\omega_2(k_\perp, \xi)$ in the ω - k_\perp plane as shown below.



For this configuration, fast (slow) wave energy incident from $\xi < 0$ is completely transformed into slow (fast) wave energy in the region $\xi > 0$. However, the ω - k_\perp dispersion curves of lower hybrid waves have a single lobe. This means that fast and slow waves keep the same group velocity orientation for all ξ , and so, if a fast (slow) wave is incident from $\xi < 0$ the transmitted branch is also a fast (slow) wave. The natural representation in this case is a single second order O.D.E. which we now construct.

$$\text{Let } k_\perp \rightarrow -i \frac{d}{d\xi} \text{ and}$$

$$k_\perp \xi \rightarrow -i\alpha \frac{d}{d\xi} (\xi\varphi) - i(1-\alpha)\xi \frac{d\varphi}{d\xi} \text{ in (3.11), where } \alpha \text{ will}$$

be fixed later.

The resulting O.D.E. is

$$\begin{aligned} \frac{d^2\varphi}{d\xi^2} - i(2k_0 + (1-\alpha)(a_1 + a_2)\xi) \frac{d\varphi}{d\xi} - i\alpha(a_1 + a_2) \frac{d}{d\xi} (\xi\varphi) \\ + (\eta - (k_0 + a_1\xi)(k_0 + a_2\xi))\varphi = 0. \end{aligned} \quad (3.13)$$

Making the transformation

$$\varphi = \exp \left[i \int k_0 - \frac{(a_1 + a_2)\xi}{2} d\xi \right] \Phi$$

(3.13) becomes

$$\frac{d^2\Phi}{d\xi^2} + \left[\frac{(a_1 - a_2)^2 \xi^2}{4} + \eta + i(a_1 + a_2)(\tfrac{1}{2} - \alpha) \right] \Phi = 0. \quad (3.14)$$

If the expression inside [] in (3.14) is real, then the equation has a first integral (Heading, 1962, p 75), namely

$$\text{Im} \left(\frac{d\Phi}{d\xi} \Phi^* \right) = \text{const} \quad (3.15)$$

We therefore take $\alpha = \frac{1}{2}$.

Finally, writing $\zeta = |a_1 - a_2|^{\frac{1}{2}}\xi$ and $a = -\eta/|a_1 - a_2|$ (3.14) becomes

$$\frac{d^2\Phi}{d\zeta^2} + \left(\frac{\zeta^2}{4} - a \right) \Phi = 0. \quad (3.16)$$

This is a standard equation describing tunnelling through a parabolic potential barrier. (See for example Heading, 1962, Ch V). In the asymptotic regions $|\zeta| \gg 0$, (3.16) has WKBJ solutions (Heading, 1962; Fröman and Fröman, 1965)

$$\left. \begin{aligned} \Phi_{1,2} &\propto q^{-\frac{1}{4}} \exp \left[\pm i \int_r^\zeta q^{\frac{1}{2}}(\zeta) d\zeta \right] \\ \text{with} \quad q(\zeta) &= \frac{\zeta^2}{4} + a \end{aligned} \right\} \quad (3.17)$$

describing two independently propagating waves. Far from the zeros of q , the general solution of (3.16) is of the form

$$\left. \begin{aligned} \Phi_+ &= C\Phi_{1+} + D\Phi_{2+}, \quad \zeta \gg 0 \\ \Phi_- &= A\Phi_{1-} + B\Phi_{2-}, \quad \zeta \ll 0 \end{aligned} \right\} \quad (3.18)$$

The key to identifying the amplitudes appearing in (3.18) with incident, transmitted and converted waves lies in the fact that the solutions Φ_\pm satisfy (3.15), from which we obtain the connection formula

$$|A|^2 - |B|^2 = |C|^2 - |D|^2. \quad (3.19)$$

The asymptotic solutions of (3.16) can also be written using Darwin's expansions (Abramowitz and Stegun, p 694)

$$\left. \begin{aligned} \Phi_+ &= (2/k)^{\frac{1}{2}} (Ek \cos \psi + F \sin \psi) e^{v_r} \\ \Phi_- &= (2/k)^{\frac{1}{2}} (E \sin \psi + Fk \cos \psi) e^{v_r} \end{aligned} \right\} \quad (3.20)$$

where $k = (1 + e^{2\pi a})^{\frac{1}{2}} - e^{\pi a}$

$$\psi = \vartheta + \pi/4 + v_i \quad (3.21)$$

and

$$\vartheta = \begin{cases} \frac{1}{4}|\zeta|(\zeta^2 - 4a)^{\frac{1}{2}} - \text{acosh}^{-1}(|\zeta|/2\sqrt{a}); & a > 0 \\ \frac{1}{4}|\zeta|(\zeta^2 - 4a)^{\frac{1}{2}} - \text{asinh}^{-1}(|\zeta|/2\sqrt{|a|}); & a < 0. \end{cases} \quad (3.22)$$

The exact forms of v_r , v_i are not needed here.

Eq (3.20) may be written as

$$\left. \begin{aligned} \Phi_+ &\propto (Ek - iF)e^{i\psi} + (Ek + iF)e^{-i\psi} \\ \Phi_- &\propto (-iE + Fk)e^{i\psi} + (iE + Fk)e^{-i\psi} \end{aligned} \right\} \quad (3.23)$$

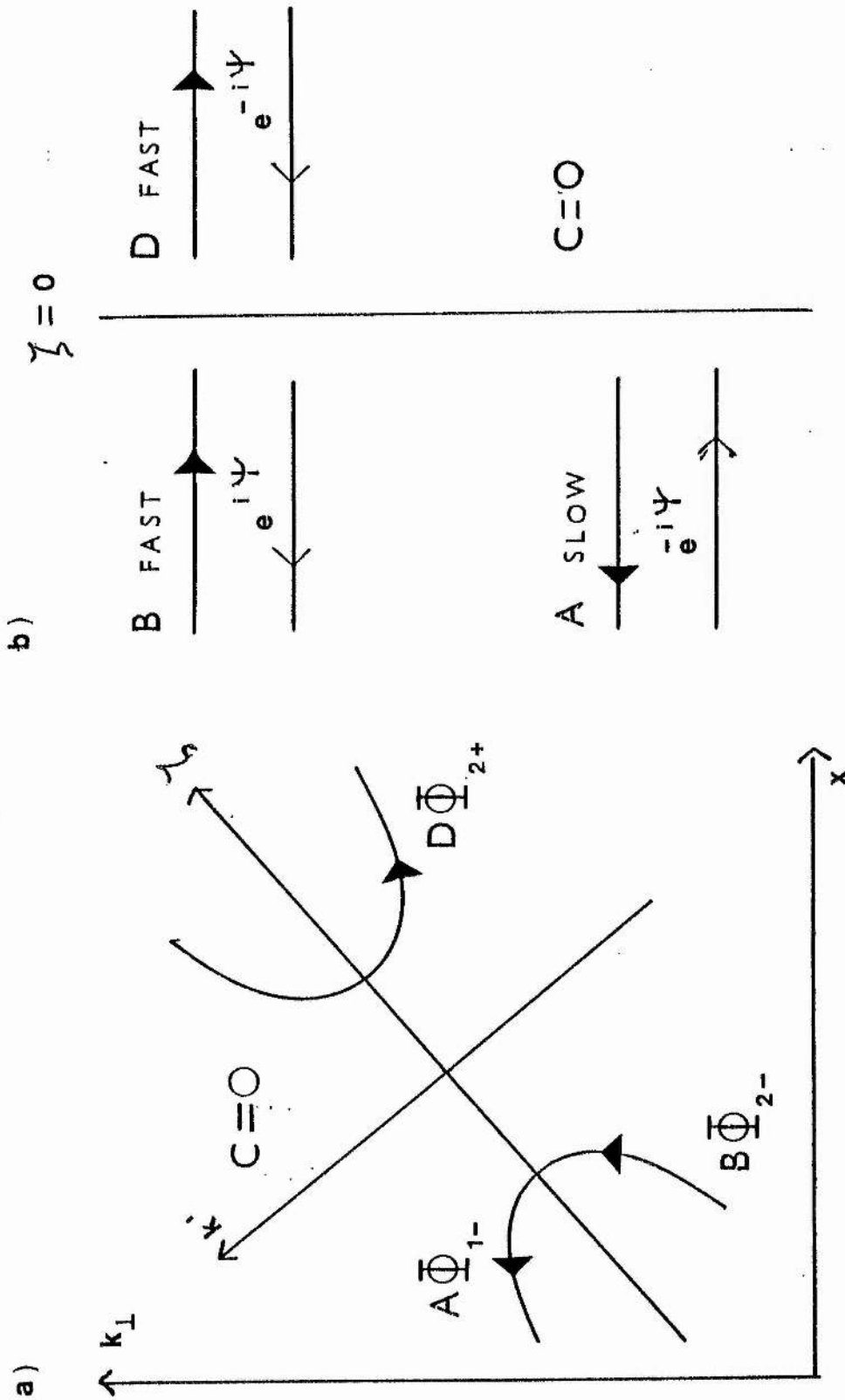
It remains to impose the boundary conditions appropriate to our problem.

Taking a configuration where, say, fast wave energy is incident from $\zeta \ll 0$, the transmitted branch must have identically oriented group velocity and is therefore also a fast wave, while the converted energy flows into the region $\zeta \ll 0$ on the slow mode. The signs of the phase velocities of the WKBJ waves $\Phi_{1,2}$, though opposite, are a matter of convention. If we take the time variation to be $\exp(-i\omega t)$, ($\omega > 0$) then

$$\begin{aligned} v_{\text{phase}} &= -\frac{\partial\psi/\partial t}{\partial\psi/\partial\zeta}; \quad \psi = \pm i \int q^{\frac{1}{2}}(\zeta)d\zeta - i\omega t \\ &= \omega/k' \end{aligned}$$

where $k' = \pm q^{\frac{1}{2}}$ are the roots of the local dispersion relation associated with (3.16). Thus the WKBJ wave Φ_1 propagates to the right, and Φ_2 to the left (see also Heading, 1962, p 75). The required boundary condition is illustrated in Figs 3.3

Figure 3.3



The transformation from k_{\perp} - x plane to k' - ζ plane represents a rotation and translation of axes.

Solid arrows denote orientation of wave group velocities. Open arrows denote orientation of wave phase velocities as measured in the k' - ζ frame.

There is no slow wave in $\zeta > 0$ and so $C = 0$. We then have from (3.19) that

$$1 = \left| \frac{D}{B} \right|^2 + \left| \frac{A}{B} \right|^2 = T + MC$$

where T and MC are the transmitted and mode converted fractions of the incident flux $|B|^2$.

Note that for this boundary condition the WKBJ amplitudes $|D|^2$ and $|A|^2$ are identical to the transmitted and converted wave fluxes respectively, suggesting that the Weber equation is the natural representation in this case. Coupling problems of the C.L-D. types arising from local dispersion relations such as (3.11) can also be handled via Weber's equation (3.16) and the connection formula (3.19) (Fuchs, Bers and Harten, 1985), but the associated boundary conditions for these cases imply a different transmitted branch from our problem, with the result that the converted wave energy is not given by one of the WKBJ amplitudes appearing in (3.19).

Identifying the WKBJ solutions (3.18) with the expansions (3.23) immediately gives

$$\begin{aligned} A &= iE + Fk, & B &= -iE + Fk \\ C &= Ek - iF = 0, & D &= Ek + iF \end{aligned}$$

so that $A = iE(1 - k^2)$, $B = -iE(1 + k^2)$, $D = 2Ek$.

Thus

$$\begin{aligned}
 & \text{and} \\
 & \left. \begin{aligned} T &= \left| \frac{D}{B} \right|^2 = \frac{1}{1 + \exp(2\pi a)} \\ MC &= \left| \frac{A}{B} \right|^2 = \frac{\exp(2\pi a)}{1 + \exp(2\pi a)} \end{aligned} \right\} \quad (3.24) \\
 & \text{where} \quad a = -\eta / |a_1 - a_2|.
 \end{aligned}$$

If $a \ll 0$, then $T \rightarrow 1$ corresponding to Fig 3.2a) in which fast and slow waves propagate independently to the lower hybrid layer, while if $a \gg 0$, $T \rightarrow 0$ corresponding to Fig 3.2c) in which incident fast (slow) wave energy is completely converted into slow (fast) wave energy propagating in the reverse direction. For $a = 0$ as in Fig 3.2b), $\frac{1}{2}$ the incident fast (slow) wave energy is transmitted on the fast (slow) mode, and $\frac{1}{2}$ converted to slow (fast) wave energy.

In order to apply the general result (3.24) to specific lower hybrid propagation problems, we need only cast the dispersion relation in the form (3.11) and identify the parameters a_1 , a_2 and η .

3.4 The result for a plasma with a linear density profile

Here, a uniform magnetic field is taken so that y^2 is a constant. We write

$$X = X_0(1 + \xi/L),$$

where L is the density gradient scale length, and, recalling the analysis of section 3.1, expand the dispersion relation (3.3) is first order in ξ for the case $n_{||} = n_c$ ($\eta = 0$).

The roots of n_{\perp}^2 are given by

$$\begin{aligned} n_{\perp}^2 &= \frac{B \pm \mu X |X - X_0|}{2A} \\ &\approx \frac{B_0 + B_1 \xi \pm \frac{\mu}{L} X_0^2 |\xi|}{2(A_0 + A_1 \xi)} \\ &\approx \frac{B_0}{2A_0} \left(1 + \left[\frac{B_1}{B_0} - \frac{A_1}{2A_0} \pm \frac{\mu X_0^2}{LB_0} \right] \xi \right). \end{aligned}$$

Forgetting the negative n_{\perp} solutions we obtain

$$k_{\perp} \approx \frac{\omega}{c} \left(\frac{B_0}{2A_0} \right)^{\frac{1}{2}} \left(1 + \frac{1}{2} \left[\frac{B_1}{B_0} - \frac{A_1}{2A_0} \pm \frac{\mu X_0^2}{LB_0} \right] \xi \right). \quad (3.25)$$

Eq (3.25) is now identified with the factors on the l.h.s. of our model dispersion relation (3.11) to give

$$\left. \begin{aligned} |a_1 - a_2| &= \frac{\mu \omega}{cL} \frac{X_0^2}{(2A_0 B_0)^{\frac{1}{2}}} \\ \text{where } A_0 &= 1 - \mu X_0 (1 - y^2) = 1 - y^2 \\ B_0 &= -X_0 [1 - n_{||}^2 - \mu X_0 (1 - 2y^2)] = 2X_0 y^2 \end{aligned} \right\} \quad (3.26)$$

For $n_{||} < n_c$ (i.e. $\eta < 0$), the equal roots of k_{\perp} in (3.11) are shifted from a double confluence at $\xi = 0$ and occur now at

$$\xi_{\Delta n}^2 = - \frac{4\eta}{(a_1 - a_2)^2}. \quad (3.27)$$

Comparing (3.27) with the separation given by (3.8) we obtain

$$\eta = 2L^2 \frac{(1-y^2)^{3/2}}{y^2} (a_1 - a_2)^2 \Delta n. \quad (3.28)$$

Using (3.26), (3.27), (3.28) and the general result (3.24) the transmission coefficient is found to be

$$\left. \begin{aligned} T &= \frac{1}{1 + \exp(-K)} \\ \text{where } K &= 2\pi \frac{\omega L}{c} \frac{1}{\mu^{1/2}} \cdot \frac{1}{(1-y^2)} \frac{\Delta n}{n_c} \end{aligned} \right\} \quad (3.29)$$

Let us estimate T for some typical operating parameters, namely those of P.L.T. where $\omega/2\pi = 800$ MHz, $B_0 = 2.5$ tesla. We assume a deuterium plasma and a density scale length $L = 0.4$ m, corresponding to the tokamak minor radius. These give

$$K \approx \frac{80}{\mu^{1/2}} \frac{\Delta n}{n_c} \approx 5000 \frac{\Delta n}{n_c}.$$

Since $K \gg 0(1)$ only for a very small spread in $n_{||}$ about its critical value, the transmission is either on or off depending as $n_{||} > n_c$ or $n_{||} < n_c$ respectively. So, in virtually all cases the mode conversion behaviour is predicted correctly by the usual ray-tracing results (see, for example, Bonoli and Ott, 1982).

3.5 Inclusion of a magnetic field gradient in the calculation

The procedure is as before, except that X is no longer the spatial gradient since the latter occurs also in y^2 .

The external magnetic field strength is now allowed to vary linearly, so that

$$\underline{B} = B\hat{z} = B_0 \left(1 + \frac{\xi}{R}\right) \hat{z}.$$

Writing

$$x = X_0 \left(1 + \frac{\xi}{L}\right), \quad y^2 = y_0^2 \left(1 - \frac{2\xi}{R}\right)$$

condition (3.5) for a confluence of the roots of n_{\pm}^2 becomes

$$\begin{aligned} & \frac{\mu X_0}{L} \left(\frac{\mu X_0}{L} + \frac{8y_0^2 n_{\parallel}^2}{R} \right) \xi^2 + \frac{2\mu X_0}{L} \left(\mu X_0 + 4n_{\parallel}^2 y_0^2 \frac{L}{R} - 1 - n_{\parallel}^2 (2y_0^2 - 1) \right) \xi \\ & + \mu^2 X_0^2 - 2\mu X_0 (n_{\parallel}^2 (2y_0^2 - 1) + 1) + (1 - n_{\parallel}^2)^2 = 0. \end{aligned} \quad (3.30)$$

If (3.30) is to have repeated roots at $\xi = 0$, we require

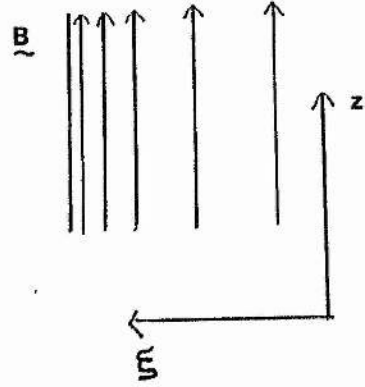
$$\left. \begin{aligned} \mu X_0 - 1 + n_{\parallel}^2 \left(2y_0^2 \left(\frac{2L}{R} - 1 \right) + 1 \right) &= 0 \\ \mu^2 X_0^2 - 2\mu X_0 (n_{\parallel}^2 (2y_0^2 - 1) + 1) + (1 - n_{\parallel}^2)^2 &= 0. \end{aligned} \right\} \quad (3.31)$$

From (3.31) we find that a single confluence of the slow and fast wave solutions occurs for a critical value of n_{\parallel} given by

$$n_{\parallel}^2 = \frac{1}{1 - y_0^2 \left(1 - \frac{4L^2}{R^2} \right)} = n_c^2$$

at the point (X_0, y_0) with X_0 and y_0 related by

$$X_0 = \frac{1}{\mu} \frac{y_0^2 (1 - 2L/R)^2}{1 - y_0^2 (1 - 4L^2/R^2)}. \quad (3.33)$$



As before, the dispersion relation (3.3) is now expanded about $\xi = 0$ in the case $n_{||} = n_c$ yielding the relevant combination,

$$\left. \begin{aligned} |a_1 - a_2| &= \frac{\omega}{c} X_0 \left(\frac{a_0}{2A_0 B_0} \right)^{\frac{1}{2}} \\ \text{with } a_0 &= \frac{\mu X_0}{L} \left(\frac{\mu X_0}{L} + \frac{8y_0^2 n_c^2}{R} \right) \\ A_0 &= 1 - \mu X_0 (1 - y_0^2) \\ B_0 &= X_0 (n_c^2 - 1 + \mu X_0 (2y_0^2 - 1)) \end{aligned} \right\} \quad (3.34)$$

where n_c^2 and X_0 are given by (3.32) and (3.33).

Away from the critical value of $n_{||}^2$, we write $n_{||} = n_c + \Delta n$ in (3.30) and obtain the new positions of the confluences of the modes to lowest order in Δn ,

$$\xi_{\Delta n}^2 = -4n_c \frac{B_0}{X_0 a_0} \Delta n; \quad \Delta n < 0. \quad (3.35)$$

Comparing (3.35) with a separation of the form (3.27) gives

$$\eta = n_c \frac{B_0}{X_0 a_0} (a_1 - a_2)^2 \Delta n. \quad (3.36)$$

Finally, we obtain the quantity characterising the range of $n_{||}$ over which partial conversion occurs

$$K = 2\pi \frac{\eta}{|a_1 - a_2|} = 2\pi \frac{\omega}{c} n_c \left(\frac{B_0}{2a_0 A_0} \right)^{\frac{1}{2}}$$

$$\text{i.e. } K = 2\pi \frac{\omega}{c} \frac{\Delta n}{n_c} \frac{L}{1 + \frac{2L}{R}} \left[\frac{(1 - 2L/R)}{\mu \left[1 - y_0^2 \left(1 - \frac{4L^2}{R} \right) \right] \left[1 - y_0^2 \left(1 - \frac{2L}{R} \right) \right]} \right]^{\frac{1}{2}}. \quad (3.37)$$

From (3.37) it would seem that this range can become large as R approaches $2L$. However the limit $2L/R \rightarrow 1$ in (3.32) and (3.33) corresponds to $n_c^2 \rightarrow 1$ and $X_0 \rightarrow 0$, so that the mode conversion point moves to the plasma edge where the waves are evanescent.

The result breaks down in this way because the analysis so far has involved the approximate dispersion relation (3.3) in which the coefficients (3.4) were obtained assuming that $\mu X \sim O(1)$.

3.6 Mode conversion at low plasma densities

In order to examine the behaviour at low densities, we must use the full dispersion relation (3.1) and retain the most significant terms assuming that

$$1 - \frac{2L}{R} \ll 1, \quad X \gg 1, \quad \mu X \ll 1,$$

where the final two inequalities guarantee a density high enough to avoid the wave cutoffs but not so high that the previous theory holds.

Condition (3.2) for a confluence of the roots of n_1^2 to occur is exactly given by

$$\begin{aligned} & \underline{\mu^2 X^2 [1 - \mu(1 - y^2)]^2} \\ & - \underline{2\mu X [n_n^2 (2y^2 - 1) + 1]} - \mu(1 - n_n^2)(1 - y^2)(2 - y^2) + \mu^3(1 - n_n^2)(1 - y^2)^3 \\ & + \underline{(1 - n_n^2)^2} + 2\mu[y^2(1 + n_n^4) - (1 - n_n^2)^2] + \mu^2(1 - y^2)^2(1 - n_n^2)^2 = 0 \end{aligned} \quad (3.38)$$

where the underlining indicates terms kept in the previous analysis.

Taking a new scaling of parameters

$$\left. \begin{aligned} X &= \mu^{-\alpha} x, & 0 < \alpha < 1 \\ 1 - 2L/R &= \mu^{\beta} \ell, & \beta > 0 \end{aligned} \right\}$$

where α and β are chosen later, the dominant terms of (3.38) are

$$\begin{aligned} & \mu^{(1-\alpha)} x^2 - 2\mu^{1-\alpha} x [n_n^2 (2y^2 - 1) + 1] + (1 - n_n^2)^2 \\ & + 2\mu [y^2 (1 + n_n^4) - (1 - n_n^2)^2] + O(\mu^{2-\alpha}) = 0. \end{aligned} \quad (3.39)$$

Writing, as usual, $x = x_0(1 + \xi/L)$, $y^2 = y_0^2(1 - 2\xi/R)$, (3.39) becomes

$$\begin{aligned} & \left[\mu^{(1-\alpha)} \frac{8n_n^2 y_0^2}{LR} + \mu^{2(1-\alpha)} \frac{x_0^2}{LR} \right] \xi^2 \\ & + \frac{2\mu^{1-\alpha}}{L} \left[\mu^{1-\alpha} x_0^2 + x_0 \left(n_n^2 \left(1 - 2y_0^2 \left(1 - \frac{2L}{R} \right) \right) - 1 \right) - 2\mu^{\alpha} \frac{L}{R} y_0^2 (1 + n_n^4) \right] \xi \\ & + \left[\mu^{2(1-\alpha)} x_0^2 - 2\mu^{1-\alpha} x_0 (n_n^2 (2y_0^2 - 1) + 1) + (1 - n_n^2)^2 \right. \\ & \quad \left. + 2\mu (y_0^2 (1 + n_n^4) - (1 - n_n^2)^2) \right] + O(\mu^{2-\alpha}) = 0. \end{aligned} \quad (3.40)$$

The ξ and constant coefficients in (3.40) are now set to zero to obtain relations between the values of n_n^2 , x_0 and y_0^2 for which a single confluence of the roots of n_n^2 occurs.

The constant coefficient, a quadratic in n_n^2 , is given by

$$n_n^4 - 2[\mu^{1-\alpha} x_0 (2y_0^2 - 1) + 1] n_n^2 + 1 - 2\mu^{1-\alpha} x_0 + O(\mu).$$

Equating this to zero we obtain

$$n_n^2 = 1 \pm 2\mu^{(1-\alpha)/2} x_0^{\frac{1}{2}} y_0 + \mu^{1-\alpha} x_0 (2y_0^2 - 1) + O(\mu^{\frac{3}{2}(1-\alpha)}), \quad (3.41)$$

but keep the + solution since $n_{\parallel}^2 > 1$ is required for propagating waves.

Substitution of (3.41) into the ξ coefficient of (3.40) gives

$$\begin{aligned} & \mu^{1-\alpha} x_0^2 - \mu^\beta 2\ell x_0 y_0^2 \left(1 + 2\mu^{(1-\alpha)/2} x_0^{\frac{1}{2}} y_0 + O(\mu^{1-\alpha}) \right) \\ & + \mu^{(1-\alpha)/2} x_0 \left(2x_0^{\frac{1}{2}} y_0 + \mu^{(1-\alpha)/2} x_0 (2y_0^2 - 1) \right) \\ & - \mu^\alpha 2y_0^2 (1 - \mu^\beta \ell) \left(1 + 2\mu^{(1-\alpha)/2} x_0^{\frac{1}{2}} y_0 + O(\mu^{1-\alpha}) \right) = 0. \end{aligned} \quad (3.42)$$

We find upon inspection of the ordering in (3.42) that fixing $\alpha = 1/3$ gives the solution which is valid as R approaches $2L$ (i.e. as $\beta \rightarrow \infty$). Also, the lower limit on the value of β for which this solution applies is $\beta = 1/3$.

Equating leading $O(\mu^{1/3})$ terms to zero in (3.42) we obtain

$$y_0 \approx \frac{x_0^{\frac{3}{2}}}{1 + \ell x_0}. \quad (3.43)$$

The by now standard calculation finally yields our mode conversion parameter,

$$K = 2\pi \frac{\omega L}{c} \frac{1}{\mu^{1/3}} y_0^{\frac{1}{2}} x_0^{\frac{1}{4}} \frac{\Delta n}{n_c} \quad (3.44)$$

with x_0 and n_c given by (3.43) and (3.41). In the limit $2L/R = 1$ ($\ell = 0$), the mode crossing point occurs at a density

$$x_0 = \frac{1}{\mu^{1/3}} y_0^{2/3} \quad (3.45)$$

while

$$K(\ell = 0) = 2\pi \frac{\omega L}{c} \frac{1}{\mu^{1/3}} y_0^{2/3} \frac{\Delta n}{n_c} . \quad (3.46)$$

Thus, $K \neq 0$ as $2L/R \rightarrow 1$. In fact the expression multiplying $\Delta n/n_c$ in (3.46) is still large so that the transmission has the same step function behaviour as for the uniform field case.

We conclude by noting however, that the presence of a magnetic field gradient shifts the mode crossing point to lower densities, as is seen by comparing (3.45) and (3.7).

CHAPTER 4

DERIVATION OF SECOND ORDER THEORY FROM EXACT FOURTH ORDER EQUATIONS

4.1 The Cold-plasma Wave Equation

The lower hybrid mode conversion is of theoretical interest because we can easily write down the exact fourth-order system of O.D.E's in the electromagnetic field amplitudes, and examine this system to discover in what approximation a second order description of the coupling process can be extracted. Starting from the cold-plasma wave equation,

$$\nabla \times \nabla \times \underline{E} - \frac{\omega^2}{c^2} \underline{\epsilon} \cdot \underline{E} = 0 \quad (4.1)$$

where $\underline{\epsilon}$ is the usual cold plasma dielectric tensor given by

$$\underline{\epsilon} = \begin{pmatrix} \epsilon_1 & -i\epsilon_2 & 0 \\ i\epsilon_2 & \epsilon_1 & 0 \\ 0 & 0 & \epsilon_3 \end{pmatrix}$$

and taking all field quantities to vary as

$$\underline{A} = \underline{A}(x) \exp(ik_z z - i\omega t),$$

we use Maxwell's curl equation $\nabla \times \underline{E} = i\omega \underline{B}$ along with (4.1) to eliminate two of the six dependent field variables, finally obtaining four coupled first order equations of the form

$$\underline{e}' \left(\equiv \frac{d\underline{e}}{d\xi} \right) = T_{4 \times 4}(\xi) \underline{e} \quad (4.2)$$

where

$$\underline{e} = (E_y, B_y, E_z, B_z)^t, \quad \xi = \frac{\omega}{c} x, \quad B_y = cB_y, \quad B_z = cB_z$$

and

$$T = \begin{pmatrix} 0 & 0 & 0 & i \\ 0 & 0 & -i\epsilon_3 & 0 \\ -\frac{\epsilon_2}{\epsilon_1} n_{||} & -i \frac{(\epsilon_1 - n_{||}^2)}{\epsilon_1} & 0 & 0 \\ -i \left[n_{||}^2 + \frac{\epsilon_2^2 - \epsilon_1^2}{\epsilon_1} \right] & -\frac{\epsilon_2}{\epsilon_1} n_{||} & 0 & 0 \end{pmatrix}$$

The eigenvalues of T , which we will denote by in^+ , in^- , $-in^+$ and $-in^-$ respectively describe the four characteristic waves whose perpendicular refractive indices n^\pm , $-n^\pm$ are the solutions of the cold plasma dispersion relation (3.1). When these eigenvalues are distinct, the waves propagate independently and are adequately described by the WKBJ approximation. However, this breaks down in the mode conversion region where the eigenvalues converge in pairs.

In general, confluence of more than two eigenvalues is unlikely, so mode conversion is expected to involve coupling between the two waves corresponding to a pair of almost coincident eigenvalues. For systems of O.D.E's such as (4.2), with embedded pairwise coupling events, Heading (1961) has given a general method of extracting the second order equation which describes the coupling. The equation is

$$\varphi'' - \beta^2 \varphi = 0, \quad (4.3)$$

where β is one half the difference between the eigenvalues, coupling to other modes being through terms involving plasma gradients. The

ideas and main results contained in Heading's 1961 paper are outlined in Section 4.2. If β^2 is real as in our case, (4.3) has a conserved quantity namely $\text{Im}(\varphi^* \varphi')$. On the other hand, our exact system (4.2) conserves the ξ -component of the Poynting flux, a property which we wish to be maintained by the second order system. Straightforward application of Heading's procedure does not yield a simple correspondence between the Poynting flux and $\text{Im}(\varphi^* \varphi')$. However, we are able to produce such a correspondence by introducing an extra transformation of the variables. This transformation also produces symmetries in the neglected coupling terms resulting in a smaller error than if Heading's method is used in its original form. In addition we have for this problem a transformation, which is well defined in the mode conversion region, relating the solutions of the second order equation (4.3) to the physical fields.

4.2 Heading's Transformation

Heading (1961) considered n dependent variables e_1, e_2, \dots, e_n satisfying the n linear first order equations

$$\underline{e}' \equiv \frac{d\underline{e}}{dz} = T \underline{e} \quad (4.4)$$

where T is an $n \times n$ matrix whose n^2 elements are given functions of z . Denoting the eigenvalues of T by q_1, q_2, \dots, q_n , let \underline{m}_j be the column matrix formed from the cofactors of $T - q_j I$ taken along any suitable row. Then under the transformation

$$\underline{e} = M \underline{\Phi} = (\underline{m}_1, \underline{m}_2, \dots, \underline{m}_n) \underline{\Phi} \quad (4.5)$$

(4.4) becomes

$$\begin{aligned}\underline{\Phi}' &= M^{-1} T M \underline{\Phi} - M^{-1} M' \underline{\Phi} \\ &= \text{diag}(q_1, q_2, \dots, q_n) \underline{\Phi} - M^{-1} M' \underline{\Phi}\end{aligned}\quad (4.6)$$

valid at all points at which M is non-singular.

Now each co-factor of $T - q_j I$ is a polynomial of degree $n-1$ at most in q_j , the coefficients being independent of the suffix j and so the eigenvectors \underline{m}_j may be written as

$$\begin{aligned}\underline{m}_j &= \begin{pmatrix} \text{polynomial 1 of degree } n-1 \text{ at most in } q_j \\ \text{polynomial 2 } q_j \\ \vdots \\ \text{polynomial } n \text{ } q_j \end{pmatrix} \\ &= P \begin{pmatrix} 1 \\ q_j \\ q_j^2 \\ \vdots \\ q_j^{n-1} \end{pmatrix}\end{aligned}$$

where P is the $n \times n$ matrix formed from the coefficients of the n polynomials.

Then

$$M = (\underline{m}_1, \underline{m}_2, \dots, \underline{m}_n) = P \begin{pmatrix} 1 & 1 & \dots & 1 \\ q_1 & q_2 & \dots & q_n \\ q_1^2 & q_2^2 & \dots & q_n^2 \\ \vdots & \vdots & & \vdots \\ q_1^{n-1} & q_2^{n-1} & & q_n^{n-1} \end{pmatrix} = PA$$

where A is the alternate matrix of the eigenvalues q_j , $j = 1, \dots, n$, and their powers arranged in order.

Since the determinant of A is given by

$$\det A = \prod_{\substack{i,j=1 \\ i > j}}^n (q_i - q_j), \quad (4.7)$$

it follows that A is nonsingular throughout any domain in which the n eigenvalues are distinct.

Equations (4.6) now take the form

$$\begin{aligned} \underline{\Phi}' &= \text{diag}(q_1, \dots, q_n) \underline{\Phi} - M^{-1} M' \underline{\Phi} \\ &= Q \underline{\Phi} - A^{-1} A' \underline{\Phi} - A^{-1} P^{-1} P' A \underline{\Phi} \end{aligned} \quad (4.8)$$

If the original matrix T in (4.4) is constant, then the coupling matrices $A^{-1} A'$ and $A^{-1} P^{-1} P' A$ vanish owing to the presence of derivatives in every element, and (4.8) constitutes a set of n independent equations whose solutions represent, in a physical interpretation, n independently propagated waves. In an inhomogeneous medium, the elements of T are functions of the variable z which describes the inhomogeneity, and equations (4.8) are rendered simultaneous through the non-diagonal elements of $A^{-1} A'$ and $A^{-1} P^{-1} P' A$. If the medium is slowly varying, the derivatives which appear in $A^{-1} A'$ and $A^{-1} P^{-1} P' A$ make these coupling terms small compared with the elements of Q , except in the vicinity of so called transition points where two or more of the roots q_j , $j = 1, \dots, n$, attain equality and A becomes singular.

The explicit form of the primary coupling matrix $A^{-1} A'$ reveals more about the nature of the coupling process. It can be shown that

$$(A^{-1}A')_{ij} = \begin{cases} \frac{q'_j}{q_j - q_i} \frac{(q_j)}{(q_i)}, & i \neq j \\ q'_i \sum_{\substack{p=1 \\ p \neq i}}^n \frac{1}{q_i - q_p}, & i = j \end{cases} \quad (4.9)$$

where the symbol (q_p) denotes the product

$$(q_p) \equiv (q_p - q_1)(q_p - q_2) \dots (q_p - q_{p-1})(q_p - q_{p+1}) \dots (q_p - q_n).$$

Consider a transition point of order two, which is defined by a solution of the equation $q_1(z) = q_2(z)$ and denoted by $z = z_{12}$. Referring to (4.9), every element of the first two rows of $A^{-1}A'$ is singular at $z = z_{12}$ due to the presence of the factor $1/(q_2 - q_1)$. However the coupling coefficients $(A^{-1}A')_{ij}$ ($i = 1, 2$) are larger in order of magnitude when $j = 1, 2$ than when $j = 3, 4, \dots, n$, since columns one and two involve the factors q'_1 and q'_2 respectively which may also be singular at z_{12} . This suggests that coupling exists mainly only between Φ_1 and $\Phi_2, \Phi_3, \dots, \Phi_n$ being relatively free from coupling with Φ_1 and Φ_2 and that the 2×2 matrix taken from the first two rows and columns of $A^{-1}A'$ is the essential feature in determining the behaviour of the solutions Φ_1 and Φ_2 near the transition point z_{12} .

Similar arguments are used to define an r th ($r \leq n$) order transition point which exists if $q_a = q_b = q_c = \dots = \alpha$, say, at $z = z_{abc\dots}$. The essential coupling between $\Phi_a, \Phi_b, \Phi_c, \dots$ is determined by the $r \times r$ matrix taken from the appropriate rows and

columns of $A^{-1}A'$. Also it is noted that of the remaining $n-r$ roots, s of these may also attain equality at $z = z_{abc\dots}$. If their common value γ is not equal to α at $z = z_{abc}$, then this set of s variables is not coupled to the previous set of r variables.

The coupled first order equations (4.8) in the n variables $\underline{\Phi}$ possessing a transition point z_0 of order $r \leq n$ may be transformed in such a way that the r variables associated with the transition point appear in a set of r coupled first order equations which are essentially decoupled from the remaining $n-r$ variables not associated with the transition point, and so that all coupling terms in all equations are nonsingular and therefore small at $z = z_0$.

It is assumed that (4.8) possesses a transition point z_0 at which $q_1 = q_2 = \dots = q_r$ and that in the vicinity of z_0 the q_j 's may be written as

$$q_j = \alpha + k^{j-1}\beta \quad j = 1, \dots, r$$

where $\beta(z_0) = 0$ and $k = \exp(2\pi i/r)$.

A new vector \underline{f} is defined by

$$\underline{\Phi} = E R^{-1} \underline{f} \quad (4.10)$$

with

$$E = \begin{pmatrix} I_r \exp \int \alpha dz & 0 \\ 0 & I_{n-r} \end{pmatrix}$$

and

$$R = \begin{pmatrix} 1 & 1 & 1 & \dots & 1 & 0 \\ \beta & k\beta & k^2\beta & & k^{r-1}\beta & 0 \\ \beta^2 & k^2\beta^2 & \vdots & & \vdots & \vdots \\ \vdots & \vdots & \vdots & & \vdots & \vdots \\ \beta^{r-1} & k^{r-1}\beta^{r-1} & k^{2(r-1)}\beta^{r-1} & & k^{(r-1)^2}\beta^{r-1} & \vdots \\ 0 & 0 & 0 & \dots & 0 & I_{n-r} \end{pmatrix} = \begin{pmatrix} BK & 0 \\ 0 & I_{n-r} \end{pmatrix}$$

where $B = \text{diag}(1, \beta, \beta^2, \dots, \beta^{r-1})$ and K is an alternant matrix of the r th roots of unity.

Then it can be shown that under transformation (4.10), equation (4.8) becomes

$$\underline{f}' = \underbrace{\begin{pmatrix} 0 & 1 & 0 & 0 & \dots & 0 \\ 0 & 0 & 1 & 0 & \dots & 0 \\ 0 & 0 & 0 & 1 & \dots & 0 \\ \vdots & & & & & \\ \beta^r & 0 & 0 & 0 & \dots & 0 \\ 0 & 0 & 0 & 0 & \dots & Q_{n-r} \end{pmatrix}}_{\text{principal term}} \underline{f} - \underbrace{E^{-1}(AR^{-1})^{-1}(AR^{-1})'E\underline{f}}_{\text{primary coupling form}} - \underbrace{E^{-1}(AR^{-1})^{-1}P^{-1}P'(AR^{-1})E\underline{f}}_{\text{secondary coupling form}}$$

where $Q_{n-r} = \text{diag}(q_{r+1}, q_{r+2}, \dots, q_n).$ (4.11)

At all points where coupling can be neglected (4.11) becomes

$$\begin{cases} f_1^{(r)} = \beta^r f_{r'} \\ f_j' = q_j f_j \quad j = r+1, \dots, n. \end{cases}$$

That is, the separation of an r th order differential equation, describing the coupling among the r variables f_1, f_2, \dots, f_r , from the $n-r$ independent variables has been achieved.

It then remains to show that the coupling terms in (4.11) are non-singular at z_0 . Heading has demonstrated that the elements of AR^{-1} are polynomials in β^r . It follows that $(AR^{-1})'$ contains β' only through such terms as $\beta^{Nr-1}\beta'$ where N is a non-negative integer.

Also $(AR^{-1})^{-1} = \text{adj } AR^{-1} / \det(AR^{-1})$ where the elements of $\text{adj } AR^{-1}$ are further polynomials in β^r . The determinant of AR^{-1} is given by

$$\begin{aligned} \det AR^{-1} &= \det A / \det R = \det A / (\det B \det K) \\ &= \prod_{\substack{i,j \\ i>j}}^n (q_i - q_j) / (\beta^{(1+2+\dots+r-1)} \det K) \end{aligned}$$

from (4.7) and (4.10).

Now the relevant factors in the numerator occur for $i, j \leq r$ and these are

$$(q_r - q_{r-1}) \dots (q_r - q_1) (q_{r-1} - q_{r-2}) \dots (q_{r-1} - q_1) \dots (q_2 - q_1)$$

which is proportional to

$$\beta^{r-1} \beta^{r-2} \dots \beta^2 \beta$$

so that $\det AR^{-1}$ does not contain β as a factor. Hence AR^{-1} is nonsingular at z_0 .

Finally, each element in the product $(AR^{-1})^{-1}(AR^{-1})'$ has terms of the form $\beta^{Nr}(\beta^{Mr})'$ where $N, M \geq 0$ are integers. This is proportional to $\beta^{(N+M)r-1}\beta'$ with $N \geq 0$, $M \geq 1$, the lowest power being $\beta^{r-1}\beta'$. If β when expanded in terms of $z - z_0$ begins with a term $(z - z_0)^b$, then $\beta^{r-1}\beta'$ is proportional to $(z - z_0)^{br-1}$ which is non-singular at z_0 provided $b \geq 1/r$. That is, the product $(AR^{-1})^{-1}(AR^{-1})'$

is nonsingular at z_0 provided the power series expansion for β^T begins with a term at least linear in $z - z_0$.

Hence the elements of the primary coupling matrix in (4.11) are nonsingular at z_0 under these conditions. The secondary coupling matrix is also nonsingular provided that P is nonsingular at z_0 .

4.3 Application and extension of Heading's transformation

Returning to our original system of coupled equations (4.2), we write these in terms of new variables $\underline{\phi}$ via the transformation

$$\underline{e} = M D \underline{\phi} = M \underline{\Phi}$$

where

$$M = (\underline{m}_1, \underline{m}_2, \underline{m}_3, \underline{m}_4) = \begin{pmatrix} c^+ & c^- & c^+ & c^- \\ -i\epsilon_3 \rho_2 n_{||} & -i\epsilon_3 \rho_2 n_{||} & -i\epsilon_3 \rho_2 n_{||} & -i\epsilon_3 \rho_2 n_{||} \\ i\rho_2 n_{||} n^+ & i\rho_2 n_{||} n^- & -i\rho_2 n_{||} n^+ & -i\rho_2 n_{||} n^- \\ n^+ c^+ & n^- c^- & -n^+ c^+ & -n^- c^- \end{pmatrix}$$

$$\text{with } c^+ = \rho_1 (n^+)^2 - \epsilon_3, \quad c^- = \rho_1 (n^-)^2 - \epsilon_3, \quad \rho_1 = \frac{\epsilon_1}{\epsilon_1 - n_{||}^2}, \quad \rho_2 = \frac{\epsilon_2}{\epsilon_1 - n_{||}^2}$$

(4.12)

The column vectors \underline{m}_i , $i = 1, \dots, 4$, are eigenvectors corresponding to the eigenvalues of T ; in other words they are polarisation vectors for the four characteristic waves, while D is a nonsingular diagonal matrix to be chosen later. M factorises as

$$M = PA = \begin{pmatrix} -\epsilon_3 & 0 & -\rho_1 & 0 \\ -i\epsilon_3\rho_2 n_{||} & 0 & 0 & 0 \\ 0 & \rho_2 n_{||} & 0 & 0 \\ 0 & i\epsilon_3 & 0 & i\rho_1 \end{pmatrix} \begin{pmatrix} 1 & 1 & 1 & 1 \\ in^+ & in^- & -in^+ & -in^- \\ -(n^+)^2 & -(n^-)^2 & -(n^+)^2 & -(n^-)^2 \\ -i(n^+)^3 & -i(n^-)^3 & i(n^+)^3 & i(n^-)^3 \end{pmatrix}$$

where A is the alternant matrix consisting of the eigenvalues and their powers arranged in order.

We note that the determinant of P given by

$$\det P = -\epsilon_3 \rho_1^2 \rho_2^2 n_{||}^2$$

is non-zero throughout the domain where the fast and slow waves propagate, so that P is nonsingular.

Then the original system (4.2) becomes

$$\begin{aligned} \underline{\varphi}' &= (MD)^{-1} T(MD) \underline{\varphi} - (MD)^{-1} (MD)' \underline{\varphi} \\ &= i \text{diag}(n^+, n^-, -n^+, -n^-) \underline{\varphi} - D^{-1} A^{-1} A' D \underline{\varphi} - A^{-1} P^{-1} P' A \underline{\varphi} \\ &\quad - D^{-1} D' \underline{\varphi}. \end{aligned} \quad (4.13)$$

Here we differ from Heading (see 4.8) by introducing an arbitrary scaling D for the eigenvectors M. A special choice of D will yield final equations similar to (4.11), but which have the additional property that the dependent variables now conserve a quantity identical to those conserved by the embedded second order equations.

Since the characteristic roots of T are the solutions of a biquadratic dispersion relation, equations (4.2) possess a second order transition point $\xi = \xi_0$, say, at which the positive n_{\perp} pair of roots become equal, as do the negative n_{\perp} pair. As is seen from (4.9), the leading order singular coupling terms in equation (4.13) occur in the matrix $D^{-1} A^{-1} A' D$ which has the following relevant factors

$$D^{-1}A^{-1}A'D = \begin{pmatrix} U & V \\ V & U \end{pmatrix} \text{ where}$$

$$V = \begin{pmatrix} (n^+)' & (n^-)' \\ (n^+)' & (n^-)' \end{pmatrix} \text{ and } U = \frac{1}{n^+ - n^-} V.$$

The difference in the order of magnitude of the singularities in U and V at ξ_0 implies that φ_1 and φ_2 are coupled to each other but not to φ_3 and φ_4 , and vice versa. Hence there are two pairwise coupling events involving the positive and negative n_{\pm} pair of waves separately.

Writing

$$in^{\pm} = \alpha \pm \beta,$$

a new column vector \underline{f} is defined (as in 4.10) by

$$\underline{\varphi} = E R^{-1} \underline{f}$$

where

$$E = \text{diag} \left(e^{\int \alpha d\xi}, e^{\int \alpha d\xi}, e^{-\int \alpha d\xi}, e^{-\int \alpha d\xi} \right)$$

and

$$R = \begin{pmatrix} 1 & 1 & 0 & 0 \\ \beta & -\beta & 0 & 0 \\ 0 & 0 & 1 & 1 \\ 0 & 0 & -\beta & \beta \end{pmatrix}$$

(4.14)

Then under transformation (4.14) equations (4.13) become

$$\underline{f}' = \underbrace{\begin{pmatrix} 0 & 1 & 0 & 0 \\ \beta^2 & 0 & 0 & 0 \\ 0 & 0 & 0 & 1 \\ 0 & 0 & \beta^2 & 0 \end{pmatrix}}_{\text{principal term}} \underline{f} - \underbrace{E^{-1}(ADR^{-1})^{-1}(ADR^{-1})'E}_{\text{primary coupling term}} \underline{f} - \underbrace{E^{-1}(ADR^{-1})^{-1}P^{-1}P'(ADR^{-1})E}_{\text{secondary coupling term}} \underline{f} \quad (4.15)$$

The form of the principal term in (4.15) shows that we will have extracted the appropriate second order equations describing the positive and negative n_{\perp} pairs of waves separately, provided it can be demonstrated that the coupling terms are nonsingular at transition points. We now fix D by considering energy conservation.

4.4 Conservation of Energy

The principal term of (4.15) yields

$$\left. \begin{aligned} f_1' &= f_2 \\ f_2' &= \beta^2 f_1 \end{aligned} \right\} \quad (4.16)$$

$$\text{i.e.} \quad f_1'' + \frac{(n^+ - n^-)^2}{4} f_1 = 0$$

and similarly for the variables f_3 and f_4 .

For (4.16) with a real potential $-\beta^2$, a conserved quantity is

$$\text{Im}(f_1^* f_1') \equiv \text{Im}(f_1^* f_2).$$

On the other hand, the exact fourth order system (4.2) conserves the ξ -component, P_{ξ} , of the Poynting flux, given by

$$P_{\xi} = \text{Re}(E_y B_z^* - E_z B_y^*).$$

Using transformations (4.12) and (4.14) to write P_{ξ} in terms of the new variables \underline{f} , we seek the choice of D which will make P_{ξ}

identical to the quantities conserved by (4.16).

Starting from (4.12) we write

$$\begin{aligned}\underline{e} &= (E_y, B_y, E_z, B_z)^t = \sum_{i=1}^4 \Phi_i \underline{m}_i \\ &= \sum_{i=1}^4 \Phi_i (E_{yi}, B_{yi}, E_{zi}, B_{zi})^t.\end{aligned}$$

Then

$$\begin{aligned}P_\xi &= \text{Re}[E_y B_z^* - E_z B_y^*] \\ &= \text{Re} \left[(\Phi_1 E_{y1} + \Phi_2 E_{y2} + \Phi_3 E_{y3} + \Phi_4 E_{y4}) \times (\Phi_1 B_{z1} + \Phi_2 B_{z2} + \Phi_3 B_{z3} + \Phi_4 B_{z4})^* \right. \\ &\quad \left. - (\Phi_1 E_{z1} + \Phi_2 E_{z2} + \Phi_3 E_{z3} + \Phi_4 E_{z4}) (\Phi_1 B_{y1} + \Phi_2 B_{y2} + \Phi_3 B_{y3} + \Phi_4 B_{y4})^* \right] \\ &= \text{Re} \left[\underbrace{|\Phi_1|^2 (E_{y1} B_{z1}^* - E_{z1} B_{y1}^*)}_{(1-1) \text{ term}} + |\Phi_2|^2 (E_{y2} B_{z2}^* - E_{z2} B_{y2}^*) \right. \\ &\quad + |\Phi_3|^2 (E_{y3} B_{z3}^* - E_{z3} B_{y3}^*) + |\Phi_4|^2 (E_{y4} B_{z4}^* - E_{z4} B_{y4}^*) \\ &\quad + \underbrace{\Phi_1 \Phi_2^* (E_{y1} B_{z2}^* - E_{z1} B_{y2}^*) + \Phi_1^* \Phi_2 (E_{y2} B_{z1}^* - E_{z2} B_{y1}^*)}_{(1-2) \text{ cross terms}} \\ &\quad \left. + (1-3) \text{ terms} + (1-4) \text{ terms} + (2-3) \text{ terms} + (2-4) \text{ terms} + (3-4) \text{ terms} \right] \end{aligned} \tag{4.17}$$

When the solutions of n_i are real, it is easy to show using the expressions in (4.12) for \underline{m}_i , $i = 1, 2, 3, 4$ that the cross terms in (4.17) are pure imaginary. In this case (4.17) becomes

$$P_{\xi} = (|\Phi_1|^2 - |\Phi_3|^2) n^+ c^+ (c^+ - c^-) + (|\Phi_2|^2 - |\Phi_4|^2) n^- c^- (c^- - c^+). \quad (4.18)$$

The roots of n_{\perp} may also occur in complex conjugate pairs, as is seen from dispersion curves for which $n_{\perp} < n_c$, with two real confluence points and a region of evanescence between them. In this region

$$(n^{\pm})^* = n^{\mp}, \quad (c^{\pm})^* = c^{\mp},$$

and the contribution to P_{ξ} , which then comes only from the (1-2) and (3-4) cross terms of (4.17), is given by

$$P_{\xi} = 2\text{Re} \left[(\Phi_1 \Phi_2^* - \Phi_3 \Phi_4^*) n^+ c^+ (c^+ - c^-) \right]. \quad (4.19)$$

From (4.12) and (4.14) we have

$$\begin{aligned} \underline{\Phi} &= D\underline{\varphi} = \text{diag}(d_1, d_2, d_3, d_4) \underline{\varphi}, \\ \left. \begin{aligned} |\varphi_1|^2 &= \frac{1}{4} \left(|f_1|^2 + \left| \frac{f_2}{\beta} \right|^2 + 2\text{Re}[f_1^* f_2 / \beta] \right) \\ |\varphi_2|^2 &= \frac{1}{4} \left(|f_1|^2 + \left| \frac{f_2}{\beta} \right|^2 - 2\text{Re}[f_1^* f_2 / \beta] \right) \\ |\varphi_3|^2 &= \frac{1}{4} \left(|f_3|^2 + \left| \frac{f_4}{\beta} \right|^2 - 2\text{Re}[f_3^* f_4 / \beta] \right) \\ |\varphi_4|^2 &= \frac{1}{4} \left(|f_3|^2 + \left| \frac{f_4}{\beta} \right|^2 + 2\text{Re}[f_3^* f_4 / \beta] \right) \\ \varphi_1 \varphi_2^* &= \frac{1}{4} \left(|f_1|^2 - \left| \frac{f_2}{\beta} \right|^2 + 2i\text{Im}[f_1^* f_2 / \beta] \right) \\ \varphi_3 \varphi_4^* &= \frac{1}{4} \left(|f_3|^2 - \left| \frac{f_4}{\beta} \right|^2 - 2i\text{Im}[f_3^* f_4 / \beta] \right) \end{aligned} \right\} \quad (4.20) \end{aligned}$$

Upon substituting of (4.20) into (4.18) we obtain the following expression for P_ξ in the case of real n_\perp ,

$$P_\xi = \frac{\rho_1 (n^+ + n^-)(n^+ - n^-)}{4} \left[n^+ c^+ \left(|d_1|^2 (|f_1|^2 + |f_2/\beta|^2 + 2\text{Re}[f_1^* f_2/\beta]) \right. \right. \\ \left. \left. - |d_3|^2 (|f_3|^2 + |f_4/\beta|^2 - 2\text{Re}[f_3^* f_4/\beta]) \right) \right. \\ \left. - n^- c^- \left(|d_2|^2 (|f_1|^2 + |f_2/\beta|^2 - 2\text{Re}[f_1^* f_2/\beta]) \right. \right. \\ \left. \left. - |d_4|^2 (|f_3|^2 + |f_4/\beta|^2 + 2\text{Re}[f_3^* f_4/\beta]) \right) \right]. \quad (4.21)$$

Setting

$$d_1 = d_3 = (n^+ c^+ \rho_1 (n^+ + n^-))^{-\frac{1}{2}} \\ d_2 = d_4 = (n^- c^- \rho_1 (n^+ + n^-))^{-\frac{1}{2}} \quad (4.22)$$

(4.21) becomes

$$P_\xi = \frac{(n^+ - n^-)}{4} \text{sgn}(c^+ \rho_1) \left[|f_1|^2 + \left| \frac{f_2}{\beta} \right|^2 + 2\text{Re}[f_1^* f_2/\beta] \right. \\ \left. - \left(|f_3|^2 + \left| \frac{f_4}{\beta} \right|^2 - 2\text{Re}[f_3^* f_4/\beta] \right) \right] \\ - \frac{(n^+ - n^-)}{4} \text{sgn}(c^- \rho_1) \left[|f_1|^2 + \left| \frac{f_2}{\beta} \right|^2 - 2\text{Re}[f_1^* f_2/\beta] \right. \\ \left. - \left(|f_3|^2 + \left| \frac{f_4}{\beta} \right|^2 + 2\text{Re}[f_3^* f_4/\beta] \right) \right].$$

Note that $0 < \epsilon_1 < 1$ in the region between the plasma edge and the lower hybrid resonance, and that we are dealing with waves whose $n_{||} > 1$. Hence $\rho_1 = \epsilon_1/\epsilon_1 - n_{||}^2 < 0$.

Also

$$c^+c^- = -\epsilon_3\rho_2^2n_{||}^2 > 0 \quad \text{and} \quad c^+ + c^- = \epsilon_1 - \epsilon_3 - \frac{\epsilon_2^2}{\epsilon_1 - n_{||}^2} > 0, \quad \forall \omega_{pe}^2 > \omega^2$$

so that $c^+ > 0$, $c^- > 0$ for real $n_{||}$.

Thus $\text{sgn}(c^+\rho_1)$ and $\text{sgn}(c^-\rho_1)$ are both negative and we finally obtain

$$P_\xi = -2(\text{Im}[f_1^*f_2] + \text{Im}[f_3^*f_4]). \quad (4.23)$$

Similarly, upon substitution of (4.20) into (4.19) and using (4.22), we find that in the case of complex conjugate roots of $n_{||}$ P_ξ is given by

$$P_\xi = \frac{\text{sgn}(\rho_1)}{2} \text{Re} \left[(n^+ - n^-) \left(|f_1|^2 - \left| \frac{f_2}{\beta} \right|^2 + 2i\text{Im}[f_1^*f_2/\beta] \right. \right. \\ \left. \left. - |f_3|^2 + \left| \frac{f_4}{\beta} \right|^2 + 2i\text{Im}[f_3^*f_4/\beta] \right) \right].$$

Since $\beta = i(n^+ - n^-)/2$ is real here, equation (4.23) is again yielded.

4.5 Properties of the transformed system

With D given by (4.22) it remains to show that the coupling terms of (4.15) are nonsingular at points where the eigenvalues n^+ and n^- coincide. Heading's proof covers the case where D is the identity matrix. However the result is not true for arbitrary D, and since (4.22) involves the eigenvalues in a complicated way, the conclusion to be drawn in our case is not obvious. We therefore exhibit the elements of ADR^{-1} in order to determine the behaviour of the coupling matrices at eigenvalue confluence points.

We have that

$$\begin{aligned}
 \text{ADR}^{-1} &= \frac{1}{2} \begin{pmatrix} 1 & 1 & 1 & 1 \\ \alpha + \beta & \alpha - \beta & -(\alpha + \beta) & -(\alpha - \beta) \\ (\alpha + \beta)^2 & (\alpha - \beta)^2 & (\alpha + \beta)^2 & (\alpha - \beta)^2 \\ (\alpha + \beta)^3 & (\alpha - \beta)^3 & -(\alpha + \beta)^3 & -(\alpha - \beta)^3 \end{pmatrix} \times \text{diag}(d_1, d_2, d_1, d_2) \\
 &\times \begin{pmatrix} 1 & 1/\beta & 0 & 0 \\ 1 & -1/\beta & 0 & 0 \\ 0 & 0 & 1 & -1/\beta \\ 0 & 0 & 1 & 1/\beta \end{pmatrix} \\
 &= \frac{1}{2} (\rho_1 (n^+ + n^-) n^+ n^- c^+ c^-)^{-\frac{1}{2}} [a_{ij}]_{4 \times 4}
 \end{aligned}$$

where

$$\begin{aligned}
 a_{11} &= s^+, a_{12} = s^-/\beta, a_{13} = a_{11}, a_{14} = -a_{12} \\
 a_{21} &= s^+ \alpha + s^- \beta, a_{22} = \frac{s^-}{\beta} \alpha + s^+, a_{23} = -a_{21}, a_{24} = a_{22} \\
 a_{31} &= s^+ \alpha^2 + 2s^- \alpha \beta + s^+ \beta^2, a_{33} = a_{31} \\
 a_{32} &= \frac{s^-}{\beta} \alpha^2 + 2s^+ \alpha + s^- \beta, a_{34} = -a_{32} \\
 a_{41} &= s^+ \alpha^3 + 3s^- \beta \alpha^2 + 3s^+ \alpha \beta^2 + s^- \beta^3, a_{43} = -a_{41} \\
 a_{42} &= \frac{s^-}{\beta} \alpha^3 + 3s^+ \alpha^2 + 3s^- \beta \alpha + s^+ \beta^2, a_{44} = a_{42}
 \end{aligned}$$

and

$$s^{\pm} = (n^- c^-)^{\frac{1}{2}} \pm (n^+ c^+)^{\frac{1}{2}}.$$

Now,

$$\begin{aligned}
 s^- &= \frac{n^- c^- - n^+ c^+}{(n^+ c^+)^{\frac{1}{2}} + (n^- c^-)^{\frac{1}{2}}} \\
 &= \frac{2i\beta}{s^+} (\rho_1 ((n^+)^2 + (n^-)^2 + n^+ n^-) - \epsilon_3).
 \end{aligned}$$

Thus the elements of ADR^{-1} are quadratics in β^2 whose coefficients are finite at confluence points.

Then $\text{adj}(ADR^{-1})$ consists of further polynomials in β^2 with nonsingular coefficients and since

$$\det(ADR^{-1}) = \det(AR^{-1})\det D = \frac{4}{\rho_1^2 c^+ c^-} \neq 0,$$

the matrix $(ADR^{-1})^{-1} = \text{adj}(ADR^{-1})/\det(ADR^{-1})$ is nonsingular at confluence points.

The elements of $(ADR^{-1})'$ involve terms in $(\beta^2)'$ arising from differentiation of the factors β^2 and β^4 . But

$$\begin{aligned} (\beta^2)' &= -\frac{1}{4} (n^+ - n^-)(n^+ - n^-)' \\ &= \frac{1}{4} \left((n^+ n^-)' - \frac{((n^+)^2 + (n^-)^2)'}{2} \right) \\ &= \frac{1}{4} \left(\frac{(\epsilon_1 + \epsilon_3)(n_{II}^2 - \epsilon_1) + \epsilon_2^3}{2\epsilon_1} + \left(\frac{\epsilon_3((\epsilon_1 - n_{II}^2)^2 - \epsilon_2^2)}{\epsilon_1} \right)^{\frac{1}{2}} \right)' \end{aligned}$$

from (3.1). This derivative exists and is finite in the region between the fast wave cutoff and the lower hybrid resonance for reasonable (continuously differentiable) density and magnetic field profiles. The elements of (ADR^{-1}) also contain terms arising from differentiation of the coefficients of the quadratics in β^2 . We note that

$$\alpha' = \frac{i}{2} (n^+ + n^-)' = \frac{i}{2} \frac{(((n^+)^2 + (n^-)^2)/2 + n^+ n^-)'}{(n^+ + n^-)}.$$

Thus α' is also defined in terms of the finite derivatives of the sum and product of the roots of n_{\perp} .

Finally we must check the behaviour of $(s^+)'$. We have

$$\begin{aligned}(s^+)' &= ((n^+c^+)^{\frac{1}{2}} + (n^-c^-)^{\frac{1}{2}})' \\ &= \frac{(n^+c^+)'(n^-c^-)^{\frac{1}{2}} + (n^-c^-)'(n^+c^+)^{\frac{1}{2}}}{2(n^+n^-c^+c^-)^{\frac{1}{2}}} \\ &= \frac{(n^+c^+)'(s^+ + s^-) + (n^-c^-)'(s^+ - s^-)}{4(n^+n^-c^+c^-)^{\frac{1}{2}}}\end{aligned}$$

$$\begin{aligned}\text{i.e. } (s^+)' &= \frac{1}{4(n^+n^-c^+c^-)^{\frac{1}{2}}} \left[s^+[(n^+ + n^-)(\rho_1((n^+)^2 + (n^-)^2 - n^+n^-) - \epsilon_3)]' \right. \\ &\quad \left. - \frac{1}{s^+} [(n^+ - n^-)^2(\rho_1((n^+)^2 + (n^-)^2 + n^+n^-) - \epsilon_3)^2]' \right],\end{aligned}$$

so that $(s^+)'$ consists of derivatives which are finite at confluence points. We have demonstrated that the elements of $(\text{ADR}^{-1})^{-1}$ and $(\text{ADR}^{-1})'$ are nonsingular at confluence points. Hence the primary coupling terms in (4.15) are nonsingular at a confluence, and, since P is nonsingular, so are the secondary coupling terms.

Moreover, it can be verified (see Appendix for details) that the total coupling matrix in (4.15) is of the form

$$[t_{ij}]_{4 \times 4} = \begin{pmatrix} \begin{bmatrix} t_{11} & 0 \\ 0 & -t_{11} \end{bmatrix} & \begin{bmatrix} t_{13} & t_{14} \\ t_{23} & -t_{13} \end{bmatrix} e^{-\int 2\alpha d\xi} \\ \begin{bmatrix} t_{13} & -t_{14} \\ -t_{23} & -t_{13} \end{bmatrix} e^{\int 2\alpha d\xi} & \begin{bmatrix} t_{11} & 0 \\ 0 & -t_{11} \end{bmatrix} \end{pmatrix}$$

where

$$t_{11} = \frac{1}{8(n^+ n^- c^+ c^-)^{\frac{1}{2}}} \left[(n^+ + n^-)' (c^+ + c^-)' + \frac{\rho_1'}{\rho_1} (n^+ + n^-) (c^+ + c^-)' - (n^+ + n^-) (c^+ + c^-)' - \frac{2\epsilon_3' \rho_2^2 n_{11}^2}{\rho_1 (n^+ + n^-)} \right] \\ - \frac{(\beta^2)'}{4(n^+ n^- c^+ c^-)^{\frac{1}{2}}} \left[\frac{(\rho_1 ((n^+)^2 + (n^-)^2 + n^+ n^-) - \epsilon_3)^2}{(s^+)^2} + \frac{(\rho_1 n^+ n^- + \epsilon_3)^2}{((n^+ c^-)^{\frac{1}{2}} + (n^- c^+)^{\frac{1}{2}})^2} \right]$$

$$t_{13} = \frac{1}{4} \left(\frac{(n^+ n^-)'}{n^+ n^-} - \frac{\epsilon_3'}{\epsilon_3} \right)$$

$$t_{14} = \frac{i}{4(n^+ n^- c^+ c^-)^{\frac{1}{2}}} \left[(c^+ + c^-)' - (c^+ + c^-) \frac{(\rho_1 \alpha)'}{\rho_1 \alpha} \right] - \frac{\alpha'}{2n^+ n^-} \\ + \frac{i}{2(n^+ n^-)^{\frac{1}{2}}} \left[\frac{(\rho_1 ((n^+)^2 + (n^-)^2 + n^+ n^-) - \epsilon_3)(\rho_1 n^+ n^- + \epsilon_3)}{s^+ ((n^+ c^-)^{\frac{1}{2}} + (n^- c^+)^{\frac{1}{2}})} \right] \\ \times \left[\frac{\epsilon_3'}{\epsilon_3 \rho_1 (n^+ + n^-)} + \frac{(\beta^2)'}{(n^+ n^- c^+ c^-)^{\frac{1}{2}}} \right]$$

$$t_{23} = \frac{i}{8} \left[c^+ + c^- + \left(\frac{c^+ c^-}{n^+ n^-} \right)^{\frac{1}{2}} (n^+ + n^-) \right] \left[\frac{(\beta^2)'}{(n^+ n^- c^+ c^-)^{\frac{1}{2}}} - \frac{\epsilon_3'}{\epsilon_3 \rho_1 (n^+ + n^-)} \right] \\ - \beta^2 \left[\frac{i}{4(n^+ n^- c^+ c^-)^{\frac{1}{2}}} \left((c^+ + c^-)' - (c^+ + c^-) \frac{(\rho_1 \alpha)'}{\rho_1 \alpha} \right) + \frac{\alpha'}{2n^+ n^-} \right].$$

(4.24)

Thus the coupling terms are seen to depend on derivatives of ϵ_i , $i = 1, 2, 3$ and on combinations of n^+ and n^- and their derivatives which are well defined at a confluence of the eigenvalues. Also,

the terms which couple the positive n_{\perp} waves to the negative n_{\perp} pair, and vice versa, have a rapidly varying phase factor which tends to cancel their effect, so that interaction between the pairs is weak compared with coupling within each pair.

We chose D to make the Poynting flux conserved by (4.15) identical with the quantities conserved by two second order equations obtained from the principal terms alone. This necessarily forces an extra symmetry among the elements of $[t_{ij}]_{4 \times 4}$ so that the coupling terms in this case have the same conservation property. That is, the system

$$\underline{f}' = [t_{ij}]_{4 \times 4} \underline{f} \quad \text{also satisfies}$$

$$Im(f_1^* f_2) + Im(f_3^* f_4) = \text{const.}$$

If the neglected terms t_{ij} ($i, j = 1, 2$) are included in the principal system (4.16), then the equation describing coupling between the f_1 and f_2 variables becomes

$$\begin{pmatrix} f_1' \\ f_2' \end{pmatrix} = \begin{pmatrix} t_{11} & 1 \\ \beta^2 & -t_{11} \end{pmatrix} \begin{pmatrix} f_1 \\ f_2 \end{pmatrix}$$

$$\text{i.e.} \quad f_1'' - (\beta^2 + t_{11}' + (t_{11})^2) f_1 = 0. \quad (4.25)$$

Since t_{11} is real, (4.25) maintains the original conservation law, while in addition the error terms t_{11}' and $(t_{11})^2$ are second order quantities in the plasma gradients. This is not true if Heading's transformation is applied with $D = I_{4 \times 4}$, in which case the neglected terms t_{ij} , ($i, j = 1, 2$) lack symmetry so that their inclusion with the principal equation destroys the conservation law and the error

terms are then of first order in the plasma gradients, being larger by a factor $\omega L/c$ (where L is the gradient scale length) than the error terms in (4.25).

Finally we indicate the relation between the embedded second order equation (4.16) and our model Weber equation constructed earlier. The function $(n^+ - n^-)^2$ has at most two zeros and so we may write

$$(n^+ - n^-)^2 = g(\xi)(\xi - \xi_1)(\xi - \xi_2); \quad g(\xi) > 0 \quad \forall \xi.$$

Let

$$\xi_m = \xi_1 + \xi_2, \quad \zeta = h(\xi - \xi_m) \quad \text{and} \quad g(\xi) = G(\zeta).$$

Then (4.16) becomes

$$\frac{d^2 f}{d\zeta^2} + \frac{G(\zeta)}{4h^2} \left(\frac{\zeta^2}{h^2} - \frac{(\xi_1 - \xi_2)^2}{4} \right) f = 0.$$

The approximation now enters through an assumption about G . Taking $G(\zeta) = G(0)$, $\forall \zeta$, and $h = G^{\frac{1}{4}}(0)$, Weber's equation with $a = \frac{(\xi_1 - \xi_2)^2}{16} G^{\frac{1}{2}}(0)$ is obtained.

4.6 Approximate expressions for the electromagnetic fields

Given that the (f_1, f_2) and (f_3, f_4) pairs of variables are weakly coupled, we might try to describe the electromagnetic fields as follows.

Using our transformation

$$\underline{e} = M D E R^{-1} \underline{f} \quad (4.26)$$

with D given by (4.22), we concentrate on the (f_1, f_2) pair which corresponds to positive n_1 waves and set

$$f_3 = f_4 = 0$$

everywhere. Variables f_1 and f_2 are then taken to be the solutions of (4.16) posed as an initial value problem. With the functional behaviour of f thus prescribed, expressions for the physical fields follow from (4.26). So, in an approximate sense,

$$\begin{pmatrix} E_y \\ B_y \\ E_z \\ B_z \end{pmatrix} = \frac{e^{\int \xi, \alpha d\xi}}{[\rho_1(n^+ + n^-)]^{\frac{1}{2}}} [a_{ij}]_{4 \times 2} \begin{pmatrix} f_1 \\ f_2 \end{pmatrix}$$

where

$$\left. \begin{aligned} a_{11} &= \frac{1}{2} \left[\left(\frac{c^+}{n^+} \right)^{\frac{1}{2}} + \left(\frac{c^-}{n^-} \right)^{\frac{1}{2}} \right] \\ a_{12} &= \frac{-i}{(n^+ - n^-)} \left[\left(\frac{c^+}{n^+} \right)^{\frac{1}{2}} - \left(\frac{c^-}{n^-} \right)^{\frac{1}{2}} \right] = \frac{-i}{2n^+n^-a_{11}} (\rho_1 n^+n^- + \epsilon_3) \\ a_{21} &= -i\epsilon_3\rho_2n_{||} \left[\frac{1}{(n^+c^+)^{\frac{1}{2}}} + \frac{1}{(n^-c^-)^{\frac{1}{2}}} \right] \\ a_{22} &= \frac{i\epsilon_3}{2n^+n^-a_{21}} \left[\rho_1((n^+)^2 + (n^-)^2 + n^+n^-) - \epsilon_3 \right] \\ a_{31} &= \frac{i\rho_2n_{||}}{2} \left[\left(\frac{n^+}{c^+} \right)^{\frac{1}{2}} + \left(\frac{n^-}{c^-} \right)^{\frac{1}{2}} \right] \\ a_{32} &= \frac{i}{2\epsilon_3a_{31}} [\rho_1 n^+n^- + \epsilon_3] \\ a_{41} &= \frac{1}{2} [(n^+c^+)^{\frac{1}{2}} + (n^-c^-)^{\frac{1}{2}}] \\ a_{42} &= \frac{-i}{2a_{41}} [\rho_1((n^+)^2 + (n^-)^2 + n^+n^-) - \epsilon_3] \end{aligned} \right\} (4.27)$$

Also,

$$E_x = (n_n B_y + i\epsilon_2 E_y)/\epsilon_1. \quad (4.28)$$

In the next chapter, these expressions are used to calculate the electric field variation. We will see that the results obtained in this way compare very well with exact field profiles calculated from the solutions of the full fourth order equation (4.2).

CHAPTER 5

SOME NUMERICAL COMPARISONS

5.1 Transmission Coefficients

In this section, transmission coefficients obtained from numerical integration of our exact fourth order equations (4.2) are compared with results given by the second order theory of Chapter 3. The comparison is carried out for the uniform magnetic field case only

The lower hybrid mode conversion is very sensitive to $n_{||}$ in that the transmission coefficients can differ significantly from 1/2 for deviations $|\Delta n|/n_c$ as small as 2×10^{-4} . Therefore the order μ corrections to expression (3.6) for n_c^2 , while not important in the final result (3.29), must be kept if we are to follow the mode conversion numerically. As before we take a linear density profile, and rework the algebra of Section 3.1, but using the full condition (3.38), rather than (3.5), for a confluence of the roots of n_{\perp}^2 to occur. The corrected forms of equations (3.6) and (3.7) are then given by

$$n_c^2 = \frac{1}{1-y^2} - \mu(1-y^2) \quad (5.1)$$

and

$$X_0 = \frac{y^2}{\mu(1-y^2)(1-\mu(1-y^2)^2)} - 1. \quad (5.2)$$

An integration routine, available from the FORTRAN NAG Library, which employs the explicit Runge-Kutta method is used to solve an initial value problem for the mode coupling configuration of Fig.5.1

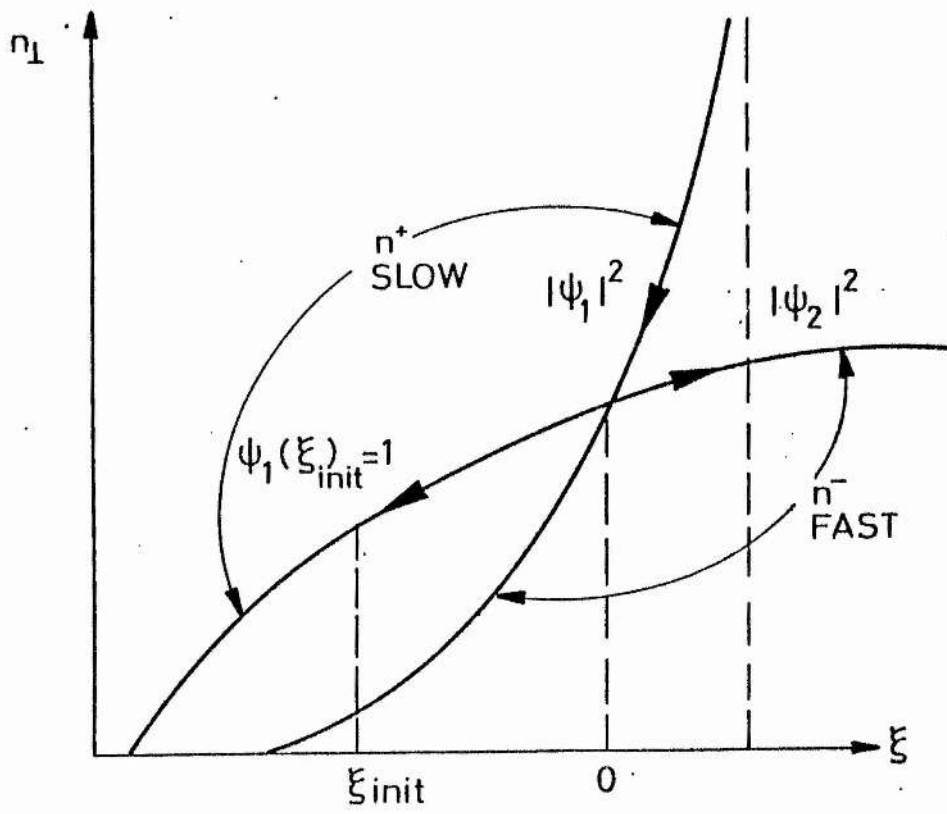


Figure 5.1 Mode coupling configuration for initial value problem (5.3)

in which a slow wave is incident from the high density side.

We solve

$$\frac{de}{d\xi} = T_{4 \times 4} e ; e(\xi_{init}) = e_1 \quad (5.3)$$

with

$$e_1 = [n^+ c^+ (c^+ - c^-)]^{-\frac{1}{2}} m_1 \Big|_{\xi = \xi_{init}}$$

(notation defined as in (4.12)), so that the initial polarisation is in the positive n_1 slow mode, and where the density dependence in $T_{4 \times 4}$ is taken as

$$\frac{\omega_{pe}^2}{\omega^2} \equiv X = X_0 \left(1 + \frac{c\xi}{\omega L} \right).$$

The starting point ξ_{init} for the integration is determined by the root of the equation

$$\frac{d}{d\xi} (n^+ - n^-) = 0.$$

That is, ξ_{init} is the point on the low density side at which the two wavenumbers are furthest apart. Of course a more natural initial value problem than that of Fig 5.1 is one for which there are incident and mode converted waves in the region $\xi < 0$, while transmitted slow wave energy proceeds towards the resonant layer. In this case, integration must start on the high density side and continue until we reach a point in the region $\xi < 0$ where convergence of the quantities which give the energy flux in each mode, and hence the transmission coefficient, is achieved. However it is not numerically feasible to solve this initial value problem since these quantities

never converge to within an acceptable accuracy (2 decimal places). This happens because the roots n^+ and n^- do not diverge sufficiently in the low density region to allow asymptotic development of the WKBJ solutions.

Transmission and conversion coefficients are calculated as follows. The solutions of (5.3) may be represented in asymptotic regions of propagation by a linear combination of the four characteristic waves so that we can write

$$\underline{e} = M\Delta\underline{\psi}$$

with

$$\Delta = \text{diag}(d_1, d_2, d_1, d_2), \quad d_1 = [n^+ c^+ (c^+ - c^-)]^{-\frac{1}{2}}, \quad d_2 = [n^- c^- (c^+ - c^-)]^{-\frac{1}{2}} \quad (5.4)$$

where Δ is chosen to normalise the Poynting flux of each mode to unity (see (4.18)) Then \underline{e}_1 is given by setting

$$\underline{\psi}(\xi_{\text{init}}) = (1, 0, 0, 0)^t.$$

We solve (5.3) for the fields \underline{e} and then invert (5.4) in the asymptotic region $\xi > 0$ to obtain the amplitudes $\underline{\psi}$ which correspond to the Poynting flux in each of the four modes. The transmission coefficient is given by

$$T = \lim_{\xi \gg 0} \left| \frac{\psi_1(\xi_{\text{init}})}{\psi_1(\xi)} \right|^2 = \lim_{\xi \gg 0} \frac{1}{|\psi_1(\xi)|^2}$$

while the fraction of energy converted to fast waves is

$$MC = \lim_{\xi \gg 0} \left| \frac{\psi_2(\xi)}{\psi_1(\xi)} \right|^2.$$

As expected, we also find that

$$T + MC = 1 \quad (\text{to four decimal places})$$

and

$$|\psi_3|^2, |\psi_4|^2 \sim O(10^{-4}) \text{ in the region } \xi \gg 0,$$

indicating that neither of the negative n_1 waves is excited. Table 5.1 compares transmission coefficients, $T_{\text{numerical}}$, obtained according to this scheme with results given by the second order theory (3.29). Good agreement is indicated.

5.2 Electric field variation in the mode coupling region

Figures 5.2, 5.4 and 5.6 show the spatial variation of the x, y and z components respectively of the electric field vector obtained from the solutions of the exact fourth order problem (5.3) for the case $n_u = n_c$. These illustrate the expected mode conversion behaviour. The waveform in $\xi > 0$, a mixture of the incident and converted modes, becomes a resonant response around $\xi = 0$ and connects to a single sinusoidal component which is the transmitted slow wave.

Next we solve the second order system

Table 5.1 Parameters $\omega/2\pi = 800$ MHz, $B_0 = 2.5$ Tesla, $L = 0.4$ m
and $m_i/m_e = 3672$.

$\Delta n/n_c$	$I_{\text{numerical}}$	I_{theory}
-1.0×10^{-3}	0.007	0.007
-5.0×10^{-4}	0.080	0.079
-4.0×10^{-4}	0.124	0.123
-3.0×10^{-4}	0.187	0.186
-2.5×10^{-4}	0.226	0.226
-2.0×10^{-4}	0.271	0.272
-1.5×10^{-4}	0.320	0.323
-1.0×10^{-4}	0.374	0.379
-5.0×10^{-5}	0.431	0.438
0.0	0.490	0.500
$+5.0 \times 10^{-5}$	0.549	0.561
1.0×10^{-4}	0.607	0.620
1.5×10^{-4}	0.662	0.675
2.0×10^{-4}	0.713	0.725
2.5×10^{-4}	0.759	0.774
3.0×10^{-4}	0.800	0.814
4.0×10^{-4}	0.866	0.877
5.0×10^{-4}	0.914	0.921
8.0×10^{-4}	0.981	0.981

Figure 5.2 Spatial variation of E_x (arbitrary units) across the mode conversion region calculated from the solutions of the full fourth order problem (5.3) for the case $n_n = n_c$, with parameters $\omega/2\pi = 800$ MHz, $B_0 = 2.5$ Tesla, $L = 0.4$ m and $m_i/m_e = 3672$.

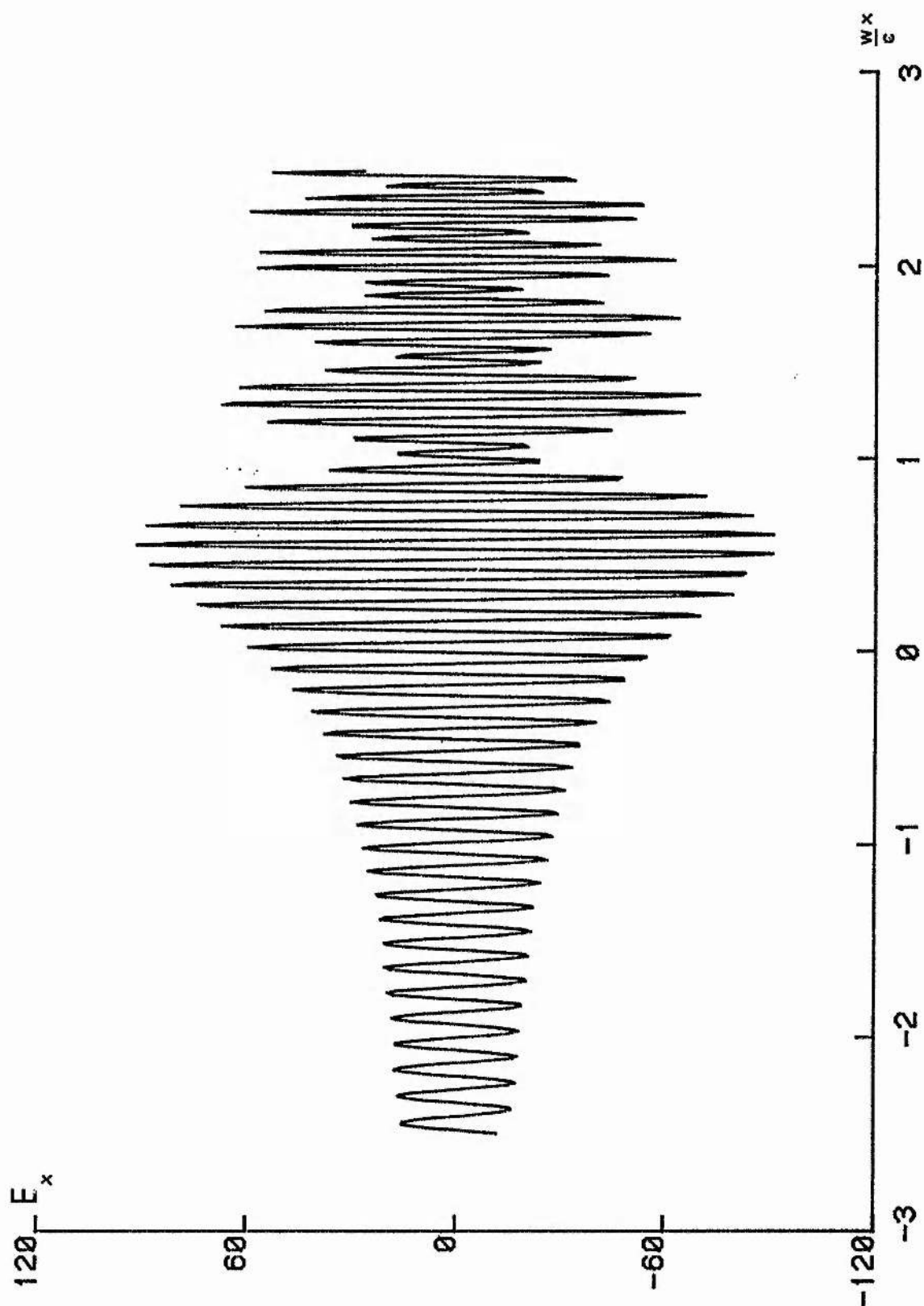


Figure 5.3 Difference between the exact E_x values of Fig 5.2 and those obtained by using the solutions of the second order initial value problem (5.5) in our transformation (4.25). That is

$$\Delta E_x = (E_x)_{4\text{th order}} - (E_x)_{2\text{nd order}}.$$

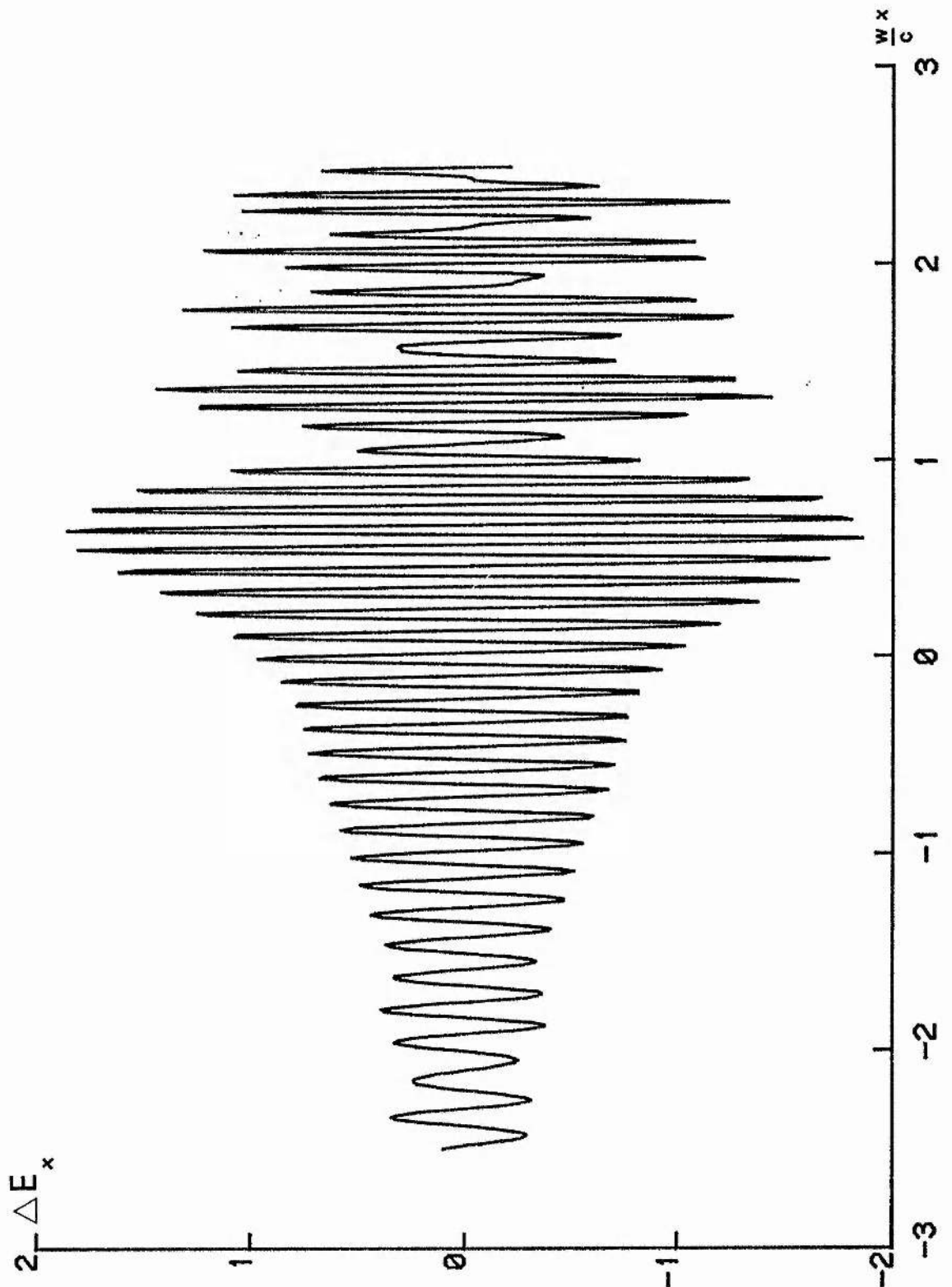


Figure 5.4 Spatial variation of E_y calculated as for Fig 5.2.

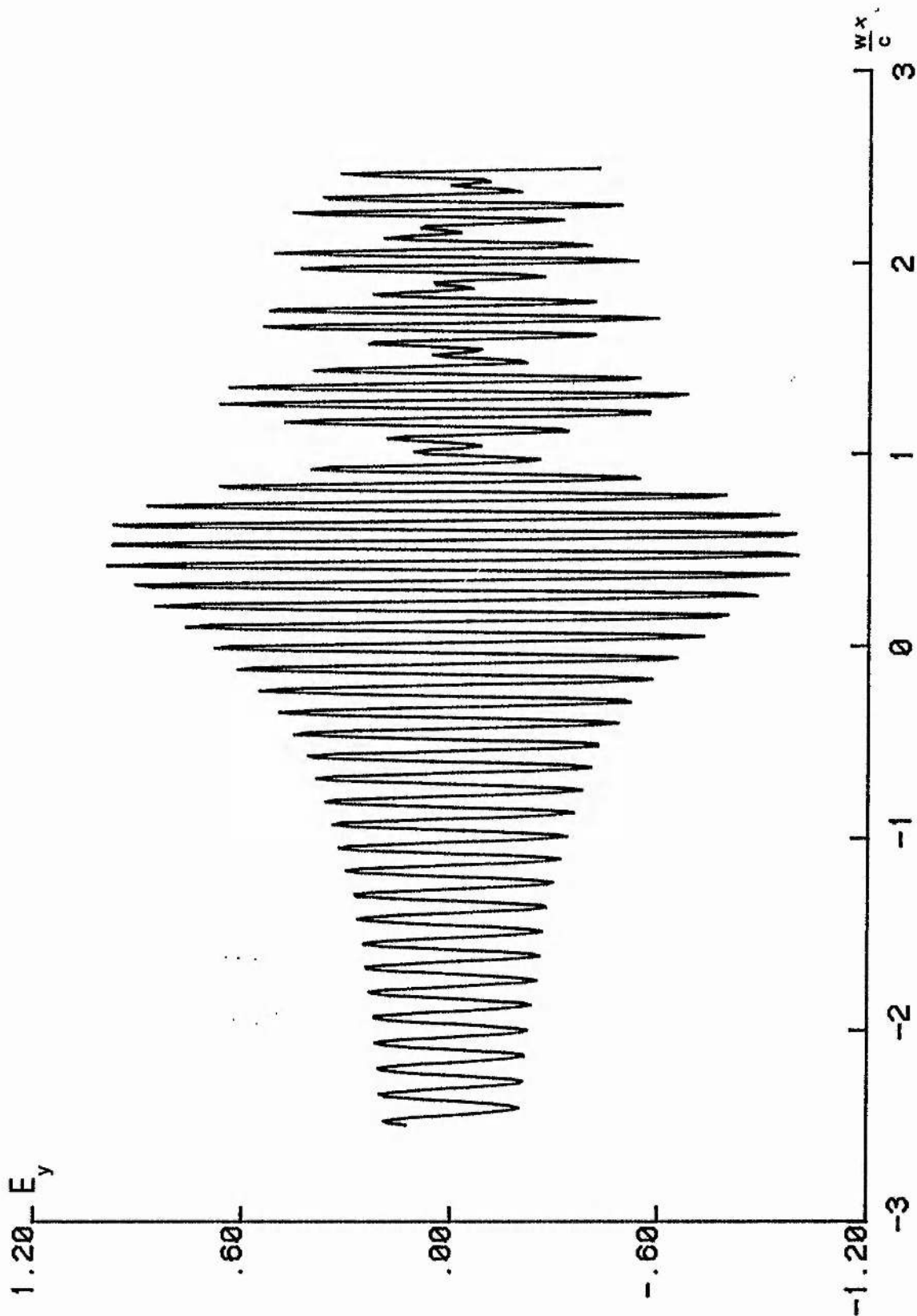


Figure 5.5 Difference between the exact E_y values of Fig 5.4 and those obtained by using the solutions of (5.5) in (4.25).

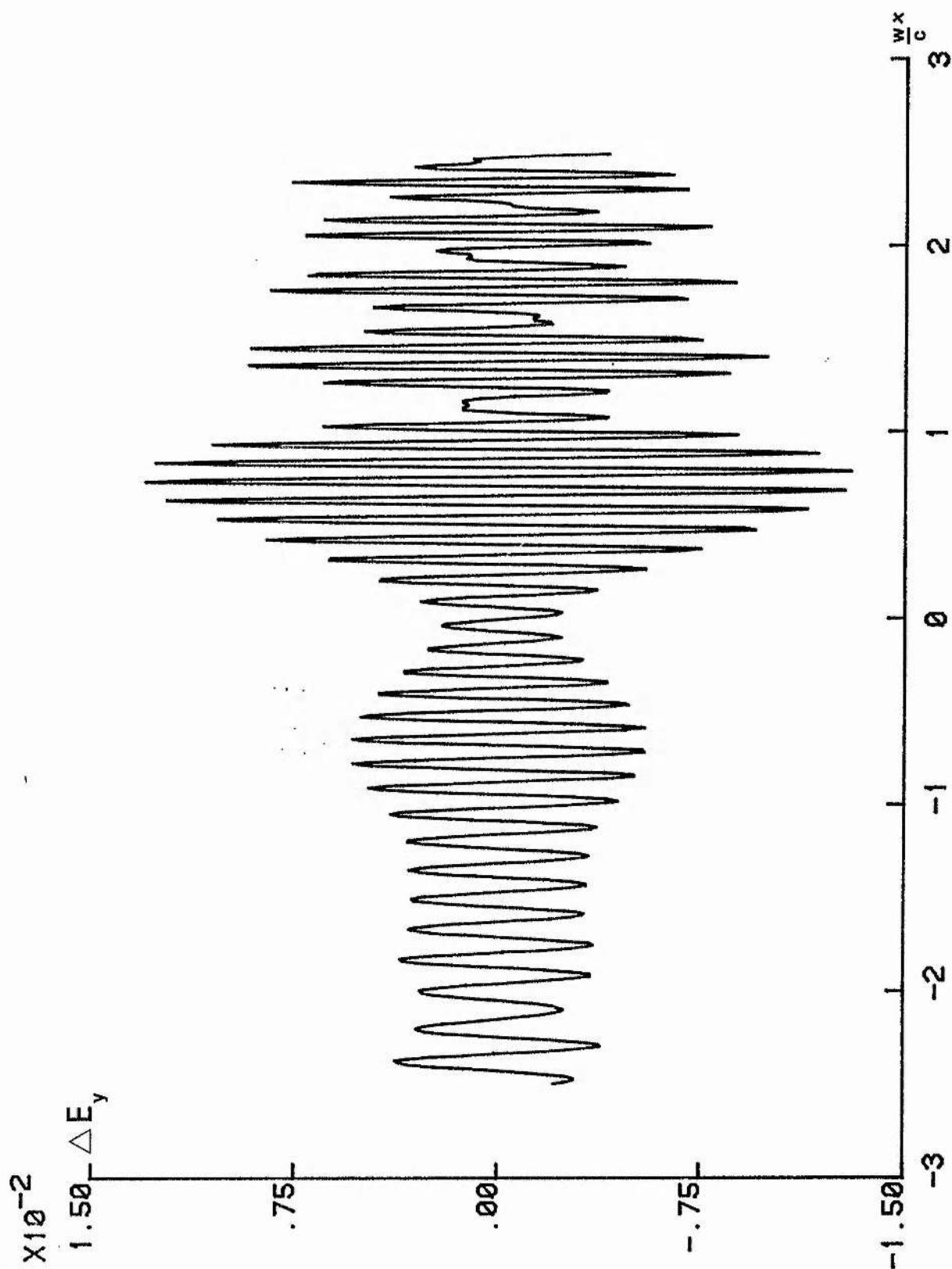


Figure 5.6 Spatial variation of E_z calculated as for Fig 5.2

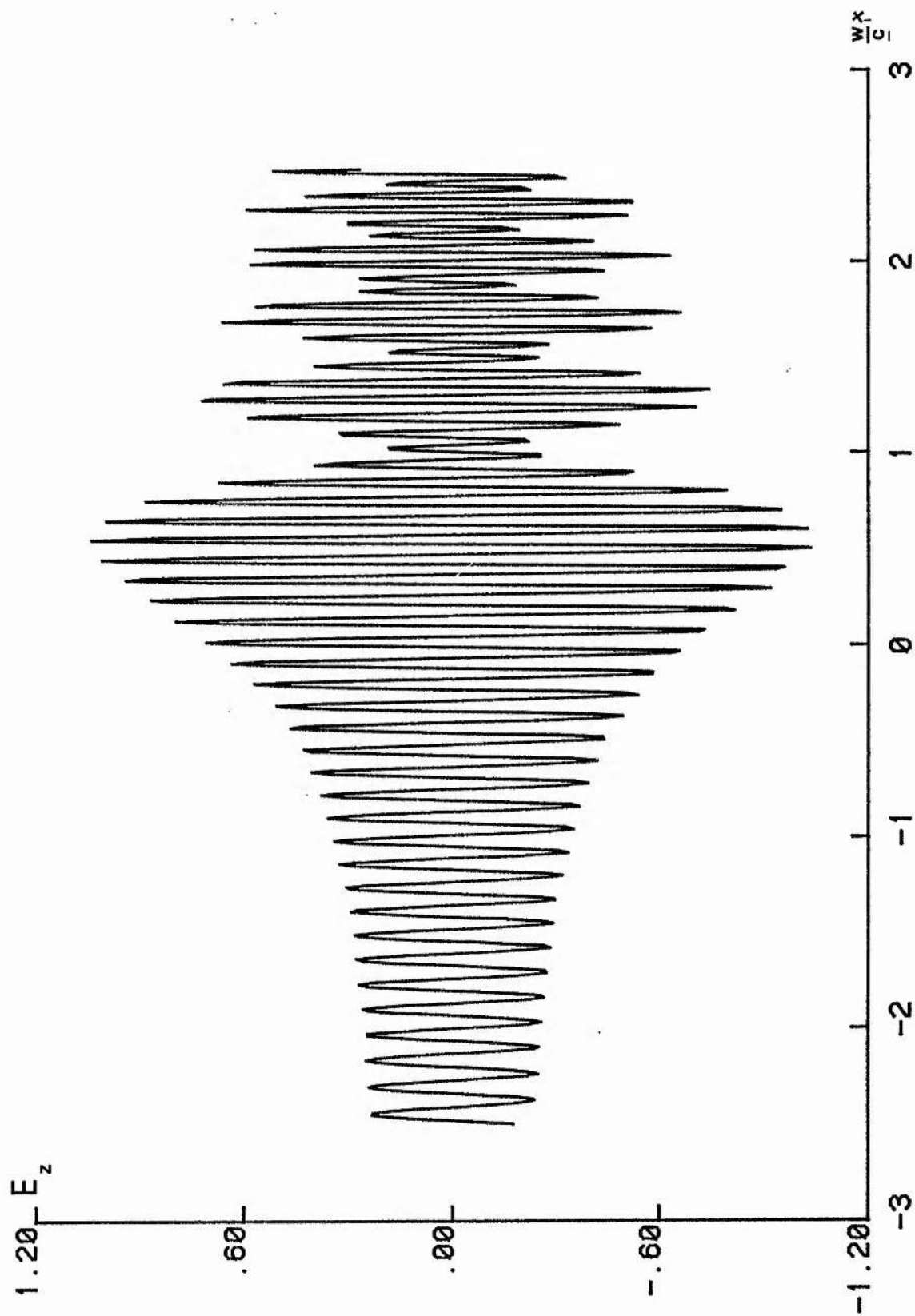
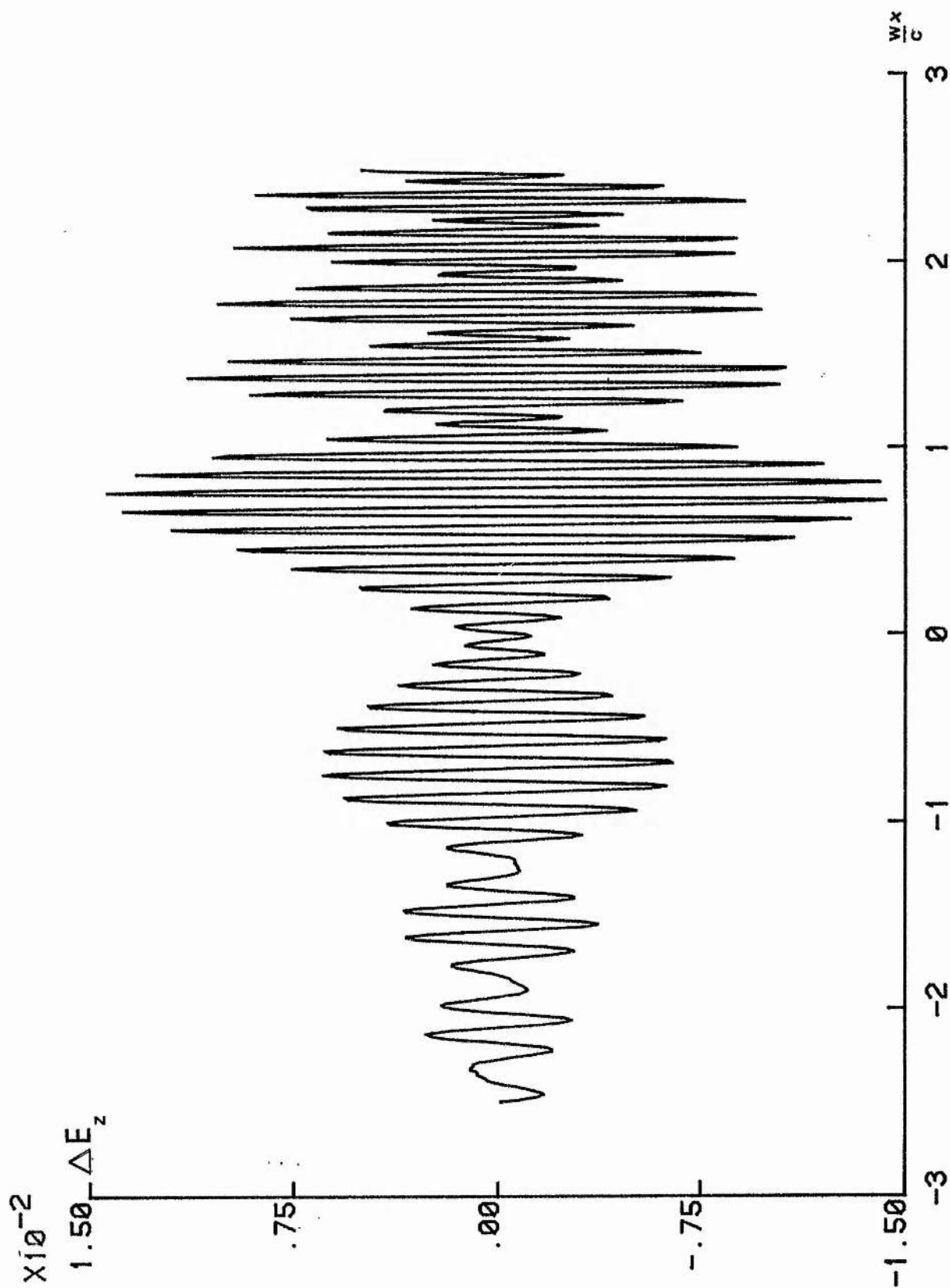


Figure 5.7 Difference between the exact E_z values of Fig 5.6 and those obtained by using the solutions of (5.5) in (4.25).



$$\left. \begin{aligned} f_1' &= f_2 \\ f_2' &= -\frac{(n^+ - n^-)^2}{4} f_1 \end{aligned} \right\} \quad (5.5)$$

where the initial values for \underline{f} are related to the full fourth order condition by

$$\underline{e}_1 = \text{MDER}^{-1} \begin{pmatrix} f_1 \\ f_2 \\ 0 \\ 0 \end{pmatrix} \bigg|_{\xi = \xi_{\text{init}}}$$

and D is as defined in (4.22).

Hence

$$f_1(\xi_{\text{init}}) = \frac{1}{(n^+ - n^-)^{\frac{1}{2}}} \bigg|_{\xi = \xi_{\text{init}}}, \quad f_2(\xi_{\text{init}}) = \frac{i}{2} (n^+ - n^-)^{\frac{1}{2}} \bigg|_{\xi = \xi_{\text{init}}}.$$

The solutions of (5.5) are now used in conjunction with (4.26), (4.27) and (4.28) to obtain expressions for the electric fields, which we compare with the full fourth order solutions by graphing their algebraic difference in Figs.5.3, 5.5 and 5.7.

Examination of Figs.5.2 and 5.3, say, together reveals that the second order values for E_x deviate from the exact fourth order values by less than 2% throughout the integration region, and similarly for the E_y and E_z components. This conclusion also holds away from the critical value of $n_{||}$ as is seen by comparing Figs.5.8, 5.10 and 5.12, which show the exact electric field variation for a case $n_{||} < n_c$, with the difference plots of Figs.5.9, 5.11 and 5.13

Figure 5.8 Spatial variation of E_x (arbitrary units) across the mode conversion region calculated from the solutions of the full fourth order problem (5.3) for the case $\Delta n/n_c = -2.5 \times 10^{-4}$, with parameters $\omega/2\pi = 800$ MHz, $B_0 = 2.5$ Tesla, $L = 0.4$ m and $m_i/m_e = 3672$.

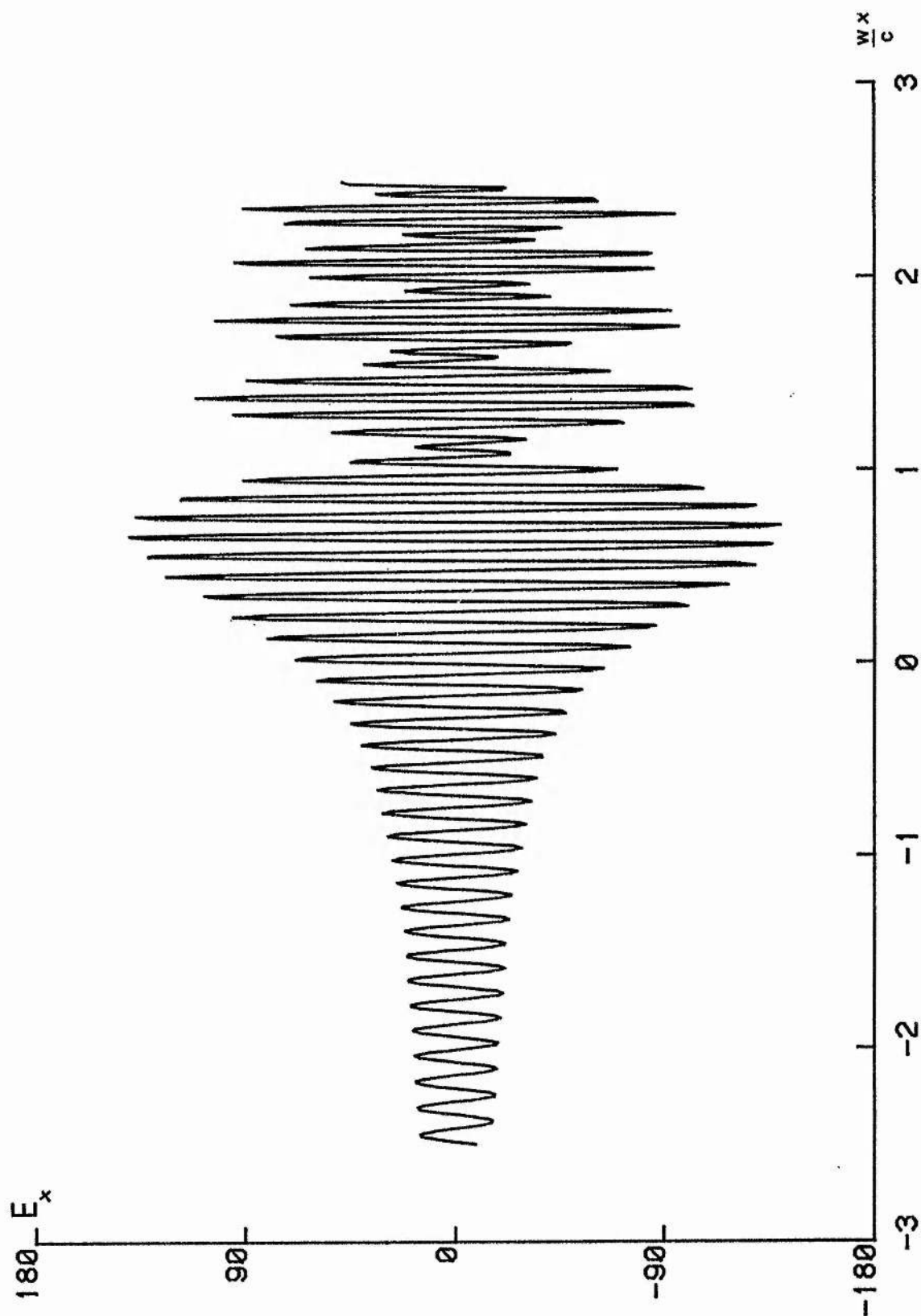


Figure 5.9 Difference between the exact E_x values of Fig 5.8 and those obtained by using the solutions of (5.5) in (4.25).

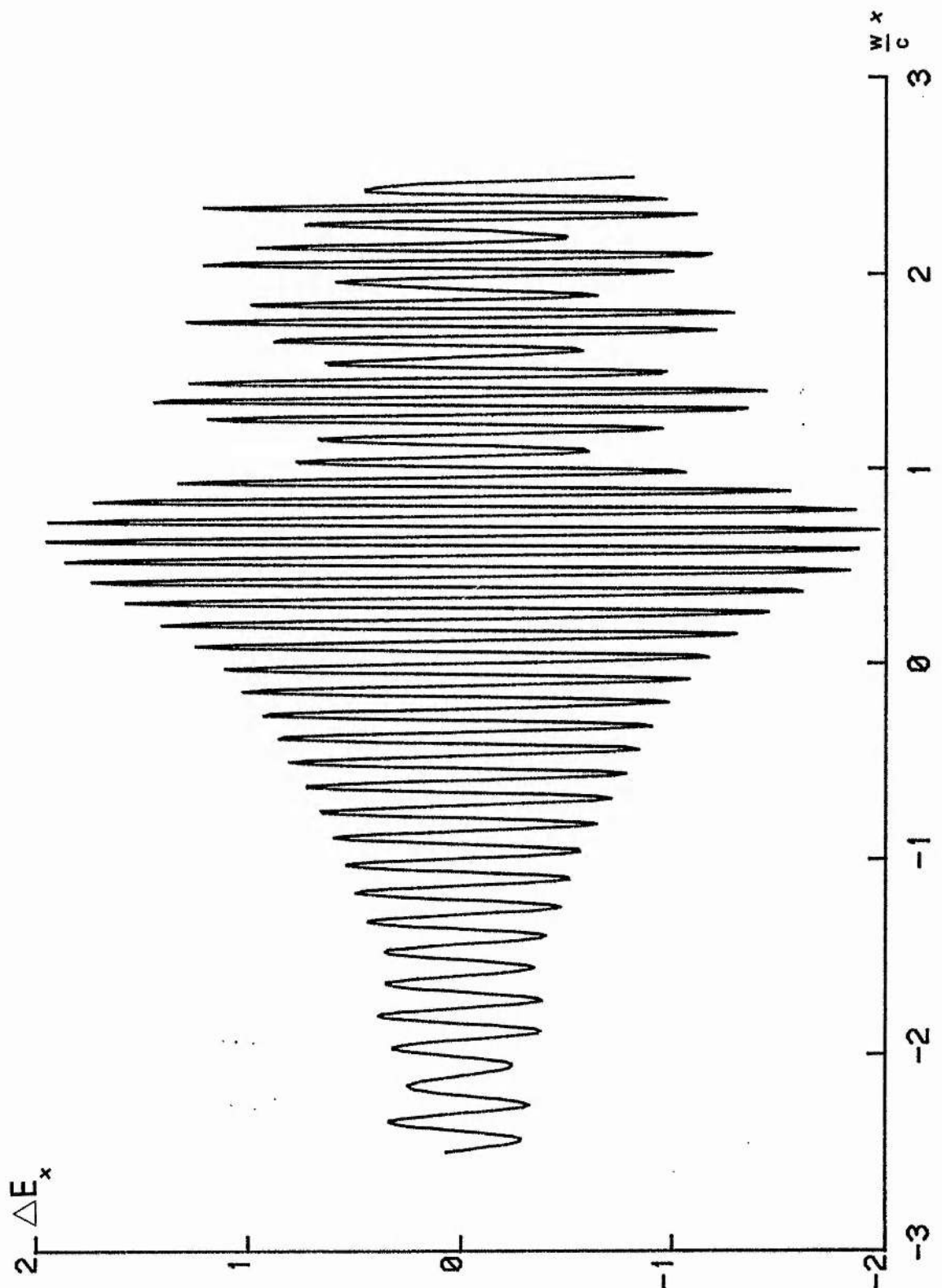


Figure 5.10 Spatial variation of E_y calculated as for Fig 5.8.

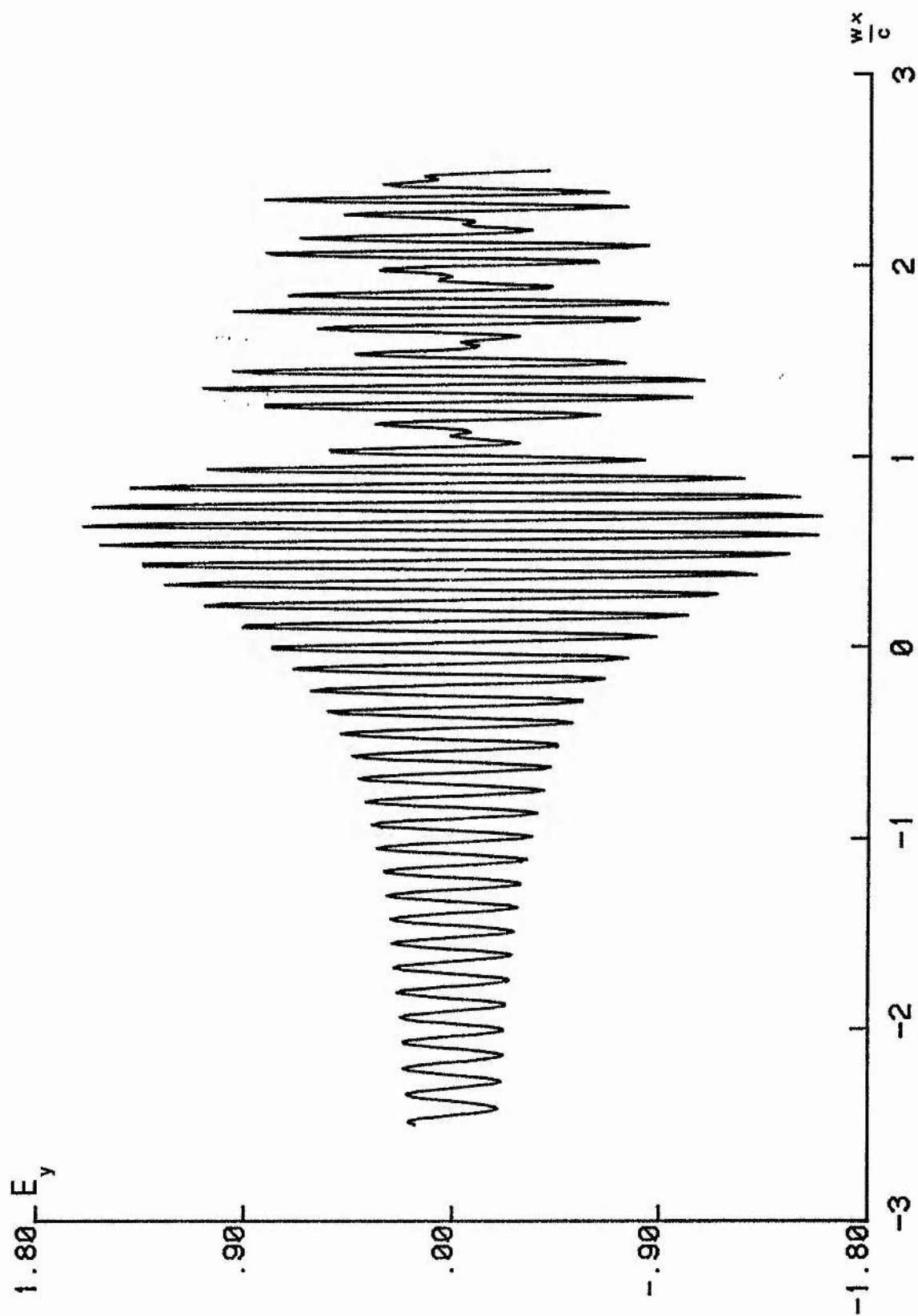


Figure 5.11 Difference between exact E_y values of Fig 5.10 and those obtained by using the solutions of (5.5) in (4.25).

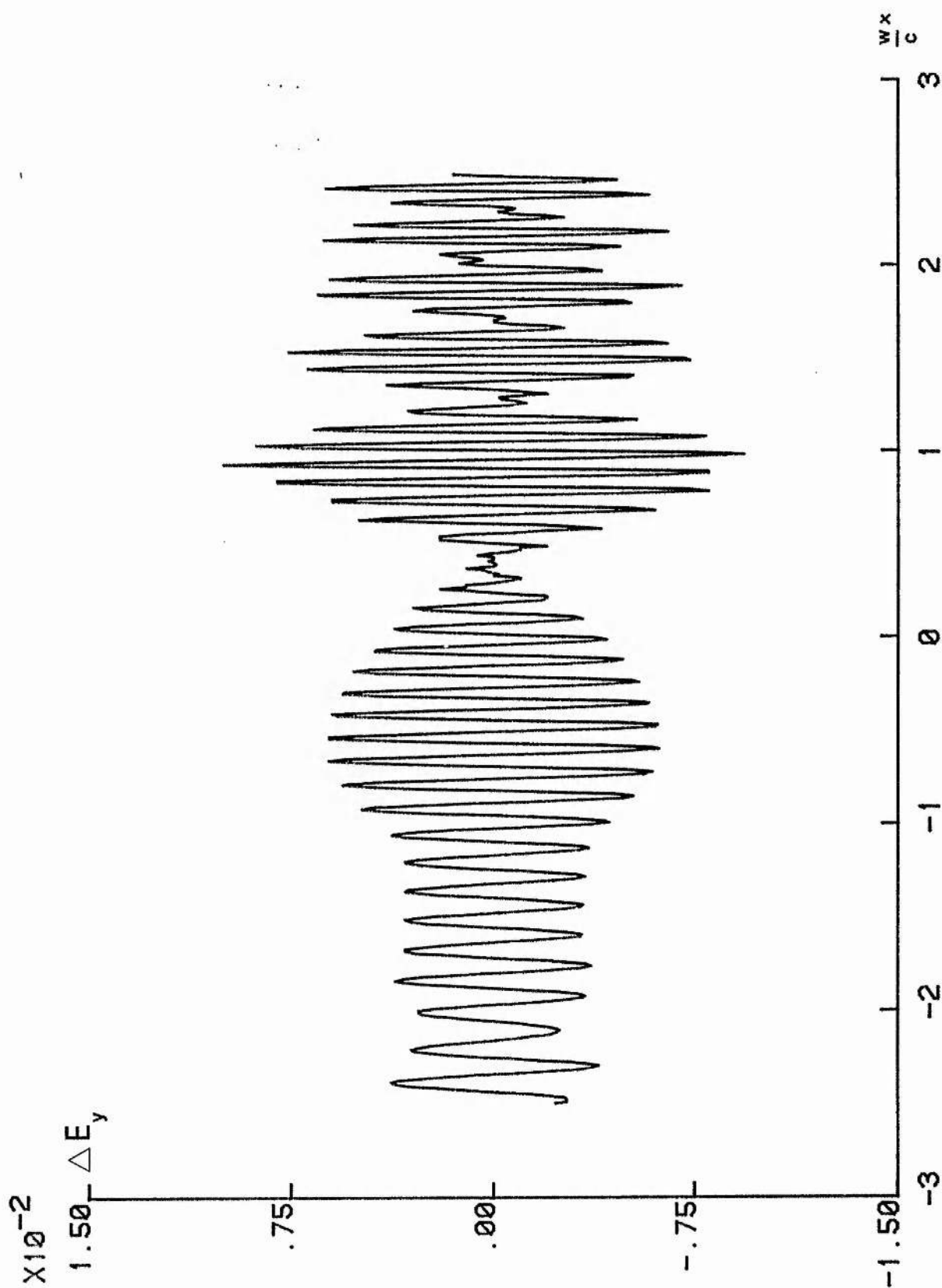


Figure 5.12 Spatial variation of E_z calculated as for Fig 5.8.

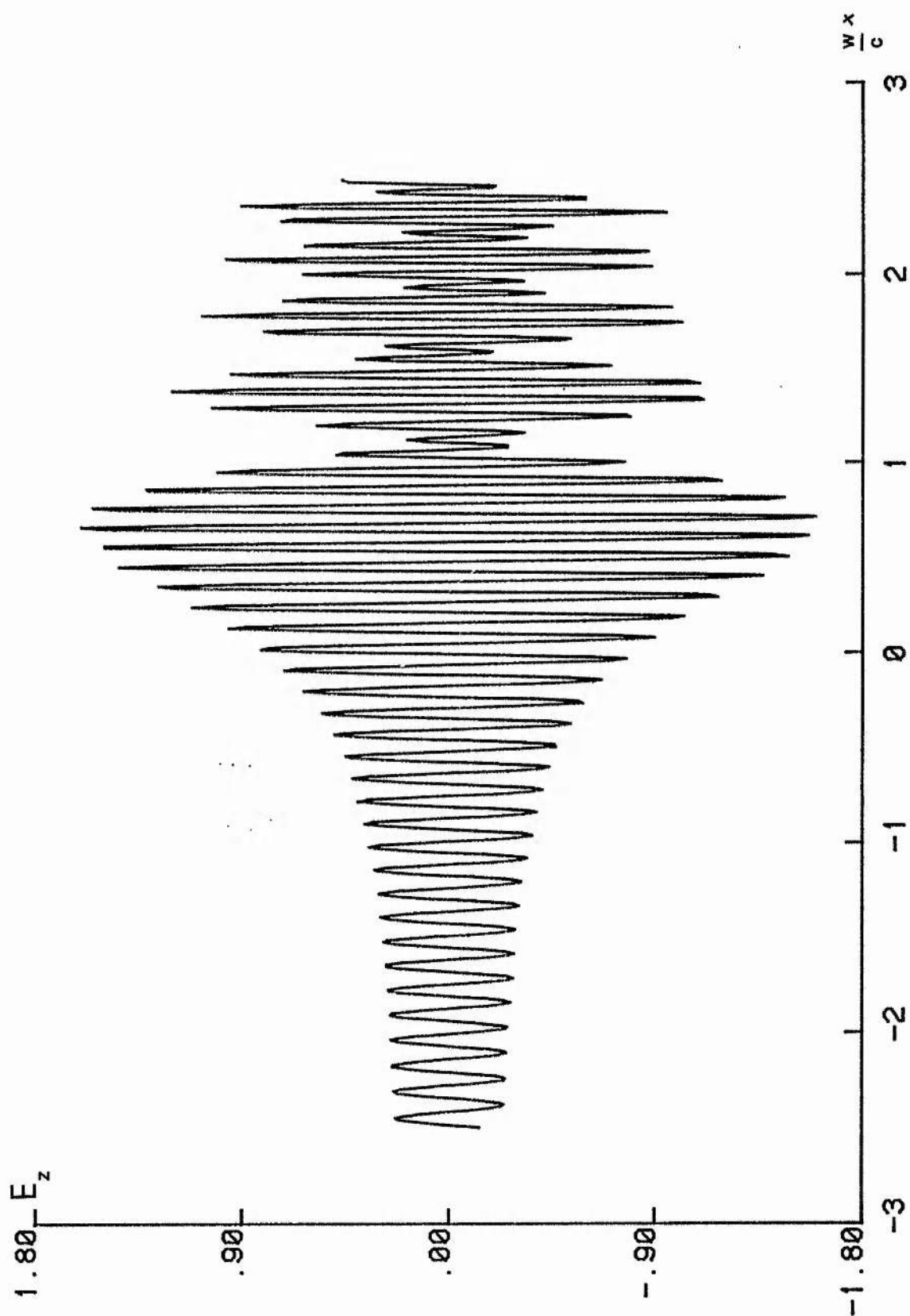
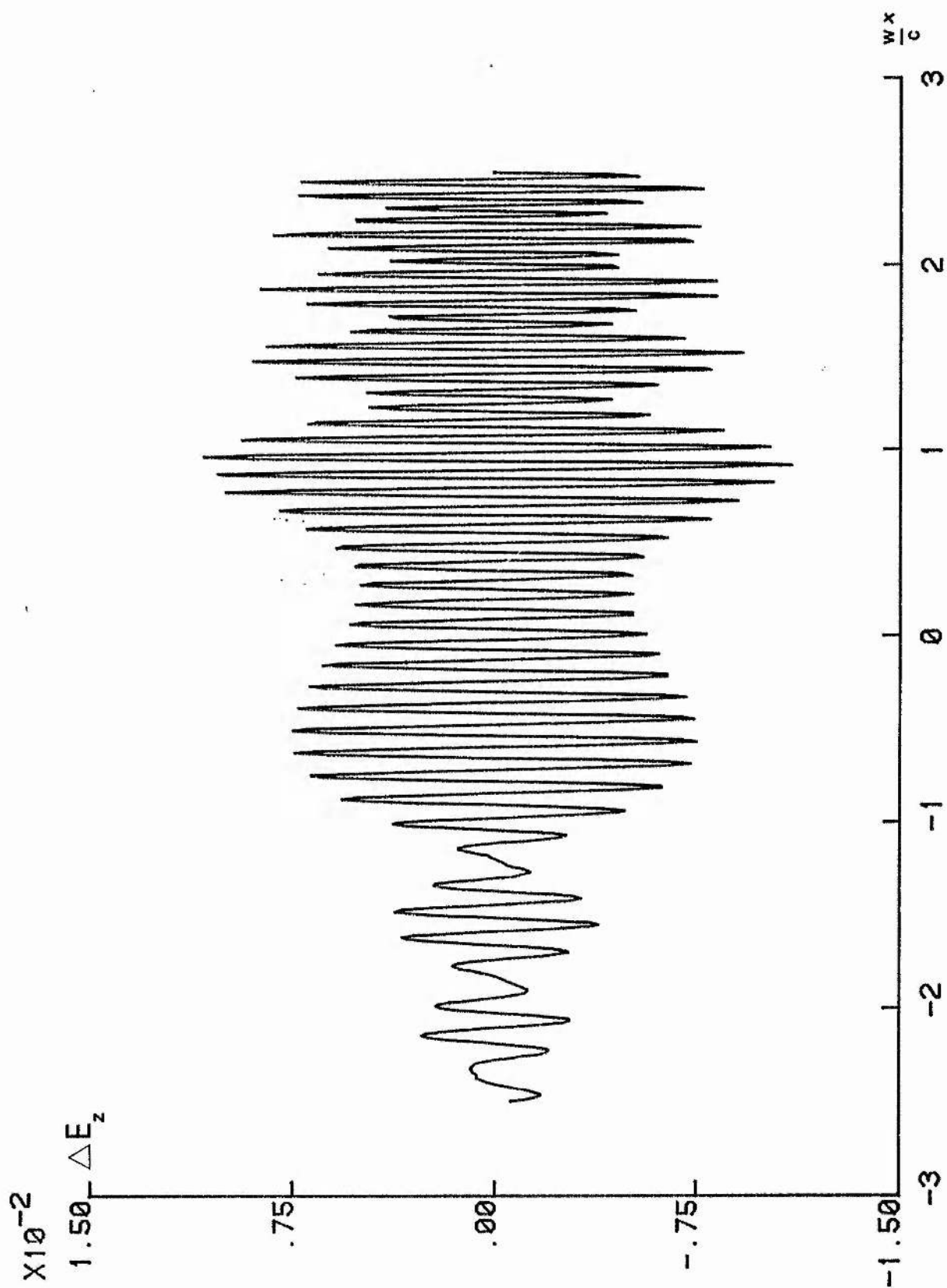


Figure 5.13 Difference between exact E_z values of Fig 5.12 and those obtained by using the solutions of (5.5) in (4.25).



respectively. For completeness we also consider a case $n_{||} > n_c$, the exact field variation being shown in Figs.5.14, 5.16 and 5.18, while the difference between exact and second order solutions is plotted in Figs.5.15, 5.17 and 5.19. Also of interest on the difference plots are the small amplitude beating structures in the region $\xi < 0$. These plots show what is left of the full solution once the positive n_{\perp} waves have been factored out, and since a single WKB solution of the fourth order equation is coupled, albeit weakly, to the other three, what we are seeing here is a small admixture of the negative n_{\perp} modes present in the full solution, which beat together as their wavenumbers converge.

As a final comparison, we solve the second order initial value problem (5.5) for the case $n_{||} = n_c$, but with $D = I_{4 \times 4}$ as in Heading's original formulation, and plot the electric field variation obtained from this procedure in Figs.5.20, 5.21 and 5.22. Comparing these graphs with Figs.5.1, 5.2 and 5.3, we find that Heading's original transformation, when applied to the solutions of (5.5), exactly reproduces the detailed phase variation of the fields, but it does not give the correct behaviour for the amplitudes of the oscillations. These differ from the amplitudes of the full fourth order solutions by a monotonically increasing factor which varies between 2 and 5 in the ξ range plotted.

In order to better approximate the field amplitudes using Heading's transformation and the solutions of a second order equation, we must retain in (5.5) the coupling terms which, as mentioned in Section 4.5, are of first order in the plasma gradients. To see

Figure 5.14 Spatial variation of E_x (arbitrary units) across the mode conversion region calculated from the solutions of the full fourth order problem (5.3) for the case $\Delta n/n_c = +2.5 \times 10^{-4}$, with parameters $\omega/2\pi = 800$ MHz, $B_0 = 2.5$ Tesla, $L = 0.4$ m and $m_i/m_e = 3672$.

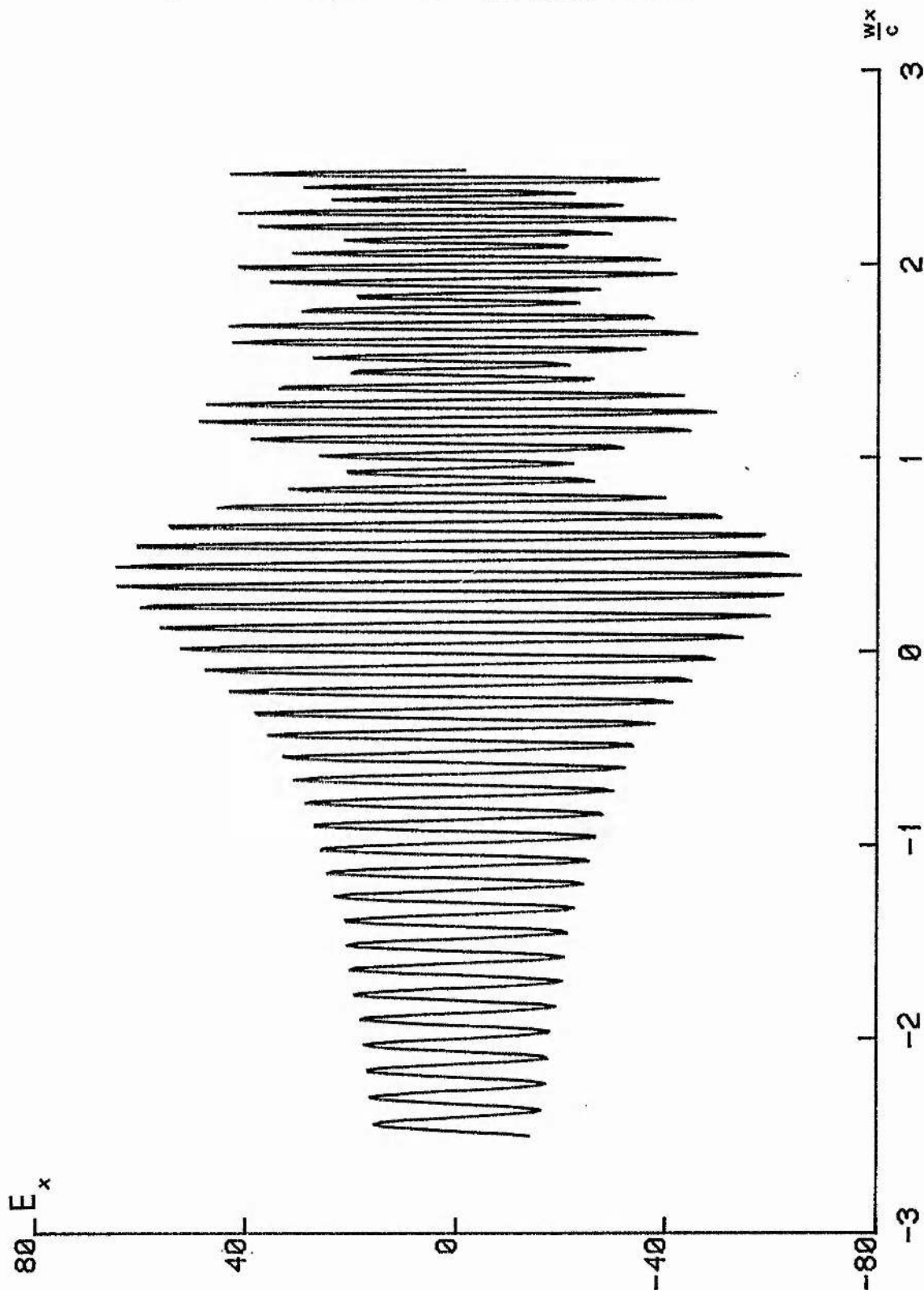


Figure 5.15 Difference between exact E_x values of Fig 5.14 and those obtained by using the solutions of (5.5) in (4.25).

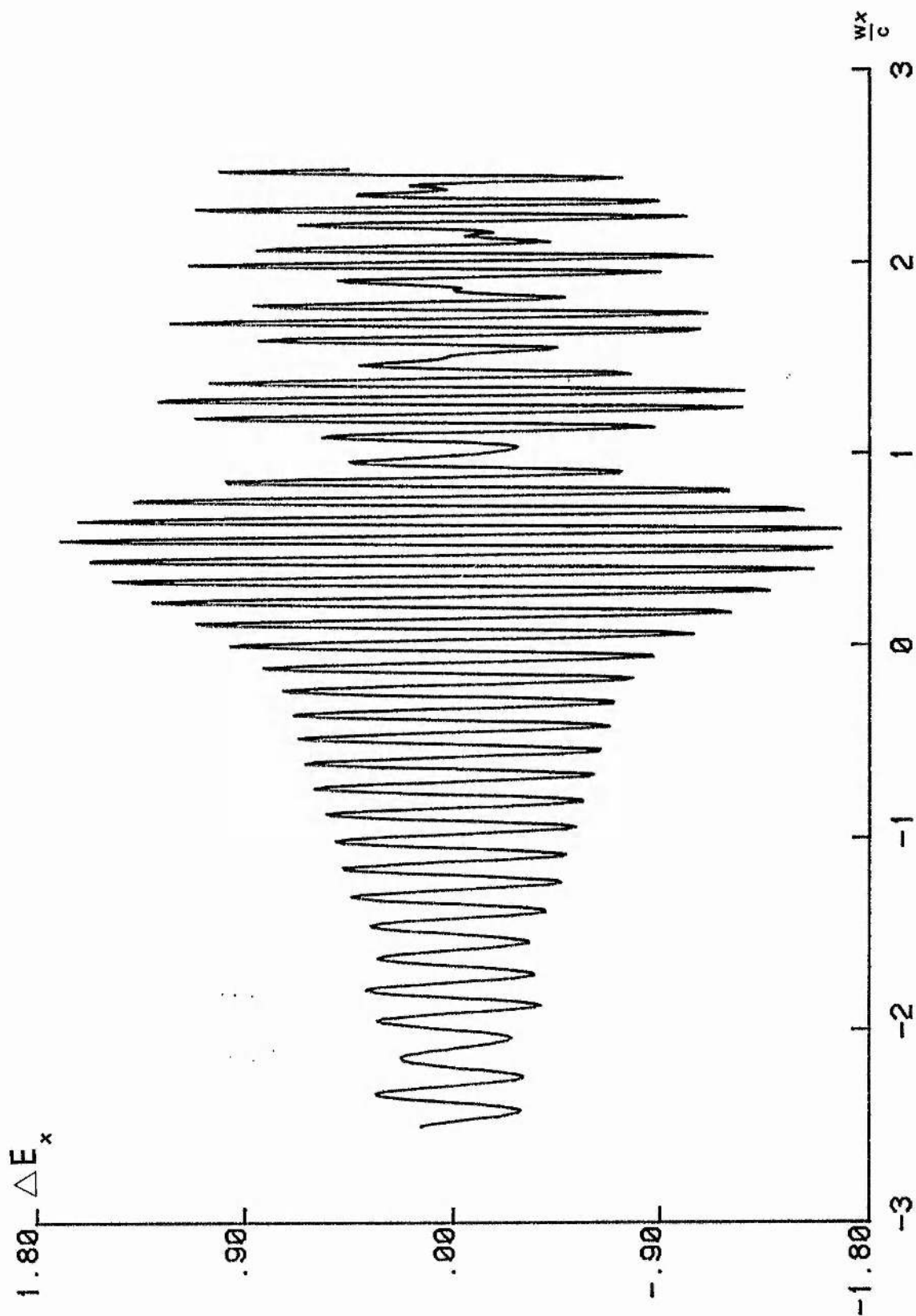


Figure 5.16 Spatial variation of E_y calculated as for Fig 5.14.

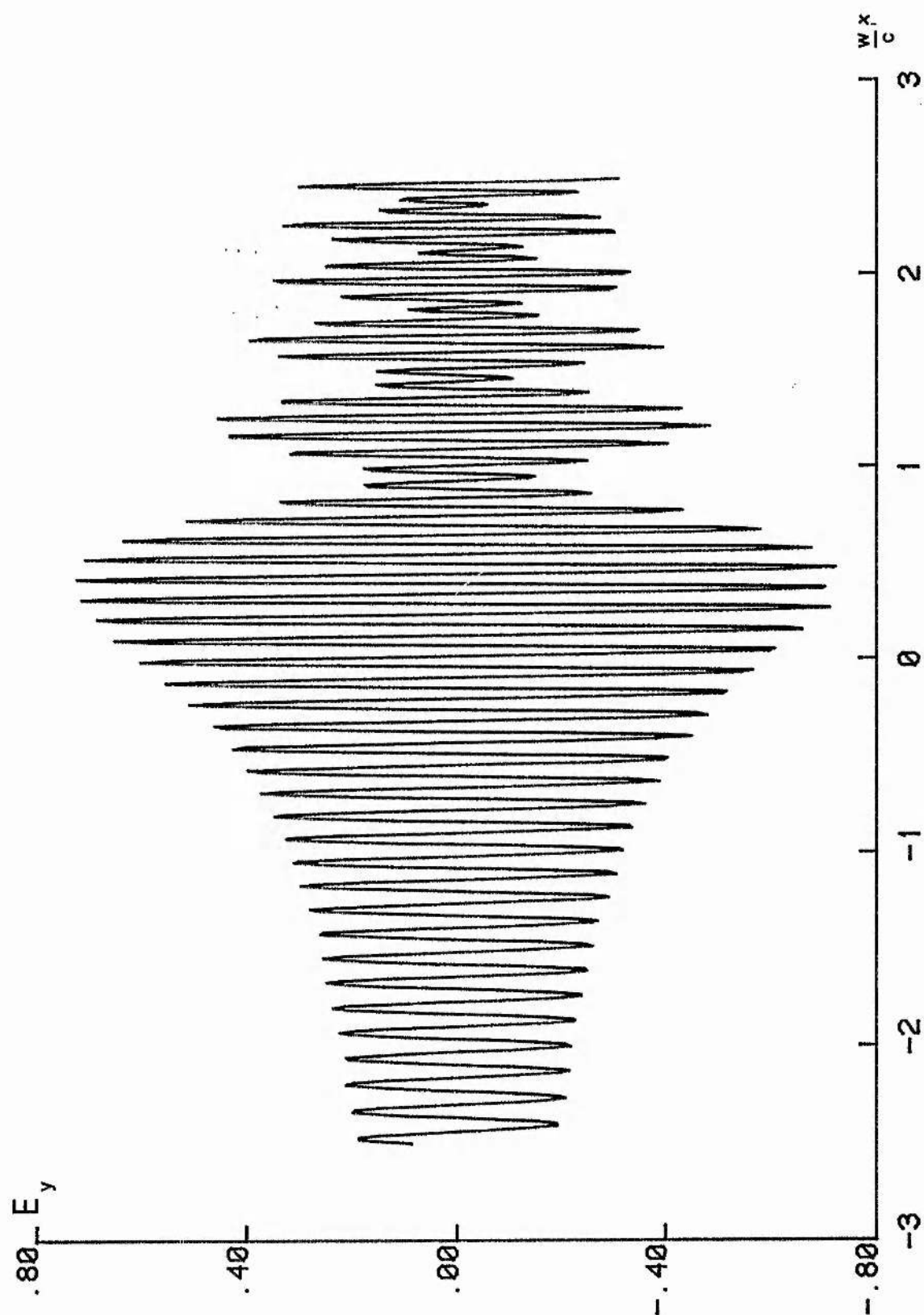


Figure 5.17 Difference between exact E_y values of Fig 5.16 and those obtained by using the solutions of (5.5) in (4.25).

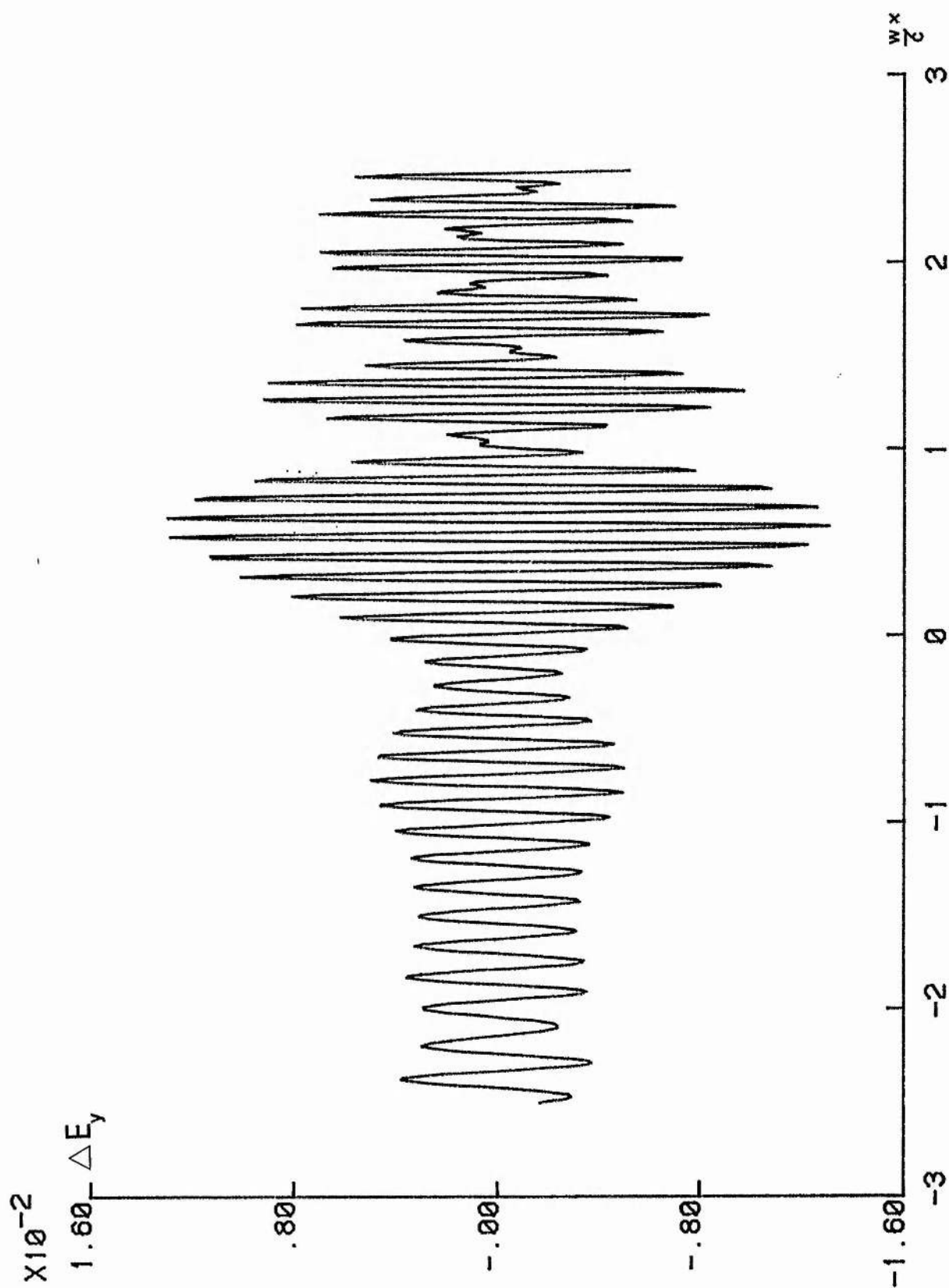


Figure 5.18 Spatial variation of E_z calculated as for Fig 5.14.

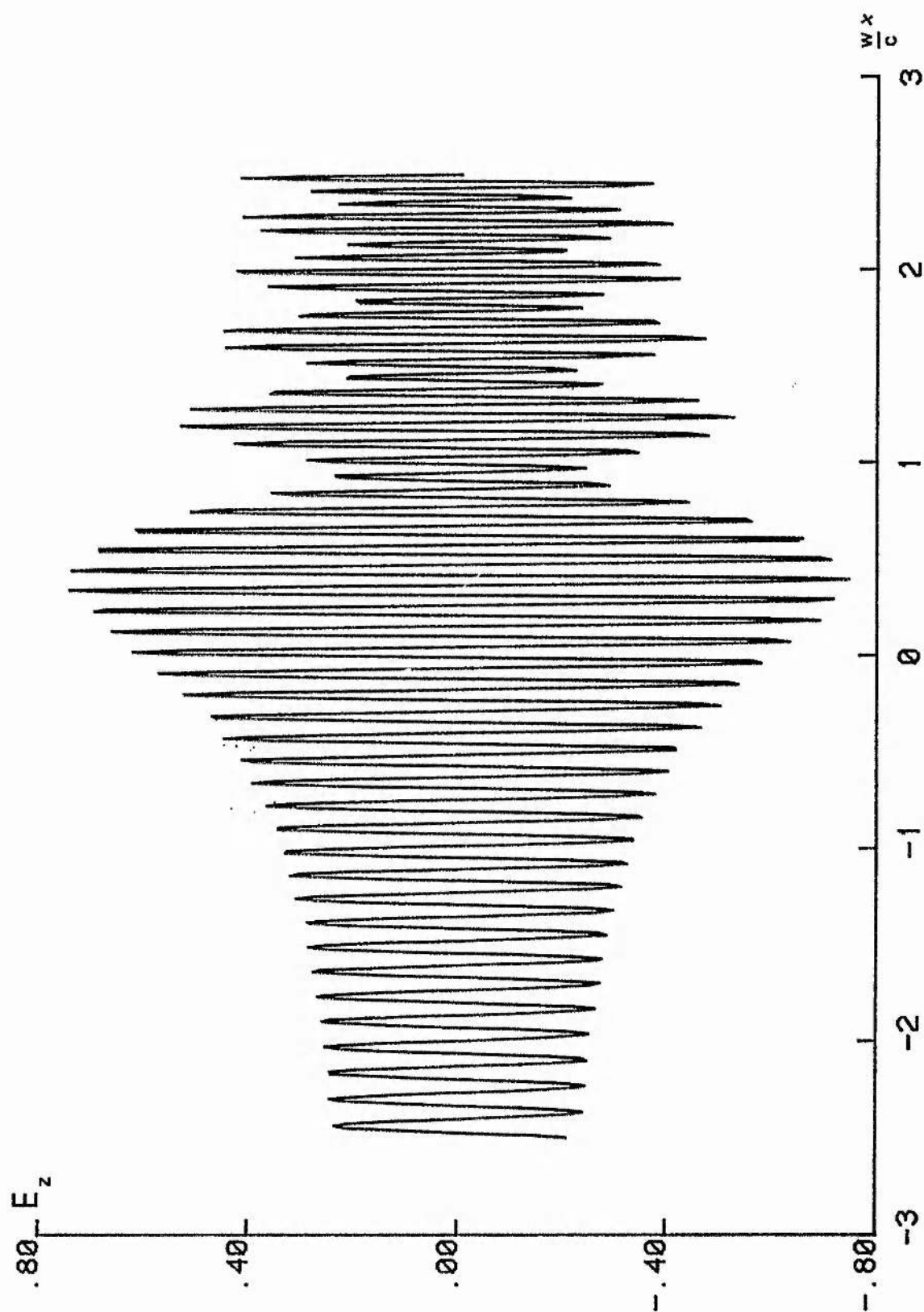


Figure 5.19 Difference between exact E_z values of Fig 5.18 and those obtained by using the solutions of (5.5) in (4.25).

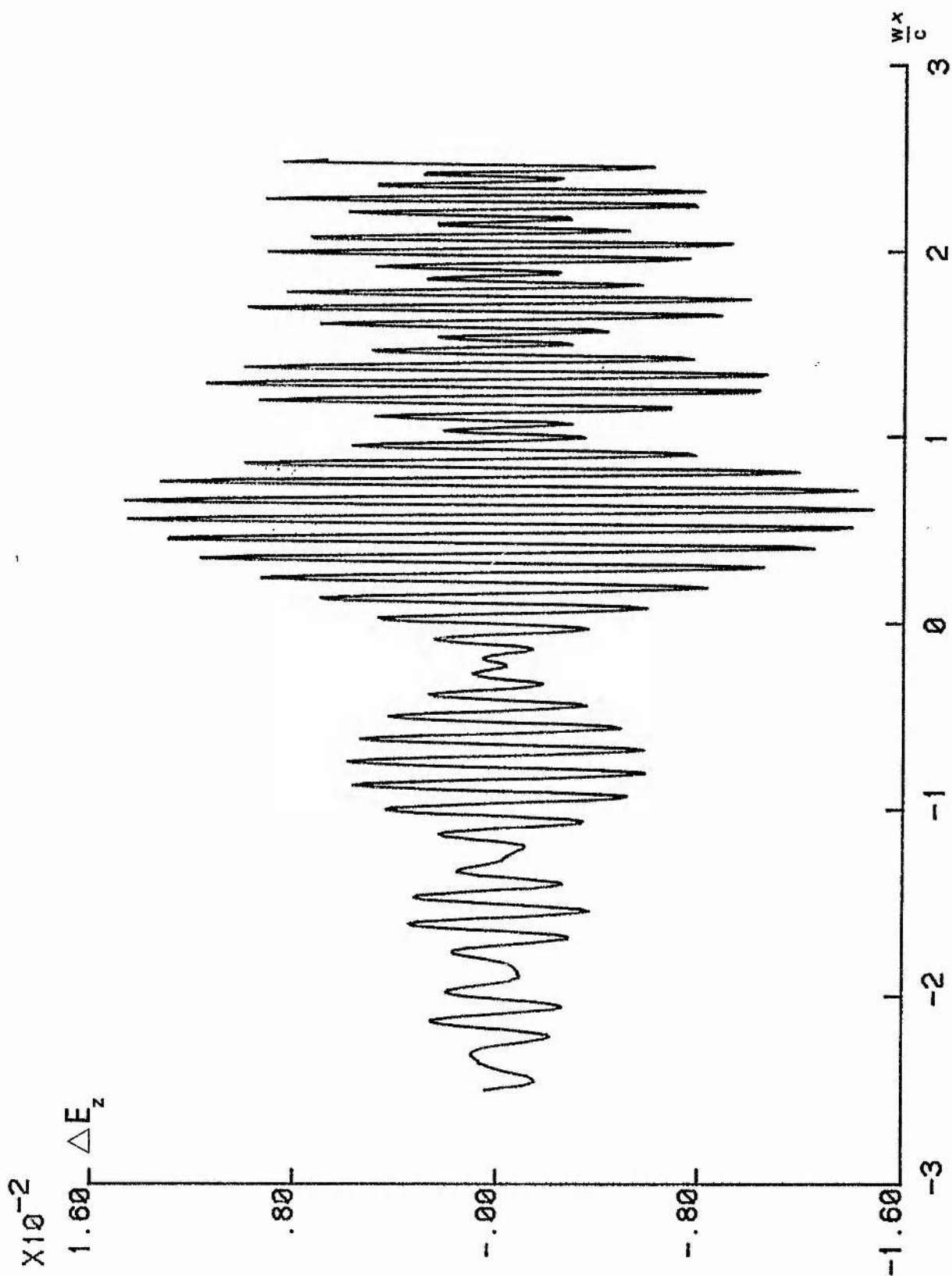


Figure 5.20 Spatial variation of E_x (arbitrary units) calculated by using the solutions of (5.5) in (4.25), but with $D = I_{4 \times 4}$ throughout, as in Heading's original formulation. Parameters $n_{||} = n_c$, $\omega/2\pi = 800$ MHz, $B_0 = 2.5$ Tesla, $L = 0.4$ m and $m_i/m_e = 3672$.

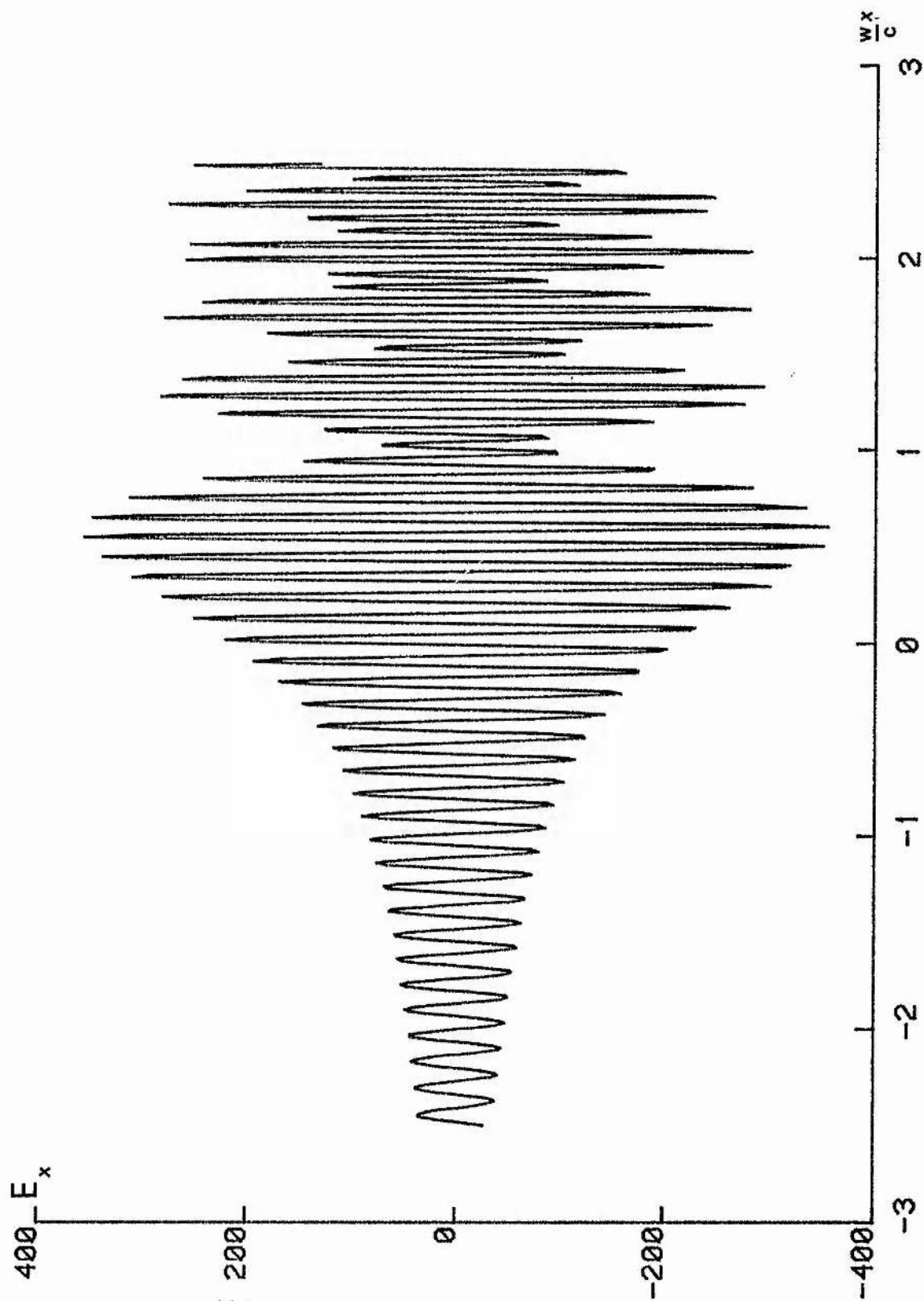


Figure 5.21 Spatial variation of E_y calculated as for Fig 5.20.

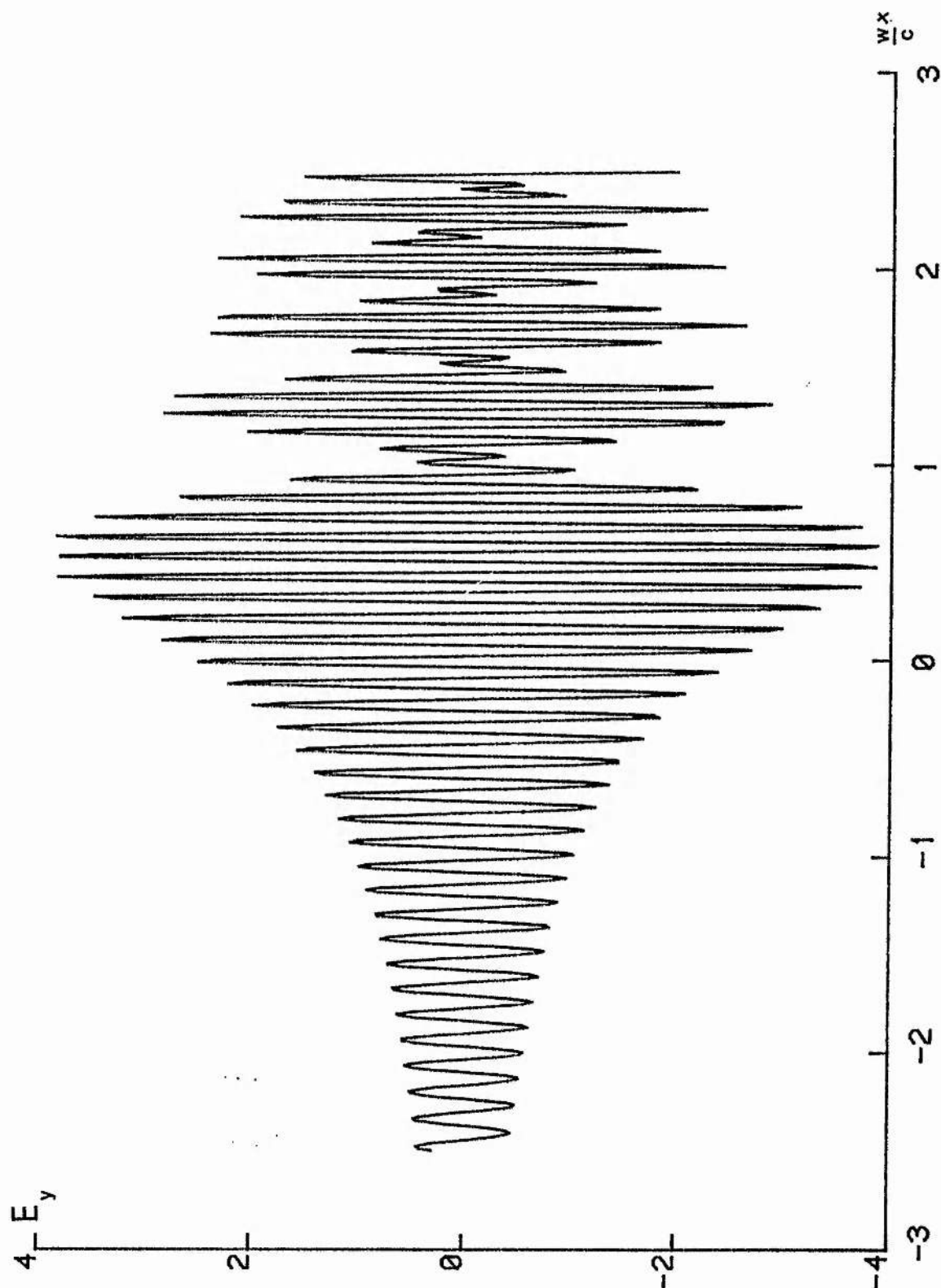
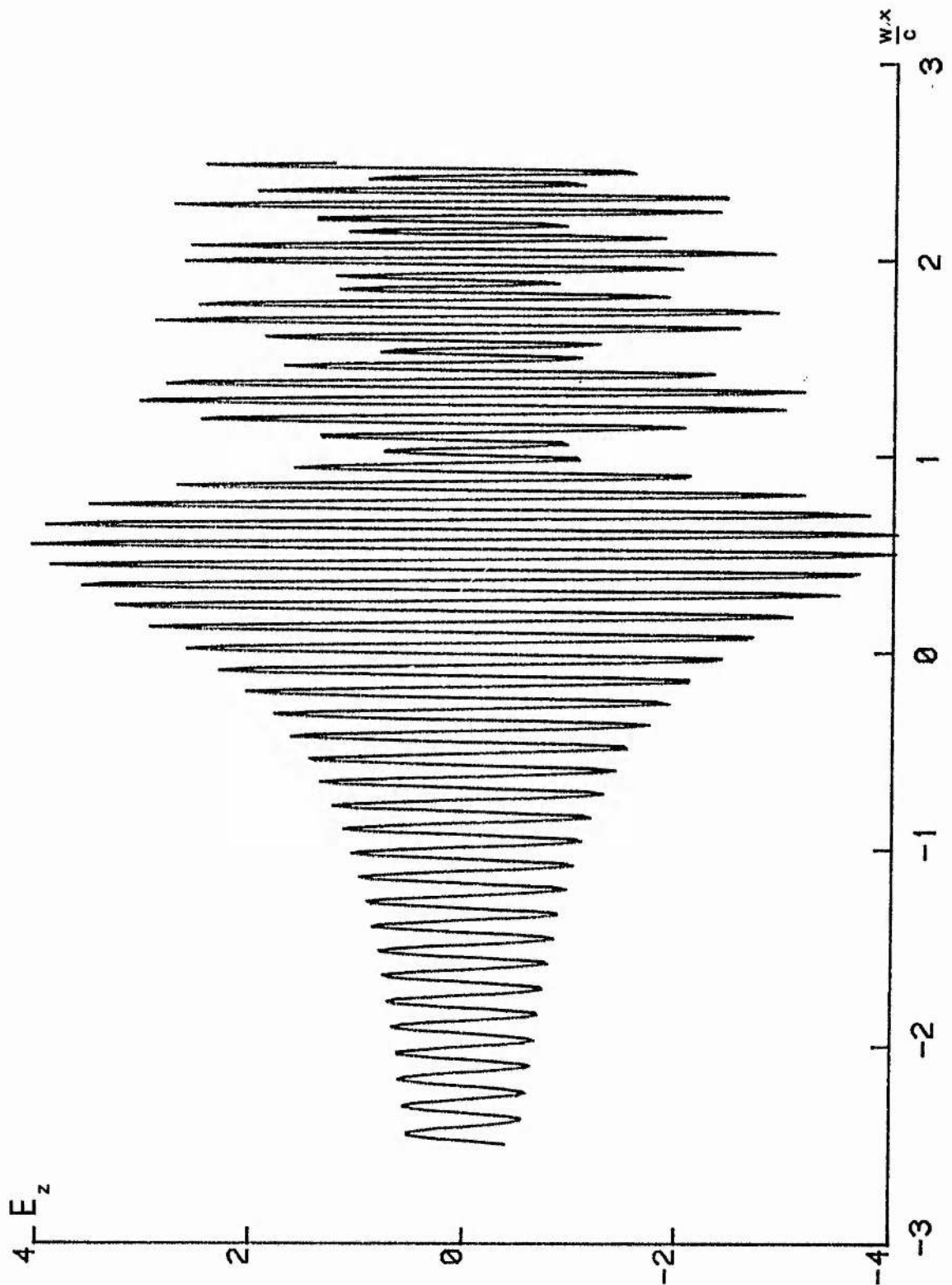


Figure 5.22 Spatial variation of E_z calculated as for Fig 5.21.



this, consider the system given by

$$\begin{pmatrix} g_1 \\ g_2 \end{pmatrix}' = \begin{pmatrix} 0 & 1 \\ \beta^2 & 0 \end{pmatrix} \begin{pmatrix} g_1 \\ g_2 \end{pmatrix} + [t_{ij}]_{2 \times 2} \begin{pmatrix} g_1 \\ g_2 \end{pmatrix} \quad (5.6)$$

where the coupling terms are obtained from (4.15) with $D = I_{4 \times 4}$. In this case, (compare with (4.24)),

$$t_{11} \text{ and } t_{22} \text{ are real but } t_{22} \neq -t_{11},$$

while t_{12} and t_{21} are both non-zero and pure imaginary.

Writing (5.6) as a single second order equation we obtain

$$g_1'' - \left(t_{11} + t_{22} + \frac{t_{12}'}{1+t_{12}} \right) g_1' - \left((\beta^2 + t_{21})(1+t_{12}) - t_{11} \frac{t_{12}'}{(1+t_{12})} + t_{11}' - t_{22} t_{11} \right) g_1 = 0.$$

This may be put in normal form via the transformation

$$g_1 = \exp \left[-\frac{1}{2} \int t_{11} + t_{22} + \frac{t_{12}'}{1+t_{12}} d\xi \right] f_1 \quad (5.7)$$

finally yielding

$$f_1'' - \left[(\beta^2 + t_{21})(1+t_{12}) + \text{higher order derivative terms} \right] f_1 = 0. \quad (5.8)$$

Now it can be shown that

$$t_{11} = -\frac{(\epsilon_3 \rho_2)'}{\epsilon_3 \rho_2} - \frac{[\rho_2(n^+ + n^-)]'}{\rho_2(n^+ + n^-)} \frac{[\rho_1((n^+)^2 + (n^-)^2 + n^+ n^-) - \epsilon_3]}{4\rho_1 n^+ n^-} + \frac{[(n^+ + n^-)[\rho_1((n^+)^2 + (n^-)^2 - n^+ n^-) - \epsilon_3]]'}{4\rho_1 n^+ n^-(n^+ + n^-)}$$

and

$$t_{22} = -\frac{[\rho_1(n^+ + n^-)]'}{\rho_1(n^+ + n^-)} + \frac{1}{4\rho_1 n^+ n^-} \left[\frac{\rho_2'}{\rho_2} [\rho_1((n^+)^2 + (n^-)^2 - n^+ n^-) - \epsilon_3] - [\rho_1((n^+)^2 + (n^-)^2 + n^+ n^-) - \epsilon_3]' \right]$$

in which case (5.7) becomes

$$\begin{aligned} g_1 &\propto (1+t_{12})^{-\frac{1}{2}}(n^+ n^- \epsilon_3 \rho_2^2)^{-\frac{1}{4}}(\rho_1(n^+ + n^-))^{-\frac{1}{2}} f_1 \\ &\propto (1+t_{12})^{-\frac{1}{2}}(n^+ n^- c^+ c^-)^{-\frac{1}{4}}(\rho_1(n^+ + n^-))^{-\frac{1}{2}} f_1 \\ &\approx (d_1 d_2)^{\frac{1}{2}} f_1, \text{ where } d_1 \text{ and } d_2 \text{ are defined in (4.22).} \end{aligned}$$

Roughly speaking, the solutions of (5.8) behave like those of (5.5), and so g_1 and g_2 can be related to the solutions f_1 and f_2 of (5.5) using (5.7). This enables us to compare, in a heuristic way, the field amplitudes obtained from the prescription of Section 4.6 with the fields, \underline{e}_H , given by the action of Heading's transformation on the solutions of (5.6). Then

$$\underline{e}_H = \text{MER}^{-1} \begin{pmatrix} g_1 \\ g_2 \\ 0 \\ 0 \end{pmatrix} \approx (d_1 d_2)^{\frac{1}{2}} \text{MER}^{-1} \begin{pmatrix} f_1 \\ f_2 \\ 0 \\ 0 \end{pmatrix}$$

so that in (4.26) our diagonal transformation D is replaced by a scalar function which is the geometric mean of the elements of D .

Clearly Heading's 'coupling' terms are important because they provide the correct order of magnitude variation for the field amplitudes. On the other hand, our transformation not only guarantees the correct amplitude variation through the matrix D , but also yields coupling terms which are an order of magnitude

smaller in the gradient scale length than those appearing in Heading's formulation. We therefore conclude that our transformation is a successful one.

CONCLUSIONS

In this thesis, we firstly investigated the hybrid resonances in a cold plasma. It was shown how these fit into the C.L-D. mode coupling model and that the Budden tunnelling coefficients are recovered.

Next we used a second order theory to examine the mode conversion between fast and slow waves in the lower hybrid frequency range. It was found that the parameter, K , which characterised the mode conversion in a plasma with linear density and/or magnetic field profiles was of order unity or less only for a very small range of n_{\parallel} about its critical value in each case. Thus the transmission coefficient for a particular mode goes very sharply from 0 to 1 as n_{\parallel} goes from $n_{\parallel} < n_c$ to $n_{\parallel} > n_c$.

The presence of a magnetic field gradient satisfying $L/R = \frac{1}{2}$ does, however, shift the mode conversion point to a density some 200 times $((m_i/m_e)^{2/3})$ for a deuterium plasma) less than in the other cases.

We then investigated the exact fourth order system of O.D.E's for the lower hybrid problem in order to discover whether the use of a second order differential equation was justified. It was demonstrated that Heading's transformation distinguishes the positive and negative n_{\perp} pairs of waves, and extracts the appropriate second order equations describing coupling events for each pair separately. An extension of Heading's transformation was used in which the Poynting flux was identified with the well known

conserved quantity of the second order equations. This modification also improved the accuracy of the second order approximation.

Transmission coefficients obtained from numerical integration of the exact fourth order system in the uniform magnetic field case were in good agreement with those given by our second order theory. Finally, we retrieved expressions for the physical fields in terms of the amplitude appearing in the second order equation. These reproduced the electric field variation across the mode conversion region in agreement with exact solutions of the fourth order equations. We therefore conclude that a second order differential equation representation obtained from a local dispersion relation valid in the coupling region does carry all the information, in a loss-free situation, about the mode coupling process.

Suggestions for further work

Very recently, Friedland (1985, 1986) has derived the mode coupling equations of Fuchs et al and C.L-D. by employing a renormalised geometrical optics perturbation expansion to solve the Maxwell-kinetic equations directly. The derivation also provides a complete physical description of the amplitudes and polarisations of the interacting modes. The analysis assumes that the plasma dielectric tensor is Hermitian which guarantees energy conservation. This conservation law is needed in order to connect the WKBJ solutions outside the coupling region.

A further area of work might be the extension of second order theories to describe situations where the mode converted wave is

strongly damped. This is the case, for example, at the second electron cyclotron harmonic resonance layer, where relativistic absorption effects greatly modify the mode conversion structure for wave propagation nearly perpendicular to the equilibrium magnetic field (Imre and Weitzner, 1985 a,b).

APPENDIX

The coupling matrix in (4.15) given by

$$(t_{ij})_{4 \times 4} = -E^{-1}(ADR^{-1})^{-1}(ADR^{-1})'E - E^{-1}(ADR^{-1})^{-1}P^{-1}P'(ADR^{-1})E$$

can be written as

$$\begin{aligned} (t_{ij})_{4 \times 4} &= -E^{-1}(ADR^{-1})^{-1}P^{-1}(PA' + P'A)DR^{-1}E \\ &\quad - E^{-1}(ADR^{-1})^{-1}(AD'R^{-1} + AD(R^{-1})')E \end{aligned}$$

i.e.

$$\begin{aligned} (t_{ij})_{4 \times 4} &= -E^{-1}RD^{-1}M^{-1}M'DR^{-1}E - E^{-1}RD^{-1}D'R^{-1}E \\ &\quad - E^{-1}R(R^{-1})'E. \end{aligned} \tag{A1}$$

We now calculate the contributions to $(t_{ij})_{4 \times 4}$ arising from each of the three terms in (A1).

Firstly,

$$\begin{aligned} &-E^{-1}R(R^{-1})'E = -R(R^{-1})' = R'R^{-1} \\ &= \begin{pmatrix} 0 & 0 & 0 & 0 \\ \beta' & -\beta' & 0 & 0 \\ 0 & 0 & 0 & 0 \\ 0 & 0 & -\beta' & \beta' \end{pmatrix} \times \frac{1}{2} \begin{pmatrix} 1 & 1/\beta & 0 & 0 \\ 1 & -1/\beta & 0 & 0 \\ 0 & 0 & 1 & -1/\beta \\ 0 & 0 & 1 & 1/\beta \end{pmatrix} \\ &= \text{diag}(0, \beta'/\beta, 0, \beta'/\beta). \end{aligned} \tag{A2}$$

Next,

$$- E^{-1} R D^{-1} D' R^{-1} E = - R D^{-1} D' R^{-1}$$

$$= - \begin{pmatrix} 1 & 1 & 0 & 0 \\ \beta & -\beta & 0 & 0 \\ 0 & 0 & 1 & 1 \\ 0 & 0 & -\beta & \beta \end{pmatrix} \times \text{diag} \left(\frac{d_1'}{d_1}, \frac{d_2'}{d_2}, \frac{d_1'}{d_1}, \frac{d_2'}{d_2} \right)$$

$$\times \frac{1}{2} \begin{pmatrix} 1 & 1/\beta & 0 & 0 \\ 1 & -1/\beta & 0 & 0 \\ 0 & 0 & 1 & -1/\beta \\ 0 & 0 & 1 & 1/\beta \end{pmatrix}$$

$$= \begin{pmatrix} u_{11} & u_{12} & 0 & 0 \\ u_{21} & u_{11} & 0 & 0 \\ 0 & 0 & u_{11} & -u_{12} \\ 0 & 0 & -u_{21} & u_{11} \end{pmatrix}$$

where

$$\begin{cases} u_{11} = -\frac{1}{2} \frac{(d_1 d_2)'}{d_1 d_2} = \frac{1}{4} \left[\frac{(n^+ n^-)'}{n^+ n^-} + \frac{(c^+ c^-)'}{c^+ c^-} \right] + \frac{1}{2} \frac{[\rho_1 (n^+ + n^-)]'}{\rho_1 (n^+ + n^-)} \\ u_{12} = -\frac{1}{2\beta} \left[\frac{d_1'}{d_1} - \frac{d_2'}{d_2} \right] = \frac{1}{4\beta} \left[\frac{(n^+)'}{n^+} - \frac{(n^-)'}{n^-} + \frac{(c^+)'}{c^+} - \frac{(c^-)'}{c^-} \right] \\ u_{21} = \beta^2 u_{12} \end{cases} \quad (A3)$$

and we have used expressions (4.22) for the elements of D.

Calculation of the final term in (A1) is straightforward but tedious.

It is convenient to evaluate this matrix product in stages.

Firstly

$$RD^{-1}M^{-1} = \begin{pmatrix} 1 & 1 & 0 & 0 \\ \beta & -\beta & 0 & 0 \\ 0 & 0 & 1 & 1 \\ 0 & 0 & -\beta & \beta \end{pmatrix} \text{diag}(d_1^{-1}, d_2^{-1}, d_1^{-1}, d_2^{-1})$$

$$\times \frac{1}{2\epsilon_3 B(c^+ - c^-)} \begin{pmatrix} \epsilon_3 B & c^- & -\epsilon_3 c^-/n^+ & \epsilon_3 B/n^+ \\ -\epsilon_3 B & -c^+ & \epsilon_3 c^+/n^- & -\epsilon_3 B/n^- \\ \epsilon_3 B & c^- & \epsilon_3 c^-/n^+ & -\epsilon_3 B/n^+ \\ -\epsilon_3 B & -c^+ & -\epsilon_3 c^+/n^- & \epsilon_3 B/n^- \end{pmatrix}$$

where we have introduced the notation

$$B = i\rho_2 n_{11}$$

i.e.

$$RD^{-1}M^{-1} = \frac{1}{2\epsilon_3 B(c^+ - c^-)} \begin{pmatrix} a_{11} & a_{12} & a_{13} & a_{14} \\ a_{21} & a_{22} & a_{23} & a_{24} \\ a_{11} & a_{12} & -a_{13} & -a_{14} \\ -a_{21} & -a_{22} & a_{23} & a_{24} \end{pmatrix}$$

where

$$\left\{ \begin{array}{ll} a_{11} = \epsilon_3 B \left(\frac{1}{d_1} - \frac{1}{d_2} \right), & a_{12} = \frac{c^+}{d_1} - \frac{c^-}{d_2} \\ a_{13} = \epsilon_3 \left(\frac{c^+}{n^- d_2} - \frac{c^-}{n^+ d_1} \right), & a_{14} = \epsilon_3 B \left(\frac{1}{n^+ d_1} - \frac{1}{n^- d_2} \right) \\ a_{21} = \epsilon_3 B \beta \left(\frac{1}{d_1} + \frac{1}{d_2} \right), & a_{22} = \beta \left(\frac{c^-}{d_1} + \frac{c^+}{d_2} \right) \\ a_{23} = -\epsilon_3 B \left(\frac{c^+}{n^- d_2} + \frac{c^-}{n^+ d_1} \right), & a_{24} = \epsilon_3 B \beta \left(\frac{1}{n^+ d_1} + \frac{1}{n^- d_2} \right) \end{array} \right. \quad (A4)$$

Also,

$$M'DR^{-1} = \begin{pmatrix} c^+ & c^- & c^+ & c^- \\ -\epsilon_3 B & -\epsilon_3 B & -\epsilon_3 B & -\epsilon_3 B \\ n^+ B & n^- B & -n^+ B & -n^- B \\ n^+ c^+ & n^- c^- & -n^+ c^+ & -n^- c^- \end{pmatrix}' \times \text{diag}(d_1, d_2, d_1, d_2)$$

$$\times \frac{1}{2} \begin{pmatrix} 1 & 1/\beta & 0 & 0 \\ 1 & -1/\beta & 0 & 0 \\ 0 & 0 & 1 & -1/\beta \\ 0 & 0 & 1 & 1/\beta \end{pmatrix}$$

i.e.

$$M'DR^{-1} = \frac{1}{2} \begin{pmatrix} b_{11} & b_{12} & b_{11} & -b_{12} \\ b_{21} & b_{22} & b_{21} & -b_{22} \\ b_{31} & b_{32} & -b_{31} & b_{32} \\ b_{41} & b_{42} & -b_{41} & b_{42} \end{pmatrix}$$

where

$$\begin{cases} b_{11} = d_1(c^+)' + d_2(c^-)', & b_{12} = \frac{d_1(c^+)' - d_2(c^-)'}{\beta} \\ b_{21} = -(\epsilon_3 B)'(d_1 + d_2), & b_{22} = -\frac{(\epsilon_3 B)'(d_1 - d_2)}{\beta} \\ b_{31} = (n^+ B)'d_1 + (n^- B)'d_2, & b_{32} = \frac{(n^+ B)'d_1 - (n^- B)'d_2}{\beta} \\ b_{41} = (n^+ c^+)'d_1 + (n^- c^-)'d_2, & b_{42} = \frac{(n^+ c^+)'d_1 - (n^- c^-)'d_2}{\beta} \end{cases}$$

(A5)

Then using (A4) and (A5),

$$\begin{aligned}
 & -E^{-1}(RD^{-1}M^{-1})(M'DR^{-1})E = \text{diag}(e^{-\int \alpha d\xi}, e^{-\int \alpha d\xi}, e^{\int \alpha d\xi}, e^{\int \alpha d\xi}) \\
 & \quad \times \frac{-1}{4\epsilon_3 B(c^+ - c^-)} (a_{ij})_{4 \times 4} (b_{ij})_{4 \times 4} \\
 & \quad \times \text{diag}(e^{\int \alpha d\xi}, e^{\int \alpha d\xi}, e^{-\int \alpha d\xi}, e^{-\int \alpha d\xi}) \\
 & = \frac{-1}{4\epsilon_3 B(c^+ - c^-)} \begin{pmatrix} c_{11} + c_{21} & c_{31} + c_{41} & \begin{bmatrix} c_{11} - c_{21} & c_{41} - c_{31} \end{bmatrix} e^{-\int 2\alpha d\xi} \\ c_{12} + c_{22} & c_{32} + c_{42} & \begin{bmatrix} c_{12} - c_{22} & c_{42} - c_{32} \end{bmatrix} e^{-\int 2\alpha d\xi} \\ \begin{bmatrix} c_{11} - c_{21} & c_{31} - c_{41} \end{bmatrix} e^{\int 2\alpha d\xi} & c_{11} + c_{21} & -(c_{31} + c_{41}) \\ \begin{bmatrix} c_{22} - c_{12} & c_{42} - c_{32} \end{bmatrix} e^{\int 2\alpha d\xi} & -(c_{12} + c_{22}) & c_{32} + c_{42} \end{pmatrix}
 \end{aligned}$$

where

$$\begin{cases} c_{11} = a_{11}b_{11} + a_{12}b_{21}, & c_{12} = a_{21}b_{11} + a_{22}b_{21} \\ c_{21} = a_{13}b_{31} + a_{14}b_{41}, & c_{22} = a_{23}b_{31} + a_{24}b_{41} \\ c_{31} = a_{11}b_{12} + a_{12}b_{22}, & c_{32} = a_{21}b_{12} + a_{22}b_{22} \\ c_{41} = a_{13}b_{32} + a_{14}b_{42}, & c_{42} = a_{23}b_{32} + a_{24}b_{42} \end{cases} \quad (A6)$$

We now substitute (A4) and (A5) into (A6) to calculate in pairs the 8 quantities

$$c_{11} \pm c_{21}, \quad c_{12} \pm c_{22}, \quad c_{31} \pm c_{41}, \quad c_{32} \pm c_{42}.$$

Hence,

$$\begin{aligned}
 & \frac{-1}{4\epsilon_3 B(c^+ - c^-)} (c_{11} \pm c_{21}) = \\
 & \frac{-1}{4\epsilon_3 B(c^+ - c^-)} \left\{ \epsilon_3 B \left(\frac{1}{d_1} - \frac{1}{d_2} \right) (d_1 c^{+'} + d_2 c^{-'}) - (\epsilon_3 B)' (d_1 + d_2) \left(\frac{c^-}{d_1} - \frac{c^+}{d_2} \right) \right. \\
 & \quad \pm \left[\epsilon_3 \left(\frac{c^+}{n^- d_2} - \frac{c^-}{n^+ d_1} \right) ((n^+ B)' d_1 + (n^- B)' d_2) \right. \\
 & \quad \left. \left. + \epsilon_3 B \left(\frac{1}{n^+ d_1} - \frac{1}{n^- d_2} \right) ((n^+ c^+)' d_1 + (n^- c^-)' d_2) \right] \right\} \\
 & = \frac{-1}{\epsilon_3 B(c^+ - c^-)} \left\{ \epsilon_3 B \left((c^+ - c^-)' - \frac{d_1}{d_2} c^{+'} + \frac{d_2}{d_1} c^{-'} \right) \right. \\
 & \quad + (\epsilon_3' B + \epsilon_3 B') \left(c^+ - c^- + \frac{d_1}{d_2} c^+ - \frac{d_2}{d_1} c^- \right) \\
 & \quad \pm \left[\epsilon_3 B \left(c^+ \frac{n^+}{n^-} \frac{d_1}{d_2} - c^- \frac{n^-}{n^+} \frac{d_2}{d_1} - c^- \frac{n^+}{n^+} + c^+ \frac{n^-}{n^-} \right) \right. \\
 & \quad + \epsilon_3 B' \left(c^+ - c^- + c^+ \frac{n^+}{n^-} \frac{d_1}{d_2} - c^- \frac{n^-}{n^+} \frac{d_2}{d_1} \right) \\
 & \quad + \epsilon_3 B \left((c^+ - c^-)' - c^{+'} \frac{n^+}{n^-} \frac{d_1}{d_2} + c^{-'} \frac{n^-}{n^+} \frac{d_2}{d_1} \right) \\
 & \quad \left. \left. + \epsilon_3 B \left(c^+ \frac{n^+}{n^+} - c^- \frac{n^-}{n^-} - c^+ \frac{n^+}{n^-} \frac{d_1}{d_2} + c^- \frac{n^-}{n^+} \frac{d_2}{d_1} \right) \right] \right\} \\
 & \hspace{25em} (A7)
 \end{aligned}$$

Note that the scored through terms sum to zero.

$$\begin{aligned}
 \text{i.e. } & - \frac{(c_{11} \pm c_{21})}{4\epsilon_3 B(c^+ - c^-)} = \\
 & \frac{-1}{4\epsilon_3 B(c^+ - c^-)} \left\{ \epsilon_3 B \left[\frac{2}{\phi} (c^+ - c^-)' - \frac{d_1}{d_2} c^{+'} \left(1 \pm \frac{n^+}{n^-} \right) \right. \right.
 \end{aligned}$$

$$\begin{aligned}
 & + \frac{d_2}{d_1} c^{-'} \left(1 \pm \frac{n^-}{n^+} \right) \pm (c^+ - c^-) \frac{(n^+ n^-)'}{n^+ n^-} \\
 & + \epsilon_3' B \left[(c^+ - c^-) + \frac{d_1}{d_2} c^+ - \frac{d_2}{d_1} c^- \right] \\
 & + \epsilon_3 B' \left[\begin{aligned} & 2_0 (c^+ - c^-) + \frac{d_1}{d_2} c^+ \left(1 \pm \frac{n^+}{n^-} \right) - \frac{d_2}{d_1} c^- \left(1 \pm \frac{n^-}{n^+} \right) \end{aligned} \right] \Bigg\}
 \end{aligned}
 \tag{A7}$$

where the notation 2_0 indicates a factor of two or zero, effective when (A7) is evaluated for the plus or the minus sign respectively. Using the following identities

$$\begin{aligned}
 \frac{d_1}{d_2} &= \left(\frac{n^- c^-}{n^+ c^+} \right)^{\frac{1}{2}} \\
 c^+ - c^- &= \rho_1 (n^+ + n^-) (n^+ - n^-) \\
 c^+ c^- &= \epsilon_3 B^2 = -\epsilon_3 \rho_2^2 n_{II}^2
 \end{aligned}$$

$$\text{and } c^+ c^{-'} - c^- c^{+'} = \frac{1}{2} \left[(c^+ + c^-)' (c^+ - c^-) - (c^+ + c^-) (c^+ - c^-)' \right], \tag{A8}$$

it is a straightforward matter to show from (A7) that

$$\begin{aligned}
 - \frac{(c_{11} + c_{21})}{4\epsilon_3 B (c^+ - c^-)} &= - \frac{(n^+ n^-)'}{4n^+ n^-} - \frac{(c^+ c^-)'}{4c^+ c^-} - \frac{[\rho_1 (n^+ + n^-)]'}{2\rho_1 (n^+ + n^-)} \\
 &+ \frac{1}{8(n^+ n^- c^+ c^-)^{\frac{1}{2}}} \left[\begin{aligned} & (n^+ + n^-)' (c^+ + c^-) + \frac{\rho_1'}{\rho_1} (n^+ + n^-) (c^+ + c^-) \\ & - (n^+ + n^-) (c^+ + c^-)' - \frac{2\epsilon_3' \rho_2^2 n_{II}^2}{\rho_1 (n^+ + n^-)} \end{aligned} \right] \\
 &- \frac{1}{2} \Delta
 \end{aligned}
 \tag{A9}$$

$$\text{where } \Delta = \frac{(n^+ - n^-)'}{(n^+ - n^-)} \left[1 - \frac{(n^+ + n^-) (c^+ + c^-)}{4(n^+ n^- c^+ c^-)^{\frac{1}{2}}} \right].$$

The behaviour of Δ near a confluence of the roots n^+ and n^- is not immediately clear. However, we can show that the [] term goes to zero like $(n^+ - n^-)^2$ in which case Δ has a $(\beta^2)'$ dependence.

We have that

$$\begin{aligned} (n^+ n^- c^+ c^-)^{\frac{1}{2}} - \frac{(n^+ + n^-)}{4} (c^+ + c^-) &= -\frac{1}{4}((n^+ c^+)^{\frac{1}{2}} - (n^- c^-)^{\frac{1}{2}})^2 \\ &\quad - \frac{1}{4}((n^+ c^-)^{\frac{1}{2}} - (n^- c^+)^{\frac{1}{2}})^2 \\ &= -\frac{1}{4} \left(\frac{n^+ c^+ - n^- c^-}{(n^+ c^+)^{\frac{1}{2}} + (n^- c^-)^{\frac{1}{2}}} \right)^2 - \frac{1}{4} \left(\frac{n^+ c^- - n^- c^+}{(n^+ c^-)^{\frac{1}{2}} + (n^- c^+)^{\frac{1}{2}}} \right)^2 \\ &= \beta^2 \left[\left(\frac{\rho_1((n^+)^2 + (n^-)^2 + n^+ n^-) - \epsilon_3}{(n^+ c^+)^{\frac{1}{2}} + (n^- c^-)^{\frac{1}{2}}} \right)^2 + \left(\frac{\rho_1 n^+ n^- + \epsilon_3}{(n^+ c^-)^{\frac{1}{2}} + (n^- c^+)^{\frac{1}{2}}} \right)^2 \right]. \end{aligned}$$

Hence,

$$\Delta = \frac{(\beta^2)'}{2(n^+ n^- c^+ c^-)^{\frac{1}{2}}} \left[\left(\frac{\rho_1((n^+)^2 + (n^-)^2 + n^+ n^-) - \epsilon_3}{(n^+ c^+)^{\frac{1}{2}} + (n^- c^-)^{\frac{1}{2}}} \right)^2 + \left(\frac{\rho_1 n^+ n^- + \epsilon_3}{(n^+ c^-)^{\frac{1}{2}} + (n^- c^+)^{\frac{1}{2}}} \right)^2 \right]. \quad (A10)$$

The minus sign in (A7) yields

$$\begin{aligned} -\frac{(c_{11} - c_{21})}{4\epsilon_3 B(c^+ - c^-)} &= \frac{-1}{4\epsilon_3 B(c^+ - c^-)} \left\{ \epsilon_3 B \left[\frac{(n^+ - n^-)}{(n^+ n^- c^+ c^-)^{\frac{1}{2}}} (c^+ c^-)' - (c^+ - c^-) \frac{(n^+ n^-)'}{n^+ n^-} \right] \right. \\ &\quad + \epsilon_3 B \left[(c^+ - c^-) - \frac{(n^+ - n^-)}{(n^+ n^- c^+ c^-)^{\frac{1}{2}}} c^+ c^- \right] \\ &\quad \left. + 2\epsilon_3 B \frac{(n^+ - n^-)}{(n^+ n^- c^+ c^-)^{\frac{1}{2}}} c^+ c^- \right\} \\ &= \frac{(n^+ n^-)'}{4n^+ n^-} - \frac{\epsilon_3}{4\epsilon_3}. \quad (A11) \end{aligned}$$

Next,

$$\begin{aligned}
 -\frac{(c_{12} \pm c_{22})}{4\epsilon_3 B(c^+ - c^-)} &= \frac{-\beta}{4\epsilon_3 B(c^+ - c^-)} \left\{ \epsilon_3 B \left(\frac{1}{d_1} + \frac{1}{d_2} \right) (d_1 c^{+'} + d_2 c^{-'}) \right. \\
 &\quad \left. - (\epsilon_3 B)' (d_1 + d_2) \left(\frac{c^-}{d_1} + \frac{c^+}{d_2} \right) \right. \\
 &\quad \left. \pm \left[\epsilon_3 B \left(\frac{1}{n^+ d_1} + \frac{1}{n^- d_2} \right) \left((n^+ c^+) ' d_1 + (n^- c^-) ' d_2 \right) \right. \right. \\
 &\quad \left. \left. - \epsilon_3 \left(\frac{c^-}{n^+ d_1} + \frac{c^+}{n^- d_2} \right) \left((n^+ B)' d_1 + (n^- B)' d_2 \right) \right] \right\} \\
 &= \frac{-\beta}{4\epsilon_3 B(c^+ - c^-)} \left\{ \epsilon_3 B \left((c^+ + c^-)' + \frac{d_1}{d_2} c^{+'} + \frac{d_2}{d_1} c^{-'} \right) \right. \\
 &\quad \left. - (\epsilon_3 B' + \epsilon_3 B) \left(c^+ + c^- + \frac{d_1}{d_2} c^+ + \frac{d_2}{d_1} c^- \right) \right. \\
 &\quad \left. \pm \left[\epsilon_3 B \left((c^+ + c^-)' + c^{+'} \frac{n^+}{n^-} \frac{d_1}{d_2} + c^{-'} \frac{n^-}{n^+} \frac{d_2}{d_1} \right) \right. \right. \\
 &\quad \left. + \epsilon_3 B \left(c^+ \frac{n^+}{n^-} + c^- \frac{n^-}{n^+} + c^+ \frac{n^+}{n^-} \frac{d_1}{d_2} + c^- \frac{n^-}{n^+} \frac{d_2}{d_1} \right) \right. \\
 &\quad \left. - \epsilon_3 B \left(c^- \frac{n^+}{n^+} + c^+ \frac{n^-}{n^-} + c^+ \frac{n^+}{n^-} \frac{d_1}{d_2} + c^- \frac{n^-}{n^+} \frac{d_2}{d_1} \right) \right. \\
 &\quad \left. - \epsilon_3 B' \left(c^+ + c^- + c^+ \frac{n^+}{n^-} \frac{d_1}{d_2} + c^- \frac{n^-}{n^+} \frac{d_2}{d_1} \right) \right] \right\}
 \end{aligned}$$

i.e.

$$\begin{aligned}
 -\frac{(c_{12} \pm c_{22})}{4\epsilon_3 B(c^+ - c^-)} &= \frac{-\beta}{4\epsilon_3 B(c^+ - c^-)} \left\{ \epsilon_3 B \left[\frac{2}{0} (c^+ + c^-)' + \frac{d_1}{d_2} c^{+'} \left(1 \pm \frac{n^+}{n^-} \right) \right. \right. \\
 &\quad \left. \left. + \frac{d_2}{d_1} c^{-'} \left(1 \pm \frac{n^-}{n^+} \right) \pm (c^+ - c^-) \left(\frac{n^+}{n^+} - \frac{n^-}{n^-} \right) \right] \right\}
 \end{aligned}$$

$$\begin{aligned}
 & - \epsilon_3 B \left[c^+ + c^- + \frac{d_1}{d_2} c^+ + \frac{d_2}{d_1} c^- \right] \\
 & - \epsilon_3 B' \left[\frac{2}{3} (c^+ + c^-) + \frac{d_1}{d_2} c^+ \left(1 \pm \frac{n^+}{n^-} \right) + \frac{d_2}{d_1} c^- \left(1 \pm \frac{n^-}{n^+} \right) \right] \Bigg\}
 \end{aligned}
 \tag{A12}$$

Taking the plus sign in (A12) we obtain

$$\begin{aligned}
 - \frac{(c_{12} + c_{22})}{4\epsilon_3 B (c^+ - c^-)} &= \frac{-\beta}{4\epsilon_3 B (c^+ - c^-)} \left\{ \epsilon_3 B \left[2(c^+ + c^-)' + \frac{(n^+ + n^-)(c^+ c^-)'}{(n^+ n^- c^+ c^-)^{\frac{1}{2}}} \right. \right. \\
 &\quad \left. \left. + (c^+ - c^-) \left(\frac{n^{+'}}{n^+} - \frac{n^{-'}}{n^-} \right) \right] \right. \\
 &\quad - \epsilon_3 B \left[(c^+ + c^-) + \frac{(n^+ + n^-)(c^+ c^-)'}{(n^+ n^- c^+ c^-)^{\frac{1}{2}}} \right] \\
 &\quad \left. - \epsilon_3 B' \left[2(c^+ + c^-) + \frac{2(n^+ + n^-)}{(n^+ n^- c^+ c^-)^{\frac{1}{2}}} c^+ c^- \right] \right\} \\
 &= - \frac{\beta}{4} \left(\frac{n^{+'}}{n^+} - \frac{n^{-'}}{n^-} \right) - \frac{\beta}{4} \left(\frac{c^{+'}}{c^+} - \frac{c^{-'}}{c^-} \right)
 \end{aligned}
 \tag{A13}$$

while the minus sign in (A12) yields

$$\begin{aligned}
 - \frac{(c_{12} - c_{22})}{4\epsilon_3 B (c^+ - c^-)} &= \frac{-\beta}{4\epsilon_3 B (c^+ - c^-)} \left\{ \epsilon_3 B \left[(c^+ c^{-'} - c^- c^{+'}) \frac{(n^+ - n^-)}{(n^+ n^- c^+ c^-)^{\frac{1}{2}}} \right. \right. \\
 &\quad \left. \left. + (n^+ n^{-'} - n^- n^{+'}) \frac{(c^+ - c^-)}{n^+ n^-} \right] \right. \\
 &\quad \left. - \epsilon_3 B \left[c^+ + c^- + (n^+ + n^-) \left(\frac{c^+ c^-}{n^+ n^-} \right)^{\frac{1}{2}} \right] \right\}.
 \end{aligned}$$

Upon use of the identities (A8) this becomes

$$\begin{aligned}
 & - \frac{(c_{12} - c_{22})}{4\epsilon_3 B(c^+ - c^-)} \\
 & = \frac{i}{8} \left[c^+ + c^- + (n^+ + n^-) \left(\frac{c^+ c^-}{n^+ n^-} \right)^{\frac{1}{2}} \right] \left[\frac{(\beta^2)'}{(n^+ n^- c^+ c^-)^{\frac{1}{2}}} - \frac{\epsilon_3'}{\epsilon_3 \rho_1 (n^+ + n^-)} \right] \\
 & - \frac{i\beta^2}{4} \left[\frac{1}{(n^+ n^- c^+ c^-)^{\frac{1}{2}}} \left((c^+ + c^-)' - (c^+ + c^-) \frac{[\rho_1 (n^+ + n^-)]'}{\rho_1 (n^+ + n^-)} \right) + \frac{(n^+ + n^-)'}{n^+ n^-} \right].
 \end{aligned}
 \tag{A14}$$

Also,

$$\begin{aligned}
 & - \frac{(c_{31} \pm c_{41})}{4\epsilon_3 B(c^+ - c^-)} \\
 & = \frac{-1}{4\epsilon_3 B\beta(c^+ - c^-)} \left\{ \epsilon_3 B \left(\frac{1}{d_1} - \frac{1}{d_2} \right) (d_1 c^{+'} - d_2 c^{-'}) - (\epsilon_3 B)' (d_1 - d_2) \left(\frac{c^-}{d_1} - \frac{c^+}{d_2} \right) \right. \\
 & \quad \pm \left[\epsilon_3 \left(\frac{c^+}{n^- d_2} - \frac{c^-}{n^+ d_1} \right) \left((n^+ B)' d_1 - (n^- B)' d_2 \right) \right. \\
 & \quad \left. \left. + \epsilon_3 B \left(\frac{1}{n^+ d_1} - \frac{1}{n^- d_2} \right) \left((n^+ c^+) d_1 - (n^- c^-) d_2 \right) \right] \right\} \\
 & = \frac{-1}{4\epsilon_3 B\beta(c^+ - c^-)} \left\{ \epsilon_3 B \left((c^+ + c^-)' - \frac{d_1}{d_2} c^{+'} - \frac{d_2}{d_1} c^{-'} \right) \right. \\
 & \quad \left. - (\epsilon_3' B + \epsilon_3 B') \left(c^+ + c^- - \frac{d_1}{d_2} c^+ - \frac{d_2}{d_1} c^- \right) \right. \\
 & \quad \pm \left[\epsilon_3 B \left(-c^- \frac{n^{+'}}{n^+} - c^+ \frac{n^{-'}}{n^-} + \cancel{c^+ \frac{n^{+'}}{n^-} \frac{d_1}{d_2}} + \cancel{c^- \frac{n^{-'}}{n^+} \frac{d_2}{d_1}} \right) \right. \\
 & \quad \left. + \epsilon_3 B' \left(-c^- - c^+ + c^+ \frac{n^+}{n^-} \frac{d_1}{d_2} + c^- \frac{n^-}{n^+} \frac{d_2}{d_1} \right) \right]
 \end{aligned}$$

$$+ \epsilon_3 B \left\{ (c^+ + c^-)' - c^{+'} \frac{n^+}{n^-} \frac{d_1}{d_2} - c^{-'} \frac{n^-}{n^+} \frac{d_2}{d_1} \right\} \\ + \epsilon_3 B \left\{ c^+ \frac{n^{+'}}{n^+} + c^- \frac{n^{-'}}{n^-} - \cancel{c^+ \frac{n^{+'}}{n^-} \frac{d_1}{d_2}} - \cancel{c^- \frac{n^{-'}}{n^+} \frac{d_2}{d_1}} \right\} \Bigg\}$$

i.e.

$$- \frac{(c_{31} \pm c_{41})}{4\epsilon_3 B \beta (c^+ - c^-)} \\ = \frac{-1}{4\epsilon_3 B \beta (c^+ - c^-)} \left\{ \epsilon_3 B \left[\frac{2}{0} (c^+ + c^-)' - \frac{d_1}{d_2} c^{+'} \left(1 \pm \frac{n^+}{n^-} \right) \right. \right. \\ \left. \left. - \frac{d_2}{d_1} c^{-'} \left(1 \pm \frac{n^-}{n^+} \right) \pm (c^+ - c^-) \left(\frac{n^{+'}}{n^+} - \frac{n^{-'}}{n^-} \right) \right] \right. \\ \left. - \epsilon_3 B \left[c^+ + c^- - \frac{d_1}{d_2} c^+ - \frac{d_2}{d_1} c^- \right] \right. \\ \left. + \epsilon_3 B \left[-\frac{2}{0} (c^+ + c^-) + \frac{d_1}{d_2} c^+ \left(1 \pm \frac{n^+}{n^-} \right) + \frac{d_2}{d_1} c^- \left(1 \pm \frac{n^-}{n^+} \right) \right] \right\}. \quad (A15)$$

Taking the plus sign in (A15) we obtain, upon use of (A8)

$$- \frac{(c_{31} + c_{41})}{4\epsilon_3 B \beta (c^+ - c^-)} = - \frac{1}{4\beta} \left(\frac{n^{+'}}{n^+} - \frac{n^{-'}}{n^-} \right) - \frac{1}{4\beta} \left(\frac{c^{+'}}{c^+} - \frac{c^{-'}}{c^-} \right) \quad (A16)$$

while the minus sign in (A15) yields

$$\frac{(c_{31} - c_{41})}{4\epsilon_3 B \beta (c^+ - c^-)} = \frac{1}{4\epsilon_3 B \beta (c^+ - c^-)} \left\{ \epsilon_3 B \left[(c^{+'} c^- - c^+ c^{-'}) \frac{(n^+ - n^-)}{(n^+ n^- c^+ c^-)^{\frac{1}{2}}} \right. \right. \\ \left. \left. - (c^+ - c^-) \left(\frac{n^{+'}}{n^+} - \frac{n^{-'}}{n^-} \right) \right] \right\}$$

$$\begin{aligned}
 & - \epsilon_3' B \left[c^+ + c^- - (n^+ + n^-) \left(\frac{c^+ c^-}{n^+ n^-} \right)^{\frac{1}{2}} \right] \Bigg\} \\
 & = \frac{i}{4} \left[\frac{1}{(n^+ n^- c^+ c^-)^{\frac{1}{2}}} \left((c^+ + c^-)' - (c^+ + c^-) \frac{[\rho_1(n^+ + n^-)]'}{\rho_1(n^+ + n^-)} \right) - \frac{(n^+ + n^-)'}{n^+ n^-} \right] \\
 & + \frac{i}{2} \left[c^+ + c^- - (n^+ + n^-) \left(\frac{c^+ c^-}{n^+ n^-} \right)^{\frac{1}{2}} \right] \times \left[\frac{1}{(n^+ - n^-)^2} \frac{\epsilon_3'}{\epsilon_3 \rho_1(n^+ + n^-)} \right. \\
 & \quad \left. - \frac{(n^+ - n^-)'}{2(n^+ - n^-)} \cdot \frac{1}{(n^+ n^- c^+ c^-)^{\frac{1}{2}}} \right].
 \end{aligned}
 \tag{A17}$$

However

$$\begin{aligned}
 & (c^+ + c^-)(n^+ n^-)^{\frac{1}{2}} - (n^+ + n^-)(c^+ c^-)^{\frac{1}{2}} \\
 & = \left[(c^+ n^-)^{\frac{1}{2}} - (c^- n^+)^{\frac{1}{2}} \right] \left[(c^+ n^+)^{\frac{1}{2}} - (c^- n^-)^{\frac{1}{2}} \right] \\
 & = (n^+ - n^-)^2 \frac{(\rho_1 n^+ n^- + \epsilon_3)(\rho_1((n^+)^2 + (n^-)^2 + n^+ n^-) - \epsilon_3)}{[(c^+ n^-)^{\frac{1}{2}} + (c^- n^+)^{\frac{1}{2}}][(c^+ n^+)^{\frac{1}{2}} + (c^- n^-)^{\frac{1}{2}}]}
 \end{aligned}$$

so that (A17) becomes

$$\begin{aligned}
 & \frac{C_{31} - C_{41}}{4\epsilon_3 B \beta (c^+ - c^-)} \\
 & = \frac{i}{4} \left[\frac{1}{(n^+ n^- c^+ c^-)^{\frac{1}{2}}} \left((c^+ + c^-)' - (c^+ + c^-) \frac{[\rho_1(n^+ + n^-)]'}{\rho_1(n^+ + n^-)} \right) - \frac{(n^+ + n^-)'}{n^+ n^-} \right] \\
 & + \frac{i}{2(n^+ n^-)^{\frac{1}{2}}} \frac{(\rho_1 n^+ n^- + \epsilon_3)[\rho_1((n^+)^2 + (n^-)^2 + n^+ n^-) - \epsilon_3]}{[(n^- c^+)^{\frac{1}{2}} + (n^+ c^-)^{\frac{1}{2}}][(n^+ c^+)^{\frac{1}{2}} + (n^- c^-)^{\frac{1}{2}}]} \\
 & \times \left[\frac{\epsilon_3'}{\epsilon_3 \rho_1(n^+ + n^-)} + \frac{(\beta^2)'}{(n^+ n^- c^+ c^-)^{\frac{1}{2}}} \right].
 \end{aligned}
 \tag{A18}$$

Finally,

$$\begin{aligned}
 - \frac{(c_{32} \pm c_{42})}{4\epsilon_3 B(c^+ - c^-)} &= \frac{-1}{4\epsilon_3 B(c^+ - c^-)} \left\{ \epsilon_3 B \left(\frac{1}{n^+ d_1} + \frac{1}{n^- d_2} \right) \left((n^+ c^+)' d_1 - (n^- c^-)' d_2 \right) \right. \\
 &\quad \left. - \epsilon_3 \left(\frac{c^-}{n^+ d_1} + \frac{c^+}{n^- d_2} \right) \left((n^+ B)' d_1 - (n^- B)' d_2 \right) \right. \\
 &\quad \left. \pm \left[\epsilon_3 B \left(\frac{1}{d_1} + \frac{1}{d_2} \right) (d_1 c^{+'} - d_2 c^{-'}) \right. \right. \\
 &\quad \left. \left. - (\epsilon_3 B)' (d_1 - d_2) \left(\frac{c^-}{d_1} + \frac{c^+}{d_2} \right) \right] \right\} \\
 &= \frac{-1}{4\epsilon_3 B(c^+ - c^-)} \left\{ \epsilon_3 B \left((c^+ - c^-)' + \frac{d_1}{d_2} c^{+'} \frac{n^+}{n^-} - \frac{d_2}{d_1} c^{-'} \frac{n^-}{n^+} \right) \right. \\
 &\quad + \epsilon_3 B \left(c^+ \frac{n^{+'}}{n^+} - c^- \frac{n^{-'}}{n^-} + \cancel{\frac{d_1}{d_2} c^+ \frac{n^{+'}}{n^-}} - \cancel{\frac{d_2}{d_1} c^- \frac{n^{-'}}{n^+}} \right) \\
 &\quad - \epsilon_3 B \left(c^- \frac{n^{+'}}{n^+} - c^+ \frac{n^{-'}}{n^-} + \cancel{\frac{d_1}{d_2} c^+ \frac{n^{+'}}{n^-}} - \cancel{\frac{d_2}{d_1} c^- \frac{n^{-'}}{n^+}} \right) \\
 &\quad - \epsilon_3 B' \left(c^- - c^+ + \frac{d_1}{d_2} c^+ \frac{n^+}{n^-} - \frac{d_2}{d_1} c^- \frac{n^-}{n^+} \right) \\
 &\quad \pm \left[\epsilon_3 B \left((c^+ - c^-)' + \frac{d_1}{d_2} c^{+'} - \frac{d_2}{d_1} c^{-'} \right) \right. \\
 &\quad \left. \left. - (\epsilon_3' B + \epsilon_3 B') \left(c^- - c^+ + \frac{d_1}{d_2} c^+ - \frac{d_2}{d_1} c^- \right) \right] \right\}
 \end{aligned}$$

i.e.

$$\begin{aligned}
 - \frac{(c_{42} \pm c_{32})}{4\epsilon_3 B(c^+ - c^-)} &= \frac{-1}{4\epsilon_3 B(c^+ - c^-)} \left\{ \epsilon_3 B \left[{}^2_0(c^+ - c^-)' + (c^+ - c^-) \frac{(n^+ n^-)'}{n^+ n^-} \right. \right. \\
 &\quad \left. \left. + \frac{d_1}{d_2} c^{+'} \left(\frac{n^+}{n^-} \pm 1 \right) - \frac{d_2}{d_1} c^{-'} \left(\frac{n^-}{n^+} \pm 1 \right) \right] \right\}
 \end{aligned}$$

$$\begin{aligned} & \pm \epsilon_3' B \left[(c^+ - c^-) - \frac{d_1}{d_2} c^+ + \frac{d_2}{d_1} c^- \right] \\ & + \epsilon_3 B' \left[\frac{2}{\rho_1} (c^+ - c^-) - \frac{d_1}{d_2} c^+ \left(\frac{n^+}{n^-} \pm 1 \right) + \frac{d_2}{d_1} c^- \left(\frac{n^-}{n^+} \pm 1 \right) \right] \Bigg\}. \quad (A19) \end{aligned}$$

Taking the plus sign in (A19) we obtain

$$\begin{aligned} - \frac{(c_{42} + c_{32})}{4\epsilon_3 B (c^+ - c^-)} &= - \frac{(n^+ n^-)'}{4n^+ n^-} - \frac{(c^+ c^-)'}{4c^+ c^-} - \frac{[\rho_1 (n^+ + n^-)]'}{2\rho_1 (n^+ + n^-)} \\ &- \frac{1}{2} \frac{(n^+ - n^-)'}{(n^+ - n^-)} - \frac{(n^+ + n^-)}{4(n^+ n^- c^+ c^-)^{\frac{1}{2}}} \frac{(c^- c^+)' - c^+ c^{-'}}{(c^+ - c^-)} \\ &- \frac{\epsilon_3' B^2}{4\rho_1 (n^+ + n^-) (n^+ n^- c^+ c^-)^{\frac{1}{2}}} \\ &= \frac{1}{8(n^+ n^- c^+ c^-)^{\frac{1}{2}}} \left[\frac{2\epsilon_3' \rho_2^2 n^2}{\rho_1 (n^+ + n^-)} + (n^+ + n^-)(c^+ + c^-)' - (n^+ + n^-)'(c^+ + c^-) \right. \\ &\quad \left. - \frac{\rho_1'}{\rho_1} (n^+ + n^-)(c^+ + c^-) \right] \\ &- \frac{(n^+ - n^-)'}{2(n^+ - n^-)} \left[1 + \frac{(n^+ + n^-)(c^+ + c^-)}{4(n^+ n^- c^+ c^-)^{\frac{1}{2}}} \right] \quad (A20) \end{aligned}$$

while the minus sign in (A19) yields

$$- \frac{(c_{42} - c_{32})}{4\epsilon_3 B (c^+ - c^-)} = - \frac{(n^+ n^-)'}{4n^+ n^-} + \frac{\epsilon_3'}{4\epsilon_3}. \quad (A21)$$

We now use (A2), (A3) and (A6) to calculate the total coupling matrix $(t_{ij})_{4 \times 4}$ of (A1).

From (A3), (A6), (A9) and (A10) we have,

$$\begin{aligned}
 t_{11} = t_{33} &= u_{11} - \frac{(c_{11} + c_{21})}{4\epsilon_3 B(c^+ - c^-)} \\
 &= \frac{1}{8(n^+ n^- c^+ c^-)^{\frac{1}{2}}} \left[(n^+ + n^-)'(c^+ + c^-) + \frac{\rho_1'}{\rho_1} (n^+ + n^-)(c^+ + c^-) \right. \\
 &\quad \left. - (n^+ + n^-)(c^+ + c^-)' - \frac{2\epsilon_3' \rho_2^2 n^2}{\rho_1 (n^+ + n^-)} \right] \\
 &\quad - \frac{(\beta^2)'}{4(n^+ n^- c^+ c^-)^{\frac{1}{2}}} \left[\left(\frac{\rho_1 ((n^+)^2 + (n^-)^2 + n^+ n^-) - \epsilon_3}{(n^+ c^+)^{\frac{1}{2}} + (n^- c^-)^{\frac{1}{2}}} \right)^2 \right. \\
 &\quad \left. + \left(\frac{\rho_1 n^+ n^- + \epsilon_3}{(n^+ c^-)^{\frac{1}{2}} + (n^- c^+)^{\frac{1}{2}}} \right)^2 \right]. \tag{A22}
 \end{aligned}$$

There is no contribution from (A2) and (A3) to t_{13} , and so (A11) yields

$$t_{13} = t_{31}^* = - \frac{(c_{11} - c_{21})}{4\epsilon_3 B(c^+ - c^-)} e^{-\int 2\alpha d\xi} = \frac{1}{4} \left(\frac{(n^+ n^-)'}{n^+ n^-} - \frac{\epsilon_3'}{\epsilon_3} \right) e^{-\int 2\alpha d\xi}. \tag{A23}$$

From (A3), (A6) and (A13) we obtain

$$t_{21} = -t_{43} = u_{21} - \frac{(c_{12} + c_{22})}{4\epsilon_3 B(c^+ - c^-)} = 0. \tag{A24}$$

There is no contribution from (A2) and (A3) to t_{23} , and so (A6) yields

$$t_{23} = t_{41}^* = - \frac{(c_{12} - c_{22})}{4\epsilon_3 B(c^+ - c^-)} e^{-\int 2\alpha d\xi} \tag{A25}$$

where this quantity is given by (A14).

From (A3), (A6) and (A16) we have

$$t_{12} = -t_{34} = u_{12} - \frac{(c_{31} + c_{41})}{4\epsilon_3 B(c^+ - c^-)} = 0 \tag{A26}$$

while

$$t_{14} = t_{32}^* = \frac{c_{31} - c_{41}}{4\epsilon_3 B(c^+ - c^-)} e^{-\int 2\alpha d\xi} \quad (A27)$$

where the appropriate quantity is defined by (A17).

Finally, we have from (A2), (A3), (A6), (A10) and (A20)

$$\begin{aligned} t_{22} = t_{44} = u_{22} + \frac{\beta'}{\beta} - \frac{(c_{32} + c_{42})}{4\epsilon_3 B(c^+ - c^-)} \\ = \frac{1}{8(n^+ n^- c^+ c^-)^{\frac{1}{2}}} \left[\frac{2\epsilon_3' \rho_2^2 n_u^2}{\rho_1 (n^+ + n^-)} + (n^+ + n^-)(c^+ + c^-)' - (n^+ + n^-)'(c^+ + c^-) \right. \\ \left. + \frac{\rho_1'}{\rho_1} (n^+ + n^-)(c^+ + c^-) \right] \\ + \frac{(\beta^2)'}{4(n^+ n^- c^- c^+)^{\frac{1}{2}}} \left[\left(\frac{\rho_1((n^+)^2 + (n^-)^2 + n^+ n^-) - \epsilon_3}{(n^+ c^+)^{\frac{1}{2}} + (n^- c^-)^{\frac{1}{2}}} \right)^2 + \left(\frac{\rho_1 n^+ n^- + \epsilon_3}{(n^+ c^-)^{\frac{1}{2}} + (n^- c^+)^{\frac{1}{2}}} \right)^2 \right]. \end{aligned} \quad (A28)$$

Comparing (A22) and (A28) we find that

$$t_{22} = -t_{11}.$$

Also, from (A21)

$$\begin{aligned} t_{24} = t_{42}^* &= - \frac{(c_{42} - c_{32})}{4\epsilon_3 B(c^+ - c^-)} e^{-\int 2\alpha d\xi} \\ &= \frac{1}{4} \left(\frac{\epsilon_3'}{\epsilon_3} - \frac{(n^+ n^-)'}{n^+ n^-} \right) e^{-\int 2\alpha d\xi} \end{aligned} \quad (A29)$$

and inspection of (A23) shows that

$$t_{24} = -t_{13}.$$

Equations (A22)-(A29) are in agreement with the expressions for the coupling matrix given by (4.24). The derivation is now completed.

REFERENCES

- M. Abramowitz and I.A. Stegun (1970), "Handbook of Mathematical Functions", Dover Publications Inc., N.Y.
- A.I. Akhiezer, I.A. Akhiezer, R.V. Polovin, A.G. Sitenko and K.N. Stepanov (1975), "Plasma Electrodynamics Vol. I", Pergamon Press, Oxford.
- A. Appert, G.A. Collins, T. Hellsten, J. Vaclavik and L. Villard (1986), Plasma Physics and Controlled Fusion, 28, 133.
- R. Behn, A. de Chambrier, G.A. Collins, P-A. Dupprex, A. Heym, F. Hofmann, Ch. Hollenstein, B. Joye, R. Keller, A. Lietti, J.B. Lister, J-M. Maret, S. Nowak, J. O'Rourke, A. Pochelan and W. Simm (1984), Plasma Physics and Controlled Fusion, 26, 173.
- I.B. Bernstein and L. Friedland (1983), "Handbook of Plasma Physics", (M.N. Rosenbluth and R.Z. Sagdeev, eds.), North-Holland, Amsterdam, Vol. 1, 367.
- R.J. Bickerton (1984), Plasma Physics and Controlled Fusion, 26, 1355.
- P.T. Bonoli and E. Ott (1982), Phys. Fluids, 25, 359.
- M. Bornatici, R. Cano, O. De Barbieri and F. Engelmann (1983), Nucl. Fusion, 23, 1153.
- T.J.M. Boyd and J.J. Sanderson (1969), "Plasma Dynamics", Nelson, London.
- M. Brambilla (1978), Nucl. Fusion, 18, 493.
- M. Brambilla (1979), Nucl. Fusion, 19, 1348.
- K.G. Budden (1961), "Radio Waves in the Ionosphere", Cambridge University Press, London.

- R.A. Cairns and C.N. Lashmore-Davies (1982), Phys. Fluids, 25, 1602.
- R.A. Cairns and C.N. Lashmore-Davies (1983), Phys. Fluids, 26, 1268.
- R.A. Cairns (1985), "Plasma Physics", Blackie, Glasgow.
- F.F. Chen (1984), "Introduction to Plasma Physics and Controlled Fusion", 2nd edn., Plenum Press, London.
- P.C. Clemmow and J.P. Dougherty (1969), "Electrodynamics of Particles and Plasmas", Addison-Wesley, Reading, Mass.
- Equipe, TFR (1982), Plasma Physics, 24, 615.
- I. Fidone and R.B. Paris (1974), Phys. Fluids, 17, 1921.
- I. Fidone, G. Granata, G. Ramponi and R.L. Meyer (1978), Phys. Fluids, 21, 645.
- I. Fidone, G. Granata and R.L. Meyer (1982), Phys. Fluids, 25, 2249.
- P.J. Fielding (1981), "Plasma Physics and Nuclear Fusion Research", (R.D. Gill, ed.), Academic Press, London, 477.
- N.J. Fisch (1978), Phys. Rev. Lett., 41, 873.
- N.J. Fisch and A.H. Boozer (1980), Phys. Rev. Lett., 45, 720.
- L. Friedland (1985), Phys. Fluids, 28, 3260.
- L. Friedland (1986), Phys. Fluids, 29, 1105.
- M. Fröman and P.O. Fröman (1965), "JWKB Approximation: Contributions to the Theory", North-Holland, Amsterdam.
- V. Fuchs, K. Ko and A. Bers (1981), Phys. Fluids, 24, 1251.
- V. Fuchs, A. Bers and L. Harten (1985), Phys. Fluids, 28, 177.
- D.J.D. Gambier and J.P.M. Schmitt (1983), Phys. Fluids, 26, 2200.
- D.J.D. Gambier and D.G. Swanson (1985), Phys. Fluids, 28, 145.
- V.E. Golant (1972), Sov. Phys.-Tech. Phys., 1980.
- J. Heading (1961), J. Res. Nat. Bur. Stand., 65D, 595.

- J. Heading (1962), "An Introduction to Phase Integral Methods",
John Wiley, New York.
- J.C. Hosea, N. Bretz, A. Cavallo, P. Colstock, C. Daughney, S. Davis,
D. Dimock, P. Efthimion, H. Eubank, J. Hovey, D. Hwang, C. Karney,
D. McNeill, D. Mikkelsen, D. Mueller, D. Post, K. Sato,
G. Schilling, S. Medley, C. Singer, A. Silverman, J. Strachan,
S. Suckewer, H. Thompson, H. Toyama and J. Wilson (1982),
Proc. 3rd Joint Varenna-Grenoble International Symposium on
Heating in Toroidal Plasmas, Vol. 1, Grenoble, 213.
- K. Imre and H. Weitzner (1985a), Phys. Fluids, 28, 133.
- K. Imre and H. Weitzner (1985b), Phys. Fluids, 28, 1757.
- F.C. Jobes, S. Bernabei, T.K. Chu, W.M. Hooke, E.B. Meservey,
R.W. Motley, J.E. Stevens and S. von Goeler (1985), Phys. Rev.
Lett., 55, 1295.
- H. Jory (1984), Proc. 4th International Symposium on Heating in
Toroidal Plasmas, (H. Knoepfel and E. Sindoni, eds.), Vol. II,
Rome, 1424.
- H.H. Kuehl (1967), Phys. Rev., 154, 124.
- H.H. Kuehl, B.B. O'Brien and G.E. Stewart (1970), Phys. Fluids, 13,
1595.
- C.N. Lashmore-Davies, R.A. Cairns and V. Fuchs (1985), Phys. Fluids,
28, 1791.
- W.M. Manheimer (1979), "Infrared and Millimeter Waves" (K. Hutton,
ed.), Academic Press, Vol. 2, 299.
- J.D. Murray (1974), "Asymptotic Analysis", Clarendon Press, Oxford.
- Y.C. Ngan and D.G. Swanson (1977), Phys. Fluids, 20, 1920.

- V.V. Parail and V.V. Alikaev (1984), Proc. 4th International Symposium on Heating in Toroidal Plasmas, (H. Knoepfel and E. Sindoni, eds.), Vol. II, Rome, 753.
- M. Porkolab, B. Lloyd, J.J. Schuss, Y. Takase, S. Texter, R. Watterson, P. Bonoli, R. Englade, C. Fiore, R. Gandy, R. Granetz, M. Greenwald, D. Gwinn, B. Lipschultz, E. Marmor, S. McCool, D. Pappas, R. Parker, Pribyl, J. Rice, J. Terry and S. Wolfe (1984), Proc. 4th International Symposium on Heating in Toroidal Plasmas, (H. Knoepfel and E. Sindoni, eds.), Vol. I, Rome, 529.
- D.C. Robinson, M.W. Alcock, N.R. Ainsworth, B. Lloyd and A.W. Morris (1982), Proc. 3rd Joint Varenna-Grenoble International Symposium on Heating in Toroidal Plasmas, Vol. 2, Grenoble, 647.
- I.P. Shkarofsky (1966a), Phys. Fluids, 9, 561.
- I.P. Shkarofsky (1966b), Phys. Fluids, 9, 570.
- M. Shoucri and H.H. Kuehl (1981), Phys. Fluids, 24, 1395.
- M.G. Smith (1966), "Laplace Transform Theory", Van Nostrand, London.
- J.E. Stevens, S. Bernabei, M. Bitter, F. Boody, N. Bowen, A. Cavallo, I.K. Chu, S. Cohen, P. Colstock, S. Davis, C. Daughney, F. Dylla, P. Efthimion, D. Herndon, E. Hinnov, W. Hooke, J. Hosea, J. Hovey, H. Hsuan, D. Hwang, D. Ignat, F. Jobes, R. Kaita, J. Lawson, A. Martin, E. Mazzucato, D. McNeill, S. Medley, E. Meservey, R. Motley, D. Mueller, D. Ruzic, J. Schivell, F. Schnabl, R. Schwartz, J. Strachan, S. Suckewer, S. von Goeler and R. Wilson (1982), Proc. 3rd Joint Varenna-Grenoble International Symposium on Heating in Toroidal Plasmas, Vol. 2, Grenoble, 455.

- T.H. Stix (1962), "The Theory of Plasma Waves", McGraw-Hill, New York.
- T.H. Stix (1965), Phys. Rev. Lett., 15, 878.
- T.H. Stix (1975), Nucl. Fusion, 15, 757.
- T.H. Stix and D.G. Swanson (1983), "Handbook of Plasma Physics",
(M.N. Rosenbluth and R.Z. Sagdeev, eds.), North-Holland,
Amsterdam, Vol. 1, 335.
- D.G. Swanson (1976), Phys. Rev. Lett., 36, 316.
- D.G. Swanson (1978), Phys. Fluids, 21, 926.
- D.G. Swanson (1980), Nucl. Fusion, 20, 949.
- D.G. Swanson (1985a), Phys. Fluids, 28, 1800.
- D.G. Swanson (1985b), Phys. Fluids, 28, 2645.
- Ting-wei Tang (1970), Phys. Fluids, 13, 121.
- R.B. White and F.F. Chen (1974), Plasma Physics, 16, 565.
- V.V. Zheleznyakov, V.V. Kocharovskii and V.I.V. Kocharovskii (1983),
Sov. Phys. Usp., 26, 877.